A STUDY OF RECYCLED PULSARS IN GLOBULAR CLUSTERS

Thesis by
Stuart Bruce Anderson

In Partial Fulfillment of the Requirements
for the Degree of
Doctor of Philosophy

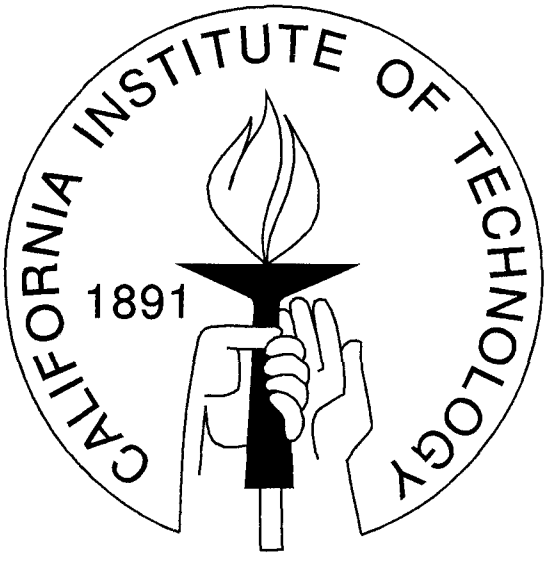

California Institute of Technology
Pasadena, California

1993

(Submitted September 23, 1992)

Acknowledgements

Thanks are due to many people for the support and encouragement I've received while searching for collapsed stars.

To my parents, for their encouragement and exemplary pursuit of excellence, I offer my warmest thanks.

I would like to thank my advisor Tom Prince, whose leadership as an academic advisor has been outstanding, and whose integrity and scholarship have been and continue to be an inspiration.

I would also like to thank Shri Kulkarni, whose foresight started an exciting search that I was fortunate enough to join; and Geoffrey Fox, in whose research group I was able to acquire the computational tools necessary for this thesis.

I would like to thank the Im's for several refreshing vacation trips, and most significantly for their invitation to walk down a church aisle at their wedding, with my as then unknown, wife to be.

This thesis is dedicated to Martha Lou Anderson, my companion for life, and wife of four months.

Abstract

We have performed a search for radio pulsars in 11 globular clusters visible from the 305 m Arecibo radio telescope. We have found 11 pulsars in the four clusters: M53, M13, NGC 6760, and M15; each containing one binary pulsar: 1310+18A, 1639+36B, 1908+00A, and 2127+11C, respectively; as well as a total of seven isolated pulsars: 1639+36A, 2127+11B, 2127+11D, 2127+11E, 2127+11F[1], 2127+11G, 2127+11H[1].

In this thesis we present the various search strategies employed and discuss the results of pulse time of arrival analysis for the seven isolated pulsars and the binary pulsar 2127+11C, as well as initial Doppler orbits for the binary pulsars 1310+18A and 1639+36B. The remaining pulsar 1908+00A is the subject of current research.

The binary pulsar 2127+11C has been found to be in an 8 hour orbit about another degenerate star. The detection of a relativistic precession of the orbit and time dilation effects constrain the pulsar and companion star masses to be $m_p = 1.34 \pm .23\, M_\odot$ and $m_c = 1.37 \pm .23\, M_\odot$.

Study of the radial positions and anomalous spin period derivatives of the seven isolated pulsars in M15 has revealed otherwise unobtainable information on the structure of this post core collapsed globular cluster. From the observed spatial pulsar distribution of $n_p \propto r^{-3}$ it is inferred that the mass of isolated pulsars in M15 is approximately $1.4\, M_\odot$. From the negative period derivative of PSR 2127+11A,D, it is inferred that the central mass-to-light ratio is $> 1.9\, M_\odot / L_{\odot,U}$ and the central mass density is $> 2.7 \times 10^6\, M_\odot\, \mathrm{pc}^{-3}$.

From the observed isolated pulsar luminosity function in M15, $\Phi(L) \propto L^{-0.93}$ and an assumed minimum luminosity of $1.0\,\mathrm{mJy\,kpc^2}$ it is inferred that the current population of observable isolated pulsars in M15 is $\mathcal{O}(100)$.

The observed dispersion measures towards the eight pulsars in M15 and their relative spatial positions indicate that the spectrum of inhomogeneities in the interstellar medium observed at smaller length scales, extends up to 10^{17} cm.

[1]Independently discovered by J. Middleditch (see page 35).

Contents

List of Figures

List of Tables

Chapter 1

Introduction

The radio pulsar population in globular clusters was only recently uncovered, beginning with the detection of a steep spectrum radio point source in the cluster M28 (Hamilton, Helfand, and Becker 1985) which was soon discovered to be the radio pulsar PSR 1821−24 by Lyne *et al.* (1987). The 32 currently published pulsars in 12 globular clusters (Table 1.1) form the majority of a class of pulsars commonly referred to as recycled pulsars. As a class, they are distinguished observationally from the $\sim$ 500 Galactic field pulsars by their short spin periods (3 ms $< P <$ 379 ms, versus $P \sim 0.6$ s), low dipole magnetic fields ($B \sim 10^9$ G, versus $B \sim 10^{12}$ G), and large spin-down ages ($\tau_c \gtrsim 10^8$ yr, versus $\tau_c \sim 10^{6.7}$ yr). It is believed that the short spin periods of recycled pulsars is due to the accretion of angular momentum during an episode of mass transfer (van den Heuvel, van Paradijs, and Taam 1986; Verbunt *et al.* 1987; Phinney and Kulkarni 1991).

The study of cluster pulsars yields information on several interesting areas of physics as well as astronomy and astrophysics. The preponderance of information obtained from and about pulsars is derived from their observed stable rotation rates. In this respect, recycled pulsars excel, exhibiting none of the rotational glitches and timing noise that are observed in young pulsars such as PSR 0531+21 in the Crab supernovae remnant (Groth 1975a; Groth 1975b; Groth 1975c). In fact, the recycled pulsar PSR 1937+21 now rivals the atomic time standard in long term stability (Davis *et al.* 1985).

As precise clocks, pulsars may be used to study both Newtonian and relativistic gravitational theories. In the case of binary pulsars in orbit about another degenerate star, precise measurements of orbital motion may be compared to theoretical calculations for a two-point mass orbit to verify relativistic effects, including the existence of gravitational

TABLE 1.1

Globular Cluster Pulsars

Globular Cluster	Pulsar(s)	Isolated	Binary	Reference
47-Tuc	0021−72 C–J,L–N†	6	5	Manchester *et al.* (1991)
M 15	2127+11 A–H	7	1	Chapter 4
M 5	1516+02 A,B	1	1	Wolszczan *et al.* (1989a)
M 13	1639+36 A,B	1	1	Chapter 5
NGC 6624	1820−30 A,B	2	-	Biggs *et al.* (1990)
M 53	1310+18	-	1	Chapter 5
M 4	1620−26	-	1	Lyne *et al.* (1988)
Ter-5	1744−24	-	1	Lyne *et al.* (1990)
NGC 6440	1746−20	1	-	Manchester *et al.* (1989)
NGC 6539	1802−07	-	1	D'Amico *et al.* (1990)
M 28	1821−24	1	-	Lyne *et al.* (1987)
NGC 6760	1908+00	-	1	Appendix B

† PSR 0021-72K has been identified as the 3rd harmonic of PSR 0021-72D (private communication, Matthew Bailes).

radiation (Taylor and Weisberg 1989; Damour and Taylor 1992; Taylor *et al.* 1992). These relativistic effects may be used to determine neutron star masses and thereby probe the equation of state for matter at nuclear densities.

Newtonian gravity may be studied using both isolated and binary pulsars as precise timing probes of the internal dynamics of globular clusters (see Spitzer (1987) and Binney and Tremaine (1987) for a general discussion of the dynamical evolution of globular clusters). As an example, we note that PSR 2127+11A and PSR 2127+11D appear to be spinning up (Table 4.2), an effect attributed to acceleration in the gravitational field of the cluster (Wolszczan *et al.* 1989b) and which may be used to estimate the mass-to-light ratio and central mass density in the core of M15 (Phinney 1992a, see Chapter 4). In addition, a large enough population of pulsars in a single cluster may be used to invert the observed distribution of pulsar spin period derivatives to obtain the distribution of line-of-sight accelerations and thereby determine the cluster's radial mass distribution (Phinney 1992a; Phinney 1992b, see Chapter 4). Of the 12 globular clusters with known radio pulsars listed above, only M15 and 47-Tuc contain more than 2 detected pulsars, making them suitable for such studies.

As a distinct class of objects characterized by short spin periods, low magnetic fields, and large ages, globular cluster pulsars provide important information on pulsar

formation and evolutionary theories. Population studies may be done to investigate such topics as magnetic field evolution, luminosity distribution and evolution (Kulkarni, Narayan, and Romani 1990, for example). The study of the distribution of pulsars among the various globular clusters may be used to infer information about recycled pulsar formation rates as a function of cluster parameters, such as the central core density (Johnston, Kulkarni, and Phinney 1991), which are important in determining the operative formation mechanism.

In order to address some of these interesting questions, we undertook a survey of Galactic globular clusters to search for a population of radio pulsars. In this thesis we present results for the pulsars found in the 11 Galactic globular clusters searched (see Table 1.2). Four clusters were found to contain a total of 11 pulsars—the four binary pulsars: 1310+18A, 1639+36B, 1908+00A, and 2127+11C in the clusters M53, M13, NGC 6760, and M15, respectively; and the seven isolated pulsars: 1639+36A, 2127+11B, 2127+11D, 2127+11E, 2127+11F[1], 2127+11G, 2127+11H[1]. All of our observations were made with the 305 m Arecibo radio telescope at either 430 MHz with a 10 MHz bandwidth or 1420 MHz with a 40 MHz bandwidth. The signal was sampled at an effective rate of 1.974 kHz using the Arecibo 40 MHz correlation spectrometer with 128 lags and three-level quantization (NAIC 1989). This work was part of a more general search of the 27 clusters visible from the Arecibo telescope ($-1° < \delta < +39°$). In the remaining 16 clusters searched elsewhere, the two binary pulsars 1516+02A,B were detected in M5 by Wolszczan *et al.* (1989a).

This thesis contains three previously published papers (Chapters 2,3,5) as well as the recently written Chapter 4—part of a manuscript in preparation for publication. The published papers have undergone editorial changes to standardize the typography, generate a single uniform bibliography, and correct typographical, stylistic, and actual errors. This work has been done in collaboration with Tom Prince, Peter Gorham, Shri Kulkarni, and Alex Wolszczan. The analysis of the radio pulsar data published in these 3 + 1 papers and the Appendices A,B was carried out as the central component of my Ph.D. research effort. The TEMPO pulsar timing software provided by J. Taylor enabled the precise timing measurements of the pulsars discovered here.

Chapter 2 appeared in *Nature* **346**, pp. 42-44 (1990) and reports the discovery of PSR 2127+11B and PSR 2127+11C in the globular cluster M15. This paper gave the first observational indication that a large population of pulsars in a single cluster might exist and

[1]Independently discovered by J. Middleditch (see page 35).

be suitable for dynamical studies of globular clusters. In addition, an initial Keplerian orbit for PSR 2127+11C indicated that this system was at that time only the second relativistic binary radio pulsar known and implied that further observations and analysis would reveal the relativistic effects reported in Chapters 3 and 4.

Chapter 3 appeared in *The Astrophysical Journal* **374**, L41–L44 (1991) and presents a timing solution for the relativistic binary pulsar 2127+11C which constrains the total binary mass to be $2.71\,M_\odot$, strengthening the case for a two neutron star system. This analysis determined that the pulsar had been ejected from the core of the cluster and partially motivated a detailed dynamical study of binaries in globular clusters (Sigurdsson 1992; Phinney and Sigurdsson 1991).

Chapter 4 contains part of a manuscript in preparation for publication in *The Astrophysical Journal* that reports a second relativistic parameter for the binary pulsar 2127+11C, enabling determination of the stellar masses, $m_p = 1.34 \pm .23\,M_\odot$ and $m_c = 1.37 \pm .34\,M_\odot$. It also presents timing solutions for the eight pulsars known to exist in M15 and discusses various implications of such a large population, including: radial mass distribution of neutron stars, mass-to-light ratio in the cluster core, spatial structure in the interstellar medium, and the recycled pulsar luminosity function.

Chapter 5 appeared in *Nature* **349**, pp. 47–49 (1991) and presents the discovery of the two pulsars, 1310+18A and 1639+36A, in the globular clusters M53 and M13, respectively. The existence of pulsars in such low-density clusters was found to be inconsistent with the conventional two-body tidal capture model (Verbunt 1988; Bailyn and Grindlay 1990) and suggested an alternative mechanism such as tidal capture between primordial binaries and a reservoir of primordial neutron stars (Phinney and Sigurdsson 1991).

Appendix A contains information on the binary pulsar 1639+36B in M13.

Appendix B contains five *International Astronomical Union* circulars announcing the discoveries of PSR 2127+11B, PSR 2127+11C, PSR 1639+36A, PSR 1310+18A, and PSR 1908+00A.

Appendix C contains an analysis of the relative sensitivities between coherent and incoherent searches for faint isolated pulsars in multiple day observations.

Appendix D contains a calculation of the expected line of sight acceleration distribution for the "core" pulsars in M15.

Appendix E discusses aspects of the computational requirements of our search.

TABLE 1.2

Globular Clusters Searched and Pulsars Found

IAU	NGC		Morph.	l	b	R_0	DM	τ_{scatt}	n_{psr}	ρ_c
1207+188	4147		KM?	252.8	77.2	17.3	32	9		3.0×10^4
1310+184	5024	M 53	KM	332.9	79.8	18.5	32	9	**1**	3.7×10^3
1339+286	5272	M 3	KM	42.2	78.7	10.4	25	9		6.7×10^3
1639+365	6205	M 13	KM	59.0	40.9	7.1	30	21	**2**	1.0×10^4
1644−018	6218	M 12	KM	15.7	26.3	5.3	74	53		2.9×10^4
1742+031	6426		KM?	28.1	16.2	17.5	120	150		—
1801−003	6535		KM?	27.2	10.4	6.9	200	440		—
1908+009	6760		KM	36.1	−3.9	4.1	200	970	**1**	—
2031+072	6934		KM	52.1	−18.9	14.9	100	110		5.8×10^3
2059+160	7006		KM	63.8	−19.8	39.1	96	97		2.5×10^2
2127+119	7078	M 15	PCC	65.0	−27.3	9.7	67	47	**5 + 2***	2.2×10^6

A list of the globular clusters searched and pulsars discovered in this thesis.* With the exception of PSR 2127+11A discovered in M15 (Wolszczan *et al.* 1989b) and the two binary pulsars in M5 (Wolszczan *et al.* 1989a) the above table is a complete list of known radio pulsars in the clusters visible from the Arecibo telescope.

The cluster morphology is taken from Chernoff and Djorgovski (1989), where KM denotes a King model cluster and PCC denotes a post-core-collapsed cluster. The Galactic longitude, latitude (l,b) and heliocentric distance, R_0 (kpc), are taken from Webbink (1985). The dispersion measure, DM ($\mathrm{cm}^{-3}\,\mathrm{pc}$) and pulse scatter-broadening at 400 MHz, τ_{scatt} (μs) are taken from Kulkarni, Narayan, and Romani (1990) when not determined directly from a pulsar detection. The central core mass density, ρ_c ($M_\odot\,\mathrm{pc}^{-3}$) is taken from Aguilar, Hut, and Ostriker (1988).

* The two pulsars 2127+11F,H were independently discovered by J. Middleditch (see page 35).

Chapter 2

Discovery of PSR 2127+11B and PSR 2127+11C

"Discovery of Two Radio Pulsars in the Globular Cluster M15"

S.B. Anderson, P.W. Gorham, S.R. Kulkarni, T.A. Prince, and A. Wolszczan

Appeared originally in *Nature*, Vol. 346, No. 6279, pp. 42–44, 5th July, 1990

DISCOVERY OF TWO RADIO PULSARS IN THE GLOBULAR CLUSTER M15

S.B. ANDERSON, P.W. GORHAM, S.R. KULKARNI AND T.A. PRINCE
Division of Physics, Mathematics and Astronomy,
California Institute of Technology, 206-49, Pasadena, CA 91125 USA

A. WOLSZCZAN
Arecibo Observatory, Arecibo, Puerto Rico 00613

ABSTRACT

We report the discovery of two radio pulsars, 2127+11B and 2127+11C, in the globular cluster M15 (NGC 7078), which also contains the 110-ms pulsar 2127+11A (Wolszczan *et al.* 1989b). Although only twenty globular cluster pulsars are known at present, the detection of three pulsars in a single cluster suggests that there might be a large total population of these objects, which would make them powerful probes of the dynamics and evolution of globular clusters. One of the new pulsars, 2127+11C, is in a highly eccentric binary system with an 8-hour period. It is thus similar to the famous PSR 1913+16 system (Taylor and Weisberg 1989) and study of the pulse arrival times can be expected to provide tests of general relativity, including gravitational wave emission. The companion of PSR 2127+11C is probably either another neutron star or a massive white dwarf, suggesting that the core of M15 contains a high density of massive stellar remnants.

2.1 Observations

The initial observations were made using the 305 m Arecibo radio telescope at a central frequency of 430 MHz and a 10 MHz receiver bandwidth. The data were sampled at an effective rate of 1.974 kHz using the Arecibo 40 MHz, three-level correlation spectrometer in a manner identical to that employed in the discovery of PSR 2127+11A (Wolszczan *et al.* 1989b). The discovery observations were made on 26 December 1988 starting at 18:51 UT. The pulse search was carried out on the Caltech nCUBE/10, a concurrent computer having 512 Central Processing Units (CPUs) with hypercube interconnection topology. A 16 Megasample de-dispersed time series was formed by padding the observed 10.9 million samples out to 2^{24} samples and by assuming a dispersion measure of 67.25 $\mathrm{cm}^{-3}\,\mathrm{pc}$ determined from earlier observations of PSR 2127+11A (Wolszczan *et al.* 1989b). The power spectrum was calculated using a concurrent implementation of the Fast Fourier Transform (FFT) algorithm (Fox *et al.* 1988) and searched for families of significant harmonic peaks.

2.2 Results

Table 2.1 and Figure 2.1 give the parameters and pulse profiles of the three pulsars detected in the 430 MHz observations. PSR 2127+11A was clearly detected in our first analysis of the December 1988 data. Further inspection revealed PSR 2127+11B with a period of 56 ms but approximately two times fainter than PSR 2127+11A. Subsequent timing measurements spanning 230 days indicate that PSR 2127+11B is an isolated pulsar with a period derivative ($\dot{P}$) of $9 \times 10^{-18}\,\mathrm{s\,s^{-1}}$, implying a characteristic age of $1 \times 10^{8}\,\mathrm{yr}$, if the observed $\dot{P}$ is due solely to magnetic braking. If, on the other hand, one assumes that the dominant effect is acceleration due to the local gravitational field, as in the case of PSR 2127+11A (Wolszczan *et al.* 1989b), then the magnitude of the acceleration is $5 \times 10^{-8}\,\mathrm{m\,s^{-2}}$. The errors quoted for PSR 2127+11B in Table 2.1 are three times the formal errors given by the temporal fitting program used in the analysis (TEMPO). The accuracy of these measurements are limited by the coupling of the timing residuals due to a position error (a one year period sine wave) and a $\dot{P}$ error (quadratic drift) over the limited 230 day observation period.

PSR 2127+11C was discovered using an algorithm specifically developed for detection of pulsars in binary orbits. The variable Doppler shift due to the orbital acceleration can spread the signal power over multiple frequency bins, resulting in a loss of sensitivity, particularly for fundamentals or harmonics with millisecond periods. In our algorithm, samples were inserted or deleted in the time series to compensate for a presumed acceleration. To reduce the computational demands of the search, we assumed a constant acceleration. A range of accelerations from $-19.2\,\mathrm{m\,s^{-2}}$ to $+19.2\,\mathrm{m\,s^{-2}}$ was explored using 2^{24}-point transforms, corresponding to the acceleration experienced by a pulsar in a circular orbit with 1 d period and a $1\,M_{\odot}$ companion. A series of 2^{22}-point transforms was also calculated for accelerations of magnitude $203\,\mathrm{m\,s^{-2}}$, corresponding to a $1\,M_{\odot}$ companion and a 4 hr circular orbit. PSR 2127+11C, with a period of 30.5 ms, was initially found in a 16 Megapoint transform at an acceleration of -9.5 $\mathrm{m/s^2}$.

Timing measurements were begun to determine the Keplerian parameters of the PSR 2127+11C orbit. Recording of the raw data stream on magnetic tape allowed us to extract timing information for all three pulsars from the same data. Because of the faintness of PSR 2127+11C, an integration time of $\gtrsim 10$ minutes was required for detection. This necessitated an acceleration search for each observation to compensate for orbital motion

TABLE 2.1

Pulsar Parameters

Timing Parameter		2127+11A	2127+11B	2127+11C
Epoch (JD)	T_0	2,447,213.15	2,447,632.9906	2,447,660.9089
Pulse Period (ms)	P_0	110.66470954(1)	56.13303358(1)	30.529(1)
Period Derivative (10^{-18} s s^{-1})	$\dot{P}$	-20 ± 1	8.8 ± 1.1	—
Right Ascension ($''$)*	α_{core}	$-1.95 \pm .15$	$+3.86 \pm .15$	—
Declination ($''$)*	δ_{core}	$+0.6 \pm .3$	$-0.8 \pm .6$	—
Dispersion Measure (cm^{-3} pc)	DM	67.25 ± 0.05	67.25 ± 1.0	67.25 ± 1.0
Flux Density (mJy)	S_{430}	$1.7 \pm .4$	$1.1 \pm .4$	$0.6 \pm .2$
Orbital Period (s)	P_b	—	—	$28{,}969 \pm 1$
Semi-Major Axis (ls)	$a_1 \sin i$	—	—	$2.52 \pm .01$
Eccentricity	e	—	—	$0.680 \pm .003$
Longitude of Periastron (deg)	ω_0	—	—	316.4 ± 1.0
Epoch of Periastron (JD)	T_0	—	—	2,447,632.46720(5)
Mass Function ($M_\odot$)	f	—	—	0.15

Numbers in parenthesis indicate the uncertainty in the last significant digit.

The values given for PSR 2127+11A are those reported by Wolszczan *et al.* (1989b) and are consistent with the results of our 430 MHz observations. The values for PSR 2127+11B are based on 430 MHz observations spanning 230 days. The Keplerian orbital parameters for PSR 2127+11C are based on 17 days of pulse arrival time analysis.

* Positions are relative to the centre of globular cluster M15 ($\alpha = 21^h\,27^m\,33\overset{s}{.}35$ and $\delta = 11^\circ\,56'\,48''.8$) (Shawl and White 1986).

and to obtain the correct apparent pulsar period. The determination of the orbital period was also complicated by the limited duration (3 hr) over which the cluster can be observed by the Arecibo telescope. The orbital period was found to be 8 hr 3 m, indicating that it would take a minimum of six weeks for a complete cycle of observable orbital phase. In Figure 2.2, we display the apparent pulsar period at the midpoint of each observation as a function of the orbital phase for observations taken primarily over an eight week period. The eccentricity of the orbit is immediately apparent.

Using the velocity curve in Figure 2.2 for an initial estimate of the orbit, pulse arrival time analysis has been performed on 17 observations taken during May 1988. The resulting Keplerian parameters, surprisingly similar to those of 1913+16 (Taylor and Weisberg 1989) are given in Table 2.1. If the secondary is another neutron star, the estimated orbital decay time and the advance of periastron will be 2×10^8 yr and 4° yr^{-1}, similar to those of PSR 1913+16. The PSR 2127+11C system should thus provide tests of general

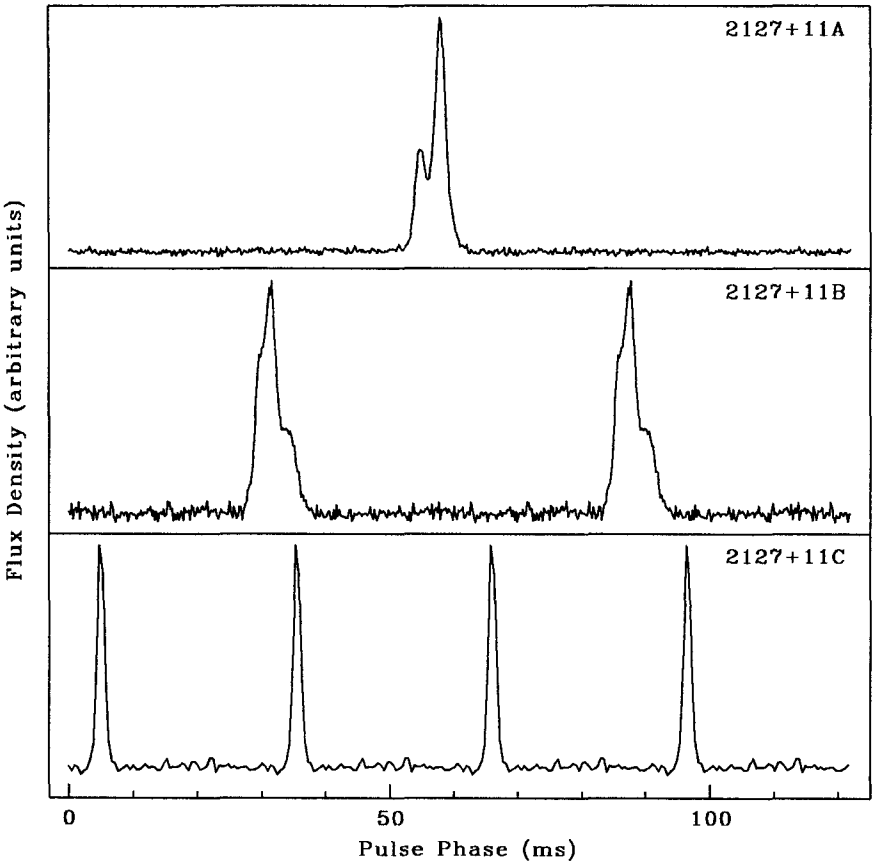

Figure 2.1: Average pulse profiles for the three known radio pulsars in globular cluster M15. The time resolution is 500 μs.

relativity in the strong field limit, including gravitational wave emission, comparable to those of PSR 1913+16. The errors quoted in Table 2.1 are our best estimates of the uncertainty due to the limited time span of observations used in this analysis and the possibility of pulse numbering ambiguities. A significantly more accurate measurement of the pulsar parameters, including a precise determination of the advance of periastron, is in progress using approximately nine months of timing observations.

Constraints can be placed on the pulsar and companion masses (m_p and m_c) by determining the mass function f, which depends on the apparent size of the pulsar's orbit and the orbital period. The value of the mass function for the 2127+11C system is $f(m_p, m_c) = (m_c \sin i)^3/(m_p + m_c)^2 = 0.15\, M_\odot$. Assuming $m_p = 1.4\, M_\odot$ for PSR 2127+11C,

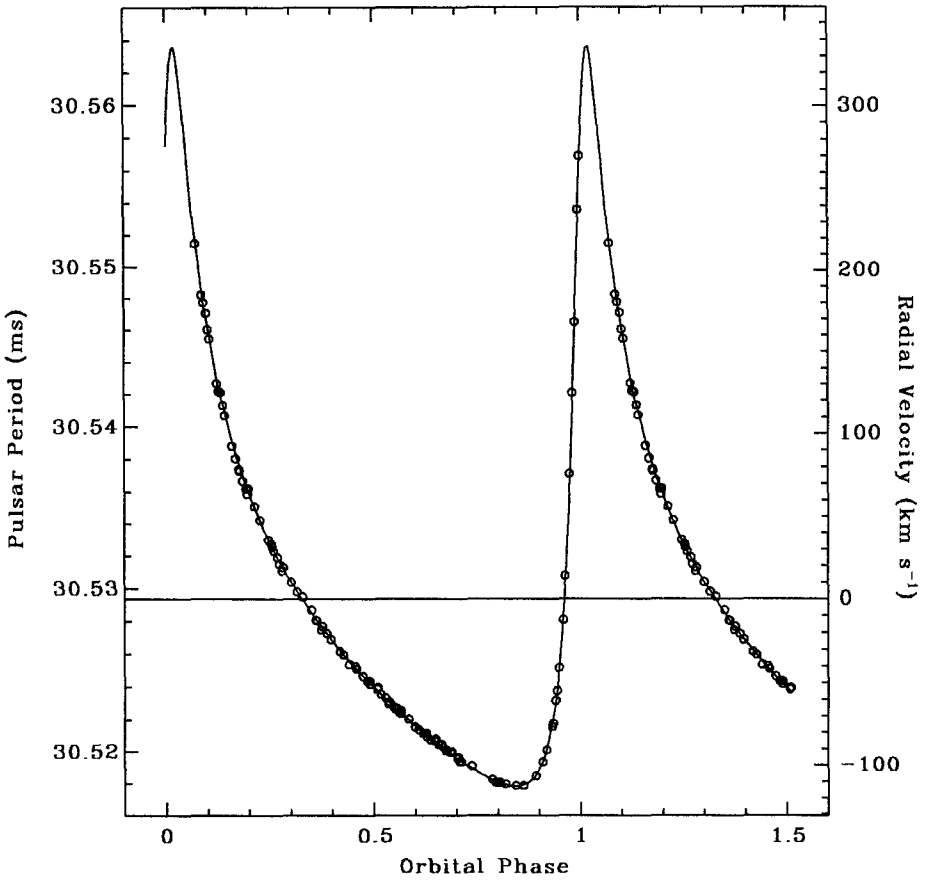

Figure 2.2: Velocity profile and observed Doppler shifted pulse periods as a function of orbital phase for PSR 2127+11C.

the minimum mass of the companion is $0.94\,M_\odot$. For $m_p = m_c = 1.4\,M_\odot$, the inclination angle i of the orbital plane to the line of sight would be 49°, close to the median inclination angle of 60°. Given the measured orbital parameters, the distance of closest approach is of the order of $1\,R_\odot$ for inclination angles corresponding to a $1\,M_\odot$ companion. Consequently, a main-sequence companion is ruled out, and the companion is most likely a second neutron star or a massive white dwarf.

2.3 Discussion

The discovery of three pulsars within a single cluster suggests that pulsars are abundant in globular clusters. Kulkarni, Narayan, and Romani (1990) have quantitatively analyzed the results of the major cluster pulsar surveys and conclude that a typical rich cluster contains about 100 active pulsars, most of which will be undetectable owing to the great distances to the clusters. Assuming a distance of 10 kpc to M15, the radio luminosities of PSR 2127+11A, B and C are respectively 170 mJy kpc^2, 110 mJy kpc^2 and 60 mJy kpc^2. These luminosities are well above the minimum luminosity of 1 mJy kpc^2 for field pulsars. Hence with increased sensitivity, additional pulsars ought to be detectable in M15. We are now in the process of analyzing all our data, over 50 hr of observations, in an effort to locate fainter pulsars.

The discovery of the binary pulsar 2127+11C strongly suggests an abundance of massive stellar remnants in the core of M15. According to the standard scenario, in some previous phase, PSR 2127+11C must have been in a binary system with a non-degenerate companion. We rule out PSR 2127+11C being a primordial binary because the formation of such systems is inevitably associated with a large systemic motion ($\gtrsim 200\,\mathrm{km\,s^{-1}}$) (Cordes and Dewey 1988; Dewey and Cordes 1987; Verbunt and Hut 1987) which would have resulted in the expulsion from the cluster. Consequently, the companion is likely the result of a capture interaction. Alternatively, PSR 2127+11C could have been a solitary, spun-up pulsar (like PSR 2127+11B) which experienced an exchange collision with a binary system.

Various authors have argued for a scenario of pulsar formation by accretion-induced collapse (AIC) of white dwarfs (Michel 1987; Chanmugam and Brecher 1987; Bailyn and Grindlay 1990). AIC scenarios invoke massive C+O white dwarfs or O-Ne-Mg white dwarfs and thus, even if AIC mechanism were to be operative (see Verbunt, Lewin, and van Paradijs (1989) for a discussion of the considerable theoretical and observational difficulties with this mechanism), the discovery of PSR 2127+11C implies an abundance of these white dwarfs. Such white dwarfs evolve from massive main-sequence stars ($M \lesssim 8\,M_\odot$). Thus in the framework of either the standard or the AIC model we conclude that, in the past, M15 contained many massive stars. To achieve reasonable rates for exchange or capture interactions, the remnants of these massive stars must have aggregated in the core of M15 by mass segregation. Even taking this effect into account, very steep initial mass functions ($\propto M^{-\alpha}$, $\alpha \geq 3.5$) are ruled out for M15 because they predict insufficient numbers of mas-

sive white dwarfs and neutron stars. A flatter IMF also explains the large abundance of pulsars inferred from other observations (Kulkarni, Narayan, and Romani 1990). However, we note that some recent theoretical studies (Chernoff and Weinberg 1990) suggest steep IMFs for most clusters which survive to the present date.

Most tidal-capture binaries, i.e., captures resulting from the transfer of kinetic energy to stellar deformation, are expected to be formed with an orbital radius of $\sim R_{\odot}$, and thus an orbital period of a fraction of day. A small fraction (10% to 30%) are expected to be wide binaries ($P_{orb} \sim 100\,\mathrm{d}$) formed by capture of giants. The formation of single pulsars like 2127+11A,B is easily understood as resulting from the breakup of a wide binary by passing stars (Verbunt *et al.* 1987; Romani, Kulkarni, and Blandford 1987). Rappaport, Putney, and Verbunt (1989) have shown this to be a very effective mechanism for breaking up wide binaries in the especially high-density collapsed core of M15. The tidal interaction model predicts that there should be between 3 to 10 times more compact binaries than isolated or wide-orbit binaries, whereas we detected only one compact binary and two isolated pulsars. Selection effects may have prevented detection of a larger number of short orbital period systems in our current survey. A quantitative analysis of selection effects is beyond the scope of this letter and will be presented elsewhere.

ACKNOWLEDGEMENTS

We thank S. Phinney for discussions and G. Fox for collaboration. This work was supported by the NSF, the Department of Energy (US) and the Alfred P. Sloan Foundation. Arecibo Observatory is operated by Cornell University under contract with the NSF.

Chapter 3

Initial Timing Model for PSR 2127+11C

"Timing Observations of the 8 Hour Binary Pulsar PSR 2127+11C
in the Globular Cluster M15"

T.A. Prince, S.B. Anderson, S.R. Kulkarni, and A. Wolszczan

Appeared originally in THE ASTROPHYSICAL JOURNAL, **374**: L41–L44, 1991 June 20

TIMING OBSERVATIONS OF THE 8-HR BINARY PULSAR 2127+11C IN THE GLOBULAR CLUSTER M15

T.A. PRINCE, S.B. ANDERSON, AND S.R. KULKARNI
Division of Physics, Mathematics and Astronomy,
California Institute of Technology, 206-49, Pasadena, CA 91125 USA

A. WOLSZCZAN
Arecibo Observatory, Arecibo, Puerto Rico 00613

ABSTRACT

We present new results on the position and characteristics of the 8 hour binary pulsar 2127+11C in the post-core-collapse (PCC) globular cluster M15. Our results indicate that PSR 2127+11C has been ejected from the cluster core via a close encounter with another binary system or isolated star. In particular, the position derived from a phase-connected timing solution places the PSR 2127+11C system 2.7 pc (projected) from the core, well outside the compact region containing the other four detected pulsars and the X-ray binary system X2127+11/AC211. While PSR 2127+11C is likely still bound to the cluster, it is nonetheless probable that other compact binary pulsars have been totally ejected, thereby contributing to the population of field binary pulsars. Timing results from PSR 2127+11C also show a relativistic advance of periastron of $4.^{\circ}46\,\mathrm{yr}^{-1}$ indicating that the total mass of the system is $2.71\,M_{\odot}$.

Subject headings: pulsars - clusters:globular - stars: binaries

3.1 Introduction

Binary star systems are expected to play a central role in the evolution of globular clusters during core collapse. In the dense environment of cluster cores, binaries are hardened through collisions with other stars, releasing binding energy which eventually halts the collapse of the core (Elson, Hut, and Inagaki 1987). When a binary becomes sufficiently hard, further collisions are expected to eject it from the core. We have determined that the 8 hr binary pulsar 2127+11C in the globular cluster M15 is such a hard binary system ejected from the core by a close encounter with another binary system or a single star.

PSR 2127+11C was discovered in observations of the globular cluster M15 taken with the 305 m Arecibo radio telescope (Anderson *et al.* 1990b, see Chapter 2). The pulsar

was first discovered at an acceleration of -9.5 m s^{-2} indicating that it was a member of a short-period binary system. Subsequent observations showed the pulsar to be in a highly eccentric 8.05 hr orbit. In the first phase of analysis (Anderson *et al.* 1990b, see Chapter 2) the five Keplerian parameters of the orbit were obtained by measurement of the apparent pulse period and pulse arrival times in 17 observations taken during May 1989. Because of the restricted time span of the observations, neither an accurate position nor relativistic orbital parameters were derived from the data.

Following these initial observations, additional observations were made at the Arecibo telescope to further refine the orbital and timing parameters of the pulsar. In this second phase of the analysis, which is reported here, we have analyzed data taken over a 372 day period to obtain a phase-connected timing solution for PSR 2127+11C which provides an accurate timing position, a measure of the precession of the periastron, and more accurate determinations of the five non-relativistic orbital parameters. These yield significant new information concerning the origin and probable history of PSR 2127+11C, which relates directly to the role of binary systems in the evolution of globular clusters. We discuss results of the timing analysis in § 3.2 and implications in § 3.3. Interpretations of the observational results presented in this *Letter* are also discussed by Phinney (1992a); Phinney and Kulkarni (1991); and Phinney and Sigurdsson (1991).

3.2 Analysis and Results

A total of 51 separate observations were made of M15, spanning the 372 day period from 1989 April 16 to 1990 April 22. The observations were taken with a central frequency of 430 MHz and a 10 MHz receiver bandwidth. The signal was sampled at an effective rate of 1.974 kHz using the Arecibo correlation spectrometer with 128 lags and three-level quantization. The resulting autocorrelation data were recorded on magnetic tape along with accurate time reference information.

The data from the digital correlation spectrometer were first folded at the apparent pulse period obtained from an ephemeris based on the values of the initial Keplerian orbital parameters. The pulse time-of-arrival (TOA) was then computed by cross-correlating the pulse profile derived from the folding process against a high signal-to-noise-ratio reference profile. Each TOA was based on 689 s of data and was measured to a typical accuracy of 70 μs. The best-fit orbital and pulsar parameters (Table 3.1) were derived using TEMPO,

a standard least-squares minimization program for pulsar timing analysis. Due to the faintness of the pulsar signal and the large orbital accelerations it was necessary to iterate the TOA measurement process several times, at each step using the improved orbital parameters computed from the previous iteration. This gradually removed artificial pulse broadening due to errors in the pulsar ephemeris, especially near periastron. The final parameters presented in Table 3.1 are based on 290 TOAs measured over the 372 day period with the corresponding timing residuals shown in Figure 3.1.

TABLE 3.1

Pulsar and Orbital Parameters

Pulsar Parameters		
Pulsar period	P	30.5292951285 (9) ms
Pulsar period derivative	$\dot{P}$	$4.99\,(5) \times 10^{-18}\,\mathrm{s\,s^{-1}}$
Dispersion measure	DM	$67.12\,(4)\,\mathrm{cm^{-3}\,pc}$
Right ascension	α	$21^{\mathrm{h}}\,27^{\mathrm{m}}\,36\overset{\mathrm{s}}{.}188\,(4)$ (B1950.0)
	$\alpha - \alpha_{core}$	$+41\overset{''}{.}65\,(5)$ §
Declination	δ	$11^{\circ}\,57'\,26\overset{''}{.}29\,(7)$ (B1950.0)
	$\delta - \delta_{core}$	$+37\overset{''}{.}49\,(7)$ §
Orbital Parameters		
Orbital period	P_b	28968.3693 (5) s
Projected semi-major axis	$a_1 \sin i$	2.520 (3) ls
Eccentricity	e	0.68141 (2)
Longitude of periastron	ω_0	$316\overset{\circ}{.}40\,(7)$
Apsidal motion	$\dot{\omega}$	$4\overset{\circ}{.}457\,(12)\,\mathrm{yr^{-1}}$
Epoch of periastron	T_0	2,447,632.4672065 (20) JD
Derived Parameters		
Mass function	f	$0.15285\,(55)\,M_\odot$
Total mass	$M = m_1 + m_2$	$2.706\,(11)\,M_\odot$
Characteristic age	τ_c	$0.96 \times 10^8\,\mathrm{yr}$
Magnetic field	B	$12 \times 10^9\,\mathrm{G}$
Predicted orbital decay time	τ_{gr}	$2 \times 10^8\,\mathrm{yr}$

Numbers in parenthesis represent a 3σ error in the last digit(s).

§ Position relative to cluster center: ($\alpha_{core} = 21^{\mathrm{h}}\,27^{\mathrm{m}}\,33\overset{\mathrm{s}}{.}35$, $\delta_{core} = 11^{\circ}\,56'\,48\overset{''}{.}8$) (Shawl and White 1986).

Table 3.1 gives the position of PSR 2127+11C relative to the cluster center obtained from the timing analysis. Figure 3.2 is a map of M15 showing the position of PSR 2127+11C, along with the timing positions of the four other known radio pulsars in M15 and the optical position of the X-ray binary system X2127+11/AC211. Pulsars

2127+11D & E are new detections, not described previously in the published literature. Both have relatively short spin periods, 4.80 ms and 4.65 ms respectively. Further details will be published in a later paper. As indicated by Figure 3.2 and Table 3.1, PSR 2127+11C has an offset from the center of the cluster of 56″, unexpectedly large compared to the much smaller offsets of the other five known neutron stars in M15. Assuming a distance of 10 kpc, the minimum radial distance of PSR 2127+11C from the cluster center is 2.7 pc, significantly larger than the core radius $\lesssim 0.13$ pc (Lauer *et al.* 1991).

3.3 Discussion

Table 3.1 gives the reduction in the spin rate, $\dot{P}$, which implies a characteristic age, $\tau_c \equiv P/2\dot{P}$ of 1×10^8 y and a dipole magnetic field strength, $B_9 \equiv B/10^9 G = 12$, where the field strength is estimated from the usual dipole formula, $B_9^2 = 10^{21} P\dot{P}$. This combination of low magnetic field strength and rapid rotation strongly suggests that PSR 2127+11C belongs to the group of pulsars which have been spun up by accretion of matter from a companion star—the so-called "recycled" pulsars.

The low stellar density at the radius of PSR 2127+11C implies a time scale of at least 10^{11} yr for either tidal capture or exchange reactions. Since at least one such event likely occurred within τ_c to form the currently observed 2127+11C system, it is almost certain that it was not formed at its current location, but rather in the highly concentrated core (King 1985) of this PCC globular cluster. Possible scenarios for ejection from the core are: (1) the 30.5 ms pulsar collided with a pre-existent binary system and replaced one of the components or (2) a pre-existent binary containing the 30.5 ms pulsar collided with an isolated star or another binary system, with a possible exchange of companion. Note that in either case a high density of degenerate stars is indicated in the core of M15 and the involvement of at least one binary system is required. The fact that four out of the five known pulsars in M15 are single supports scenario (1). It has been suggested that single recycled pulsars in clusters are the result of catastrophic tidal encounters of neutron stars with main sequence stars (Phinney and Kulkarni 1991).

Either of the two formation scenarios for PSR 2127+11C requires a collision involving a binary system. The PSR 2127+11C system is thus likely to be a direct manifestation of processes predicted to occur in globular clusters, namely, the heating of the cluster core through release of binary binding energy (Elson, Hut, and Inagaki 1987). Core collapse of

dense globular clusters is an inevitable consequence of dynamical evolution. The collapse is halted by the formation of tidal binaries and the release of energy through additional close interactions which cause a decrease in the binary semi-major axis ("hardening"), thereby releasing binding energy. For close binaries, exothermic interactions are kinematically favored over endothermic reactions which tend to disrupt the binary. The highly eccentric PSR 2127+11C system is likely to have resulted from such an exothermic collision with the potential energy released in the collision being converted into kinetic energy, resulting in the ejection of PSR 2127+11C from the core. If the products of such collisions do not escape the cluster, their excess kinetic energy is eventually distributed to other stars in the core upon subsequent passes through it, thus contributing to the overall heating of the core.

With the exception of PSR 2127+11C, all the cluster pulsars known to date and the dozen cluster low-mass X-ray binaries are located within the core of clusters, or within a few core radii. It is highly unlikely that PSR2127+11C is on an escape trajectory from the cluster because of the very short time to escape to its current radius ($< 10^5$ y). Rather, it is almost certainly in a highly eccentric orbit with its pericenter in the cluster core, (Phinney and Sigurdsson 1991, for a discussion of the distribution and evolution of orbits of ejected pulsars). However, a slightly larger initial velocity kick ($\gtrsim 60\,\mathrm{km\,s^{-1}}$) would have resulted in escape from the cluster, raising the possibility that other systems such as the remarkably similar binary pulsar 1913+16 may have been formed in and ejected from a cluster and are currently masquerading as field binary pulsars. PSR 2127+11C was found during a systematic search of globular clusters observable from Arecibo, most of which are in the range $-30^\circ \lesssim l \lesssim 70^\circ$ in galactic longitude. Given the relative volumes probed by this survey and the galactic plane survey which discovered PSR 1913+16, and given the characteristic ages of the pulsars, a birth rate for compact binary systems may be crudely estimated for each of the two systems separately. Assuming that several binaries are ejected for every binary like PSR 2127+11C retained by the cluster, the birth rates are the same within an order of magnitude. Globular clusters may thus turn out to be a significant source of compact binary pulsars. We further note that the proper motion measured for PSR 1913+16 (Taylor and Weisberg 1989) is consistent with it originating in a globular cluster several kiloparsecs from its present position.

In addition to position information, the timing solution for PSR2127+11C also yields new information concerning the nature of the companion to the pulsar and therefore on its evolutionary history. Interpretation of the observed orbital precession as a general

relativistic (GR) advance of periastron at a mean rate of $\dot{\omega} = 4.^{\circ}46 \pm 0.^{\circ}01\,\mathrm{yr}^{-1}$ (Table 3.1) implies a total mass of $2.71 \pm .01\,M_{\odot}$ for the binary system. It is necessary, however, to consider alternative classical explanations which, if present, would corrupt the above mass estimate. In particular, significant classical contributions can be expected if the companion star is an extended object with either a tidally or rotationally induced gravitational quadrupole moment. A main sequence star companion is ruled out, since it would induce a rate of precession $\mathcal{O}\ (10^3)$ times that observed (Masters and Roberts 1975). A helium star companion is also excluded since the current maximum mass of a helium star in M15 is $\lesssim 0.38\,M_{\odot}$ (Iben and Tutukov 1985)—more massive stars having completed their evolution in the $\sim 10^{10}\,\mathrm{yr}$ age of the cluster, implying a pulsar mass $< 0.22\,M_{\odot}$ and a rate of precession based on the structure of helium stars (Roberts, Masters, and Arnett 1976) substantially different from that observed.

In the case of a white dwarf companion, a gravitational quadrupole moment might arise from rapid rotation. However, given the lack of an observed variation in the projected semi-major axis $a_1 \sin i$, a limit of $\sim 0.^{\circ}001\,\mathrm{yr}^{-1}$ may be placed on the precession of the orbital inclination angle. This in turn places a limit on a classical contribution to $\dot{\omega}$ due to a quadrupole moment (Smarr and Blandford 1976). For instance, a rotating white dwarf companion generating more than a 1% classical contribution to the observed $\dot{\omega}$ would need to have its spin axis aligned to better than $\sim 1.^{\circ}5$ of the orbital plane or its normal vector (or a similar restriction on the dynamical longitude). Such an alignment seems unlikely given the nearly uniform *a priori* distribution of orientations expected from the collisional interaction which resulted in the observed binary system. In summary, we conclude that the current companion is either a white dwarf, neutron star, or black hole, and is not significantly contributing to the observed rate of precession. Hence, the total mass of the system is $2.71\,M_{\odot}$.

One consequence of the large total mass and the small characteristic age of this system compared to the age of M15 is that the current companion could not have been the mass donor responsible for the "recycling" of the pulsar. For, unless the pulsar mass alone exceeds $2.1\,M_{\odot}$ (a value which seems unlikely given the mass measurements of PSR 1913+16 (Taylor and Weisberg 1989) and X-ray binary systems (Rappaport and Joss 1983), the mass of the progenitor of the presumed white dwarf companion would exceed the $0.7\,M_{\odot}$ turn off mass of the cluster, i.e., the companion star would have evolved off the main sequence and initiated mass transfer prior to the inferred pulsar age τ_c. As a result of this, unless

PSR 2127+11C was orbiting a star with just the right mass to evolve and initiate mass transfer during the last $\sim 10^8$ yr, it has undergone at least two collisional interactions in the last $\sim 10^8$ yr—the first to "recycle" it and the second to replace the mass donor with a degenerate star and eject it from the core.

PSR 2127+11C provides another astronomical system in which the effects of GR can be observed along the lines of PSR 1913+16 (Taylor and Weisberg 1989), with two caveats: (1) the radio flux density at 430 MHz of PSR 2127+11C is 0.6 mJy, considerably smaller than the 6 mJy of PSR 1913+16, resulting in noisier TOAs (70 μs versus 15 μs for PSR 1913+16); (2) the pulsar parameters of PSR 2127+11C will be perturbed by gravitational effects of the cluster stars. The latter is an intrinsic effect and arises from an unknown gravitational acceleration of the binary system from both nearby stars and a cumulative effect from the cluster as a whole. Using the equation for the acceleration along the line of sight given in Phinney (1992a), we find that the maximum acceleration that PSR 2127+11C may be undergoing due to the cluster potential is of order $\sim 1 \times 10^{-7}\,\mathrm{cm\,s^{-2}}$ (the perturbation from neighboring stars is only $\sim$ 4% of this value). This corresponds to a 1.7% corruption of $\dot{P}$ (rotational spin decay) and a 2.1% corruption of $\dot{P}_b$ (orbital period decay). Observations of PSR 2127+11C over the next few years will thus allow a quantitative test of GR in the strong field limit accurate to $\sim$ 2%, compared to the 0.8% now obtained by PSR 1913+16 and the even better accuracy expected for PSR1534+12 (Wolszczan 1991). Conversely, one may assume that GR is the correct theory and use any observed deviation in $\dot{P}_b$ to determine the line-of-site acceleration and hence the intrinsic $\dot{P}$. This may then be used to infer the correct characteristic age of the system as well as information on the mass distribution of the cluster. Higher order time derivatives of the observed parameters will be dominated by the cluster environment (Blandford, Romani, and Applegate 1987), and rather than yielding new information about the pulsar, will provide interesting information on the gravitational potential of the globular cluster.

ACKNOWLEDGEMENTS

We are grateful to J. H. Taylor for supplying the TEMPO software package; E.S. Phinney for stimulating discussions; S. Djorgovski for an optical image of M15; and Jose Navarro for help in observations. This work was supported by the National Science Foundation (NSF), the US Department of Energy, and the Alfred P. Sloan Foundation. Arecibo

Observatory is part of the National Astronomy and Ionosphere Center, operated by Cornell University under contract with the NSF.

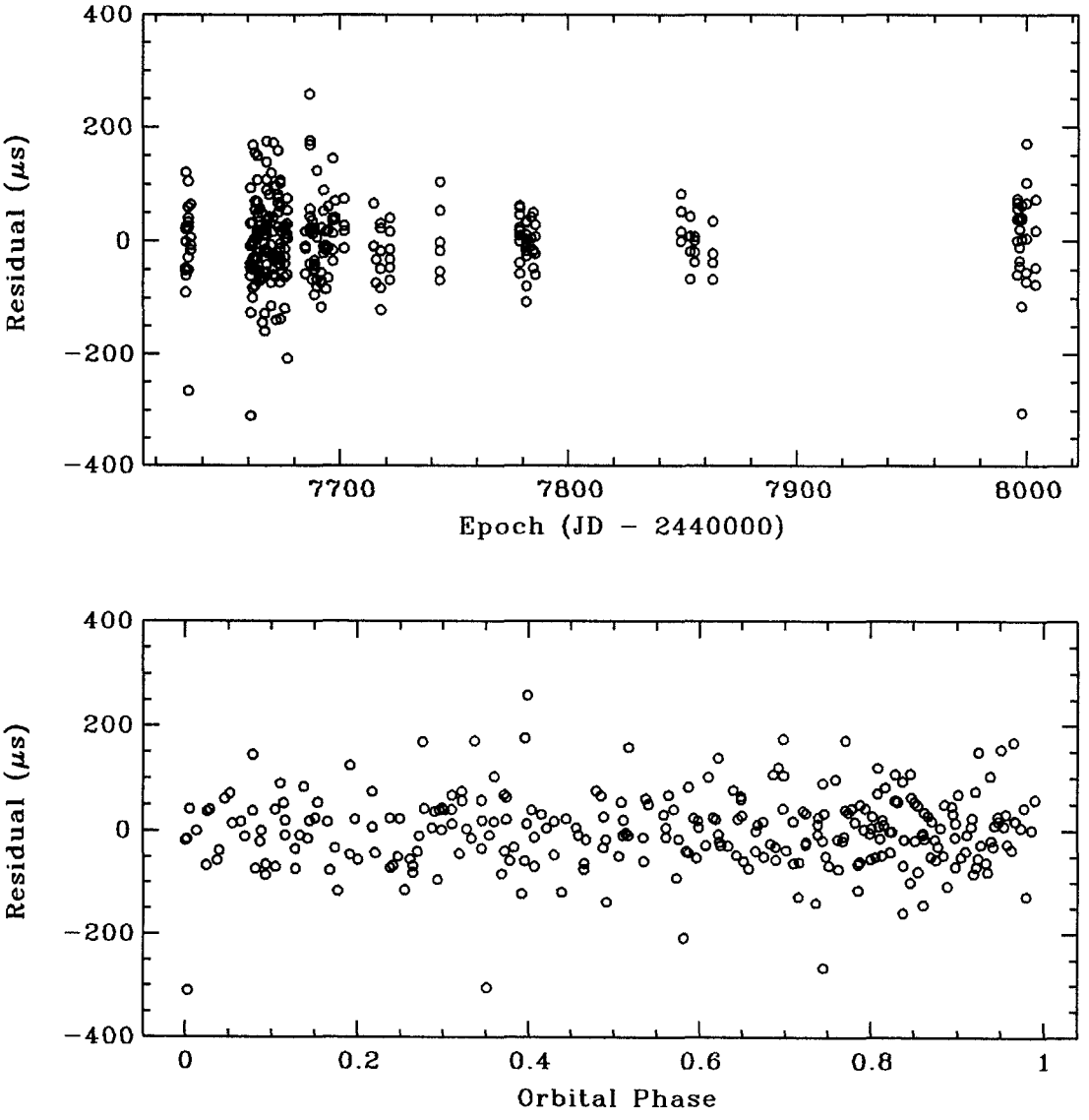

Figure 3.1: Timing residuals for the timing solution given in Table 3.1 as a function of both observation epoch and orbital phase.

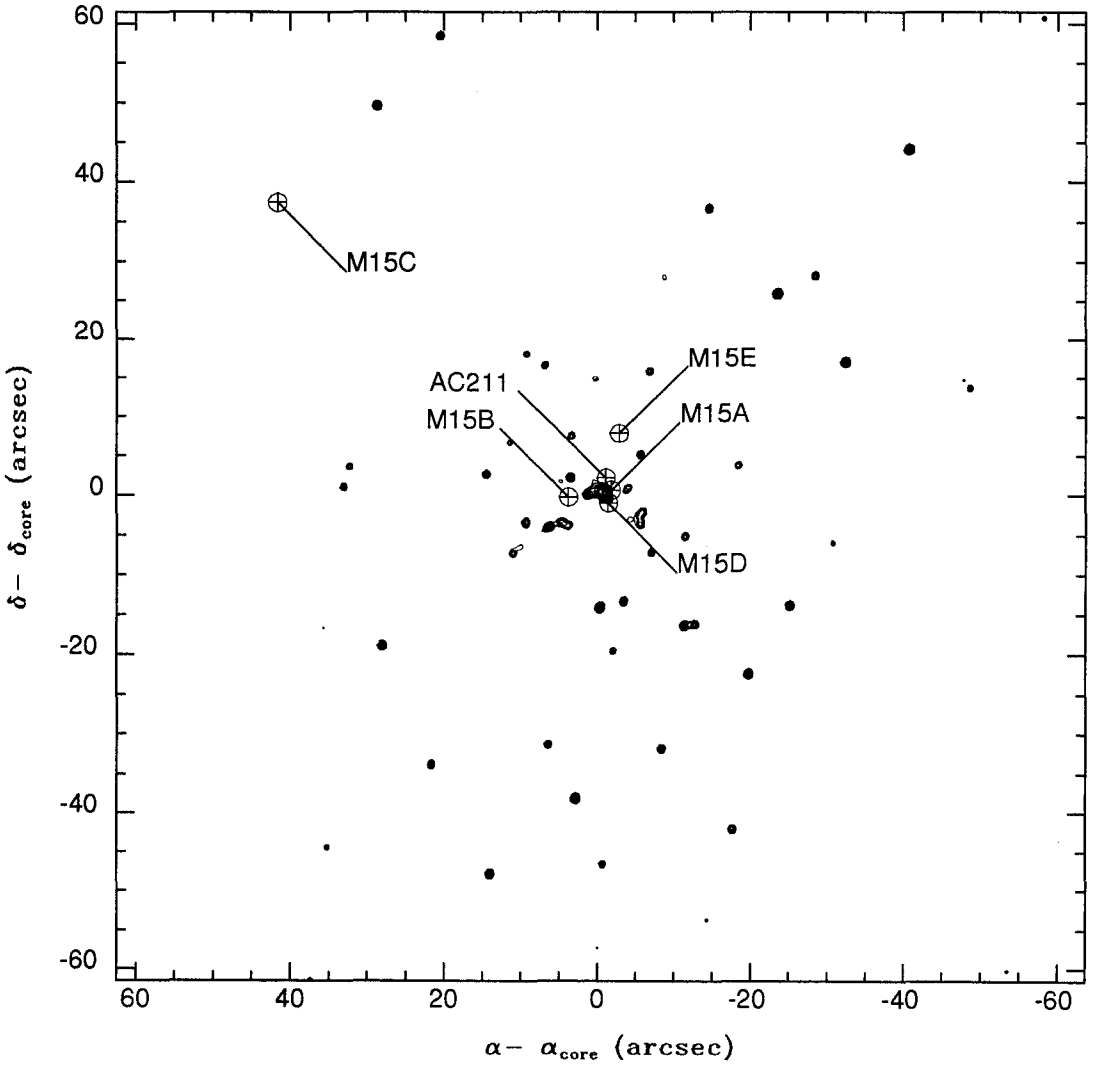

Figure 3.2: Optical image of the globular cluster M15 with the positions of the 5 known pulsars and the X-ray binary X2127+11/AC211 indicated relative to the cluster core $\alpha_{core} = 21^h\,27^m\,33\overset{s}{.}35$ and $\delta_{core} = 11^\circ\,56'\,48\overset{''}{.}8$ (Shawl and White 1986). The position of AC211 is from Geffert *et al.* (1989). Positions of PSR 2127+11A–E (M15A–E) relative to the cluster core are $(-1\overset{''}{.}9, 0\overset{''}{.}8)$, $(3\overset{''}{.}8, -0\overset{''}{.}3)$, $(41\overset{''}{.}7, 37\overset{''}{.}5)$, $(-1\overset{''}{.}4, -0\overset{''}{.}9)$, and $(-2\overset{''}{.}7, 8\overset{''}{.}0)$ respectively, accurate to within $0\overset{''}{.}3$ in all cases.

Chapter 4

Study of 8 Pulsars in the Globular Cluster M15

Part of a manuscript in preparation for publication in THE ASTROPHYSICAL JOURNAL

ABSTRACT

Radio observations of the globular cluster M15 were made on 63 days over a 1.2 year period to study the binary pulsar PSR 2127+11C. In addition to measuring two relativistic orbital parameters for PSR 2127+11C, we detected seven isolated pulsars and have successfully performed pulse time-of-arrival analysis for all eight pulsars in M15: PSR 2127+11A–H. Some results of particular interest are the following: (1) for the binary system 2127+11C, the pulsar and companion star masses are determined to be $m_p = 1.34 \pm .23\,M_\odot$ and $m_c = 1.37 \pm .23\,M_\odot$, (2) for PSR 2127+11D, an increasing spin rate is observed, placing a distance independent lower limit on the central mass density ($\rho_c > 2.7 \times 10^6\,M_\odot\,\mathrm{pc}^{-3}$) and mass to light ratio ($M/L_U > 1.9\,M_\odot\,/\,L_{\odot,U}$), (3) spatial structure in the dispersion measure towards the eight pulsars is detected, and (4) a flux limit of 300 μJy is placed on pulsations from the companion star to PSR 2127+11C.

4.1 Introduction

Recent observations of globular clusters have revealed a surprisingly large population of radio pulsars. The unique environment found in these extremely old star systems produces a class of pulsars that is significantly different from the more populous collection of field pulsars. While field pulsars are characterized by long spin periods ($P_{median} \simeq 0.62\,\mathrm{s}$) and high magnetic fields ($B \simeq 10^{12}\,\mathrm{G}$), the globular cluster population is characterized by spin periods and magnetic fields several orders of magnitude lower, i.e., $P_{median} \simeq 5.4\,\mathrm{ms}$ and $B \simeq 10^{8-10}\,\mathrm{G}$. As a distinct population, the study of globular cluster pulsars provides important information on pulsar formation and evolution theories, as well as the structure and dynamics of globular clusters. In addition, the study of individual exotic binaries formed in the dense central cores of clusters provides precise neutron star mass measurements as well as information on the various stellar interactions operative in globular clusters.

Globular clusters offer an excellent test case for the physics of large ensembles of self gravitating particles—see Spitzer (1987) for a recent treatment of the dynamical evolution of globular clusters. Furthermore, radio pulsars, with their rapid rotation rates and large moments of inertia, may be used as precise timing probes of the internal dynamics of globular clusters. As an example, we note that PSR 2127+11A and PSR 2127+11D appear to be spinning-up (Table 4.2), an effect attributed to acceleration of the pulsars in the gravitational field of the cluster (Wolszczan *et al.* 1989b). More particularly, the observed

anomalous spin period derivatives may be used to place limits on the central mass density and mass to light ratio. It may also be possible with a large enough population to invert the observed pulsar spin period derivatives to obtain a distribution of line of sight accelerations and thereby determine the cluster radial mass distribution (Phinney 1992a; Phinney 1992b). Of the 12 globular clusters with known radio pulsars, only M15 and 47-Tuc contain more than 2 detected pulsars (Table 4.1), making them amenable to such studies.

TABLE 4.1

Globular Cluster Pulsars

Globular Cluster	Pulsar(s)	Isolated	Binary	Reference
47-Tuc	0021−72 C–J,L–N†	6	5	Manchester *et al.* (1991)
M 15	2127+11 A–H	7	1	Chapter 4
M 5	1516+02 A,B	1	1	Wolszczan *et al.* (1989a)
M 13	1639+36 A,B	1	1	Chapter 5
NGC 6624	1820−30 A,B	2	-	Biggs *et al.* (1990)
M 53	1310+18	-	1	Chapter 5
M 4	1620−26	-	1	Lyne *et al.* (1988)
Ter-5	1744−24	-	1	Lyne *et al.* (1990)
NGC 6440	1746−20	1	-	Manchester *et al.* (1989)
NGC 6539	1802−07	-	1	D'Amico *et al.* (1990)
M 28	1821−24	1	-	Lyne *et al.* (1987)
NGC 6760	1908+00	-	1	Appendix B

† PSR 0021-72K has been identified as the 3rd harmonic of PSR 0021-72D (private communication, Matthew Bailes).

Globular clusters are evidently efficient producers of binary pulsars—13 out of 32 in GC's versus 10 out of 489 for the Galactic plane population. The study of binary pulsars provides a wealth of interesting information. Analysis of their orbital motion provides the only accurate means of determining pulsar masses, which are important in understanding the formation process of isolated and binary pulsars as well as investigating the equation of state of nuclear density material. In addition, timing studies of binary pulsars may be used as strong field tests of relativistic gravity (Damour and Taylor 1992; Taylor *et al.* 1992), and provide the only experimental evidence for the existence of gravitational radiation (Taylor and Weisberg 1989).

The discovery of PSR 2127+11C (Anderson *et al.* 1990b, see Chapter 2) and its subsequent timing (Prince *et al.* 1991, see Chapter 3) have yielded information on binary pulsar formation scenarios in globular clusters (Sigurdsson 1992, and references therein).

In addition, the more accurate timing results reported here have determined two neutron star masses and future timing studies should show the effects of gravitational radiation.

In this work we describe the detection analysis and timing results obtained from 63 observations of M15 over a 1.2 year period for the eight pulsars PSR 2127+11A–H. In § 4.2 we describe the observations made with the 305 m Arecibo telescope. Section 4.3 describes the various searches performed: (§ 4.3.1) an acceleration search for binary pulsars, (§ 4.3.2) an incoherent multiple day search for faint isolated pulsars, (§ 4.3.3) a coherent multiple day search, (§ 4.3.4) a full Keplerian orbit search for pulsations from the companion star to PSR 2127+11C, (§ 4.3.5) a halo search for ejected pulsars, and (§ 4.3.6) an optical pulsation search for PSR 2127+11A–H. In § 4.4 we present our timing results for the seven isolated pulsars: PSR 2127+11A,B,D–H. In § 4.5 we present our timing results for the binary pulsar: PSR 2127+11C. In § 4.6 we discuss the implications of our findings for the population of pulsars in M15: (§ 4.6.1) relative positions, (§ 4.6.2) pulsar accelerations, (§ 4.6.3) search sensitivities and flux measurements, (§ 4.6.4) relative radio luminosities, and (§ 4.6.5) relative dispersion measures. Appendix C contains an analysis of the relative sensitivities for coherently and incoherently combining multiple day observations. In Appendix D we derive the expected line of sight acceleration for the seven "core" pulsars. Appendix E contains aspects of the computational requirements of our search. Finally, in § 4.7 we conclude with comments on the possibilities for future research.

4.2 Observations

The 305 m Arecibo radio telescope was used to make 63 observations of M15 during the 422 day period from 16 April 1989 to 11 June 1990, with an average duration of 62 minutes. The observations were taken at a central frequency of 430 MHz with a 10 MHz receiver bandwidth. The signal was sampled at an effective rate of 1.974 kHz using the Arecibo correlation spectrometer with 128 lags and three-level quantization (NAIC 1989). The resulting autocorrelation data were recorded on magnetic tape along with accurate time reference information.

Most pulsar timing programs are similar in that they generate a sequence of time tagged pulse profiles (see Figure 4.1), that are later used to determine a sequence of pulse times of arrival (TOAs)—an exception being Lestrade *et al.* (1990), who determine a pulse TOA from the corresponding frequency of arrival. These TOAs are used to generate a

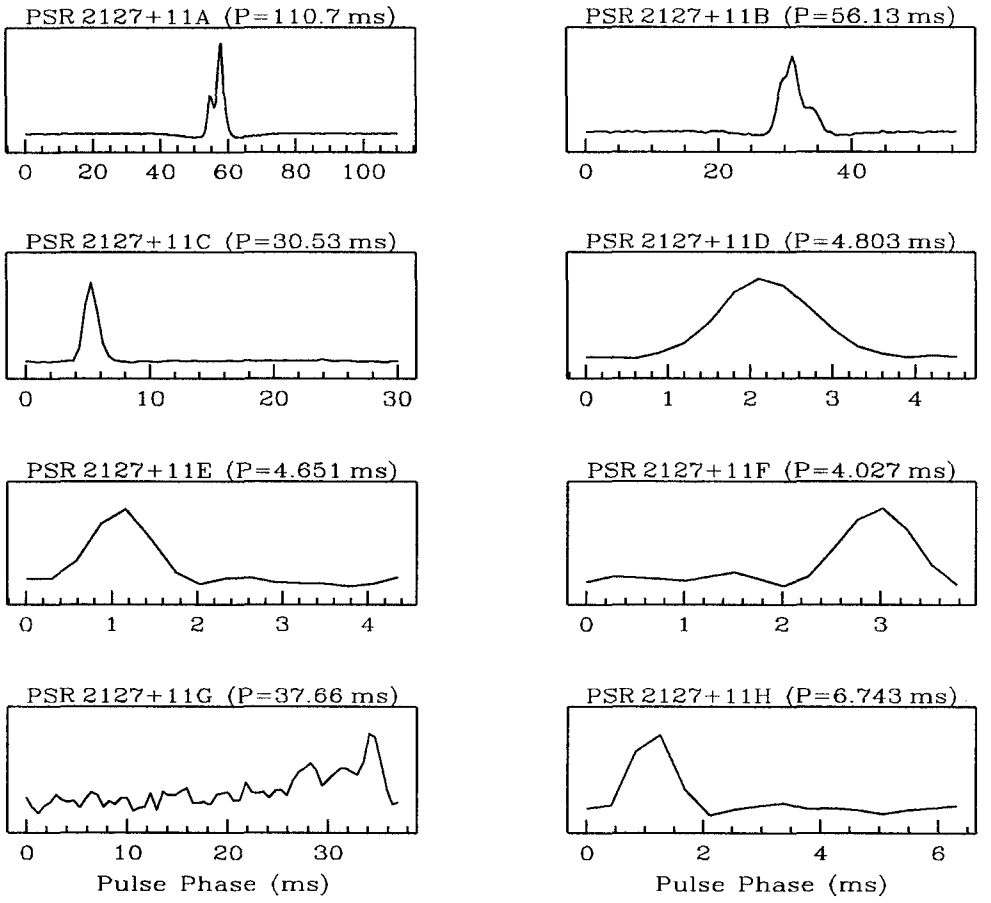

Figure 4.1: Pulse profiles for 8 pulsars in M15.

timing model for the pulsar and determine system parameters such as the mass of two neutron stars (see Table 4.4). However, our observations differ from most current timing efforts in the method of generating the pulse profiles. Rather than folding the data in real time at a precomputed pulse period, the "raw" (post-detection) signal was recorded on magnetic tape and later processed to generate pulse profiles. This recording scheme removes the requirement for special purpose hardware and prior knowledge of the pulsar parameters. As a dramatic example of the benefits of archiving the "raw" data (at least in the case of globular cluster observations) we note that the five pulsars (PSR 2127+11D–H) were detected and successfully timed using the observations of PSR 2127+11C *ex post facto.* Of additional benefit for timing PSR 2127+11C, with the relatively long integration times of 10 minutes necessary to obtain significant pulse profiles, is the ability to iterate the

determination of the initial 11 dimensional timing model.

The conversion of pulse profiles to TOAs requires precise timing information. The accuracy of the time reference information required here is dictated by the TOA measurement precision of $\sim 15\,\mu$s for PSR 2127+11A. Arecibo maintains two precise clocks (Rubidium and Cesium) as well as receiving the LORAN C broadcast time standard. The Rubidium clock is used as the frequency standard for the observatory clock (EECO), which has its phase adjusted daily to agree with the LORAN C signal. In addition, the Cesium clock is routinely read by the National Institute of Standards and Technology (NIST) via a Global Positioning System (GPS) of satellites in common view from Arecibo. For our pulsar timing observations the correlator was slaved to the observatory clock and forced to start on a 10-second interval. To refer the observations to coordinated universal time (UTC), a frequency counter was used to measure the time difference between the EECO 10-second tick and the cesium clock, while the difference between the cesium clock and UTC is published by the NIST. The resulting absolute time tag for each observation is in principle limited to a $1\,\mu$s uncertainty in the start time of the correlator (Perillat 1989).

In addition to the observatory clocks, the pulsars themselves may be considered as an ensemble of precise clocks, providing several internal consistency checks between the various pulsar timing models. The most dramatic instance of this was the recovery of 11 days of observations (9 June 1989 thru 25 June 1989) for which the timing information was incorrectly recorded. The start times for these observations were uncertain by $\pm 10\,$s, whereas $\lesssim 40\,\mu$s accuracy is required to be useful in timing PSR 2127+11C. By requiring the fractional pulse phase of PSR 2127+11A at the beginning of each observations to agree with the predicted value, the start time uncertainty was reduced to a discrete set, i.e., one of a few hundred integral pulse numbers. The same phase alignment of PSR 2127+11B then selected the proper PSR 2127+11A pulse number and the start time was determined to the $15\,\mu$s (rms) timing precision of PSR 2127+11A. This data could then be used in the timing of the remaining seven pulsars (excluding only PSR 2127+11A) and was crucial in the original orbit determination for PSR 2127+11C.

4.3 Detection Algorithms

Of the eight pulsars known in M15, only PSR 2127+11A,B are readily detected in a standard pulsar search—see Nice (1992) for a recent discussion of standard search tech-

niques. Of the remaining six pulsars, 2127+11C,D and possibly 2127+11E are detectable if repeated observations are searched until the orbital phase and/or interstellar scintillation conditions are fortuitous for detection. We consider here the methods employed to detect the binary pulsar and faint isolated pulsars in M15 below the single day detection limit.

4.3.1 Acceleration Search

PSR 2127+11C was discovered using an algorithm specifically developed for the detection of pulsars in binary orbits (Anderson *et al.* 1990b, see Chapter 2). Standard Fourier analysis techniques assume a strictly periodic signal, whereas the pulse periods of binary pulsars are modulated by orbital motion. This time variable Doppler shift spreads the pulsed signal power over multiple Fourier bins, drastically reducing sensitivity to short orbital and spin period pulsars. In Figure 4.2 we demonstrate this loss in signal power for PSR 2127+11C during a 35 minute Fourier transform made near the most favorable detection orbital phase ($\phi_{orb} \sim 0.5$, i.e., near apastron). PSR 2127+11C was discovered at $\phi_{orb} \sim 0.8$ with an acceleration of -9.5 $\mathrm{m\,s^{-2}}$. The line of sight orbital acceleration near periastron is 300 $\mathrm{m\,s^{-2}}$, and the measurements of the apparent pulsar period near periastron shown in Figure 4.7 were determined by performing a two-dimensional search over a and $\dot{a}$, i.e., acceleration and jerk.

4.3.2 Incoherent Multiple Day Search ("Stack Search")

PSR 2127+11D,E were discovered in a "stack" search designed to detect faint isolated pulsars. By incoherently adding multiple observations an improved flux limit may be reached for signals with a frequency drift less than a Fourier bin width, i.e.,

$$\left|\frac{\partial f}{\partial t}\right| T_{run} < \frac{1}{T_{obs}} \qquad \text{or} \qquad \left|\dot{P}\right| T_{run} < \frac{P^2}{T_{obs}}, \tag{4.1}$$

where f is the pulsation frequency, T_{obs} is the duration of a single observation, T_{run} is the time span of the observations to be incoherently stacked, and P is the pulsation period.

There are four potential sources of such a frequency/period shift in a "stack" search: (1) intrinsic pulsar spin evolution, (2) acceleration in a GC gravitational field, (3) positional offset from the center of the telescope beam, and (4) orbital motion in a binary system. All of these effects are strongly dependent on the putative pulsar's spin period, being significant predominantly for millisecond periods.

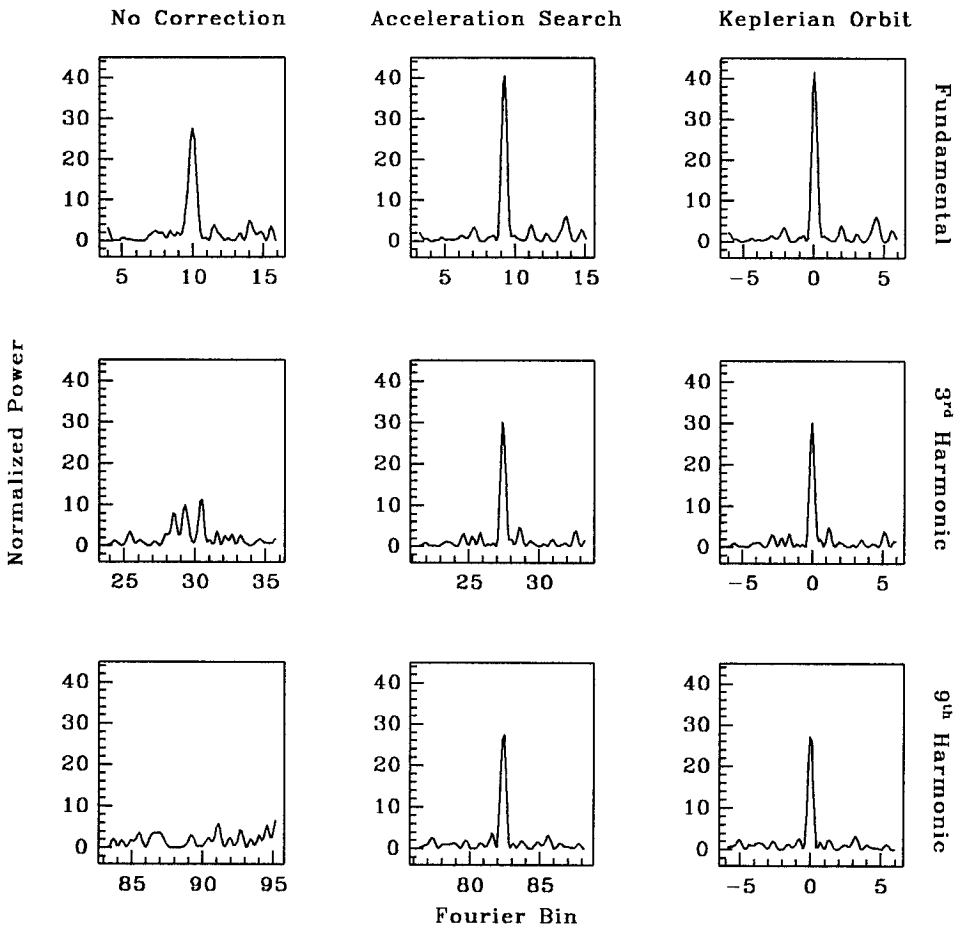

Figure 4.2: Effects of orbital acceleration on signal power. The three rows show the normalized power at the first, third and ninth harmonics of PSR 2127+11C. The three columns show the results of applying: no orbital correction, constant acceleration search ($a = 1.0\,\mathrm{m\,s^{-2}}$), and a full Keplerian orbit.

Intrinsic $\dot{P}$ in Stack Search

We show that the Fourier bin drift from an intrinsic $\dot{P}$, while significant for a population of young pulsars ($\tau_c < 10^6$ yr), is negligible for the old recycled pulsar population observed in globular clusters. To maintain sensitivity to 1.0 ms pulsations (the Nyquist period of our data is 1.012 ms), with observation times of 3 hours (transit time of the Arecibo Telescope) the requirement of Equation (4.1) is, $\dot{P}\, n_{day} < 1.07 \times 10^{-15}\,\mathrm{s\,s^{-1}}$, where n_{day} is the number of days spanned by the observations. Expressed in terms of the characteristic

age of the putative pulsar,

$$\tau_c \equiv \frac{P}{2\dot{P}} > \frac{T_{obs}T_{run}}{2P} \qquad \text{or} \qquad \tau_c > n_{day}\,(1.5 \times 10^4\,\mathrm{yr}).$$

Consequently, stacks of $\lesssim 18\,\mathrm{yr}$ may be performed before selecting against the observed population of old recycled pulsars, $\tau_c \gtrsim 10^8\,\mathrm{yr}$ (Table 4.5).

Globular Cluster Acceleration in Stack Search

The effects of acceleration in the core of M15 are comparable to the intrinsic spin-down, as may be immediately inferred from the negative $\dot{P}$ of PSR 2127+11A,D. In particular, a pulsar with intrinsic spin period P and line of sight velocity v_l will have an observed Doppler shifted spin period $P_{obs} = (1 + v_l/c)P$. Consequently, gravitational acceleration along the line of sight, a_l, will manifest itself as a shift in $\dot{P}$,

$$\dot{P}_{obs} = \dot{P} + \frac{a_l}{c}P,$$

potentially spreading the signal power over multiple Fourier bins and selecting against millisecond pulsars. However, the requirement for the cluster acceleration component of $\dot{P}_{obs}$ to satisfy Equation (4.1) is (for $P = 1\,\mathrm{ms}$ and $T_{obs} = 3\,\mathrm{hr}$),

$$\frac{|a_l|}{c}P < \frac{P^2}{T_{run}T_{obs}} \qquad \text{or} \qquad |a_l| < \frac{3.2 \times 10^{-2}\,\mathrm{cm\,s^{-2}}}{n_{day}}.$$

A typical globular cluster with core velocity dispersion $\sigma_c \sim 10\,\mathrm{km\,s^{-1}}$ and core radius $r_c \sim 1\,\mathrm{pc}$, has a characteristic acceleration of $|a_l| \sim \sigma_c^2/r_c \simeq 3 \times 10^{-7}\,\mathrm{cm\,s^{-2}}$ (Phinney 1992a), implying $n_{day} \lesssim 10^5$. However, for M15, a classic example of a post-core-collapsed globular cluster (King 1985), it is found that $|a_l|/c < 4 \times 10^{-16}\,\mathrm{s^{-1}}$ in the core region, or $|a_l| < 1.2 \times 10^{-5}\,\mathrm{cm\,s^{-2}}$ (see § 4.6.2), implying $n_{day} < 2.7 \times 10^3$. Consequently, the effects of cluster acceleration in M15 place a similar limit of $\sim 7\,\mathrm{yr}$ on the length of a stack search.

Position Offset in Stack Search

In order to compare power spectra from different observations it is necessary to account for the time varying Doppler shift of the Earth's orbital motion. This may be accomplished in either the time domain, by referring each time sample to its solar system barycenter (SSB) arrival time, or in the frequency domain by Doppler shifting each observation by the orbital velocity of the Earth projected along the assumed pulsar direction.

In either case the correction to the SSB requires *a priori* knowledge of the pulsar position. With an unknown offset from the nominal position of the telescope beam center, there is an uncorrected residual Doppler term which constrains the length of observations that may be stacked before a signal will drift into adjacent Fourier bins. The SSB Doppler shift of a signal with frequency f is simply,

$$\delta f \equiv f_{ssb} - f_{obs} = -f(\vec{V}_\oplus \cdot \vec{n})/c = f R_\oplus \Omega_\oplus \cos\beta \, \sin\phi,$$

where $\vec{n}$ is the unit vector (λ, β) towards the pulsar in ecliptic coordinates, $\vec{V}_\oplus$ is the velocity vector of the Earth, $R_\oplus$ is half the light travel time across the Earth's orbit, $\Omega_\oplus$ is the angular velocity of the Earth's orbit, and $\phi \equiv \lambda_{psr} - \lambda_\oplus$ is the relative heliocentric longitude of the pulsar. Consequently, if one parametrizes the pulsar position relative to the beam center by a direction angle γ, and a small angular displacement ϵ, the residual Doppler shift, $\delta f \rightarrow \delta f + \delta f_{err}$, is given by

$$\left.\begin{aligned} \lambda &\rightarrow \lambda + \epsilon \left(\frac{\cos\gamma}{\cos\beta}\right) \\ \beta &\rightarrow \beta + \epsilon \sin\gamma \end{aligned}\right\} \quad \Rightarrow \quad \delta f \rightarrow \delta f + \epsilon f R_\oplus \Omega_\oplus (\cos\phi \, \cos\gamma - \sin\beta \, \sin\phi \, \sin\gamma),$$

or

$$\left.\begin{aligned} A^2 &= \cos^2\gamma + \sin^2\beta \, \sin^2\gamma \\ \phi_0 &= \tan^{-1}\left[\frac{\cos\gamma}{\sin\beta \, \sin\gamma}\right] \end{aligned}\right\} \quad \Rightarrow \quad \delta f_{err} = -\epsilon f R_\oplus \Omega_\oplus A \sin(\phi - \phi_0).$$

The maximum δf_{err} is obtained for $A = 1$ from position offsets along the ecliptic, i.e., $\gamma = \{0, \pi\}$, and is independent of the ecliptic latitude of the observations. The requirement for the pulsar signal to remain in a single Fourier bin may now be expressed as (for A=1),

$$\begin{aligned} \left|\delta f_{err}^{end} - \delta f_{err}^{beg}\right| &< \frac{1}{T_{obs}}, \\ \epsilon R_\oplus \Omega_\oplus \left|\sin(\phi + T_{run}\frac{\Omega_\oplus}{2} - \phi_0) - \sin(\phi - T_{run}\frac{\Omega_\oplus}{2} - \phi_0)\right| &< \frac{P}{T_{obs}}, \\ 2\epsilon R_\oplus \Omega_\oplus \left|\sin(T_{run}\frac{\Omega_\oplus}{2}) \cos(\phi - \phi_0)\right| &< \frac{P}{T_{obs}}. \end{aligned}$$

The maximum δf_{err} is obtained for $\phi = \phi_0$, where ϕ is measured at the middle of the run. This implies that to maintain sensitivity to 1.0 ms period signals in a $5'$ radius beam for $T_{obs} = 3$ hr individual observations that $n_{day} < 39$. Alternatively, it implies that if $2\epsilon R_\oplus \Omega_\oplus T_{obs} < P$ then the residual SSB Doppler correction will always remain within a Fourier bin, i.e., there is no limit imposed on n_{day} by the Earth's orbit. For example, if $T_{obs} < 1$ hr then there is no limit to n_{day} for $P > 1$ ms.

Binary Motion in Stack Search

The detection of a binary pulsar in a stack search is subject to the same requirement that the orbital velocity of the pulsar not Doppler shift the signal over multiple Fourier bins. This may be accomplished by reducing the length of individual transforms. While this technique has the distinct advantage of being equally sensitive to all binary pulsars with orbital velocities below a fixed level, it suffers a severe drop in sensitivity compared to that obtained for isolated pulsars in a single coherent transform (see Appendix C). The requirement may be expressed as, $|\beta_{max}|\, f\, T_{obs} < 1$, where $\beta_{max} \equiv V_{max}/c$ is the maximum orbital line of sight velocity. For PSR 2127+11C, with $|V_{max}| < 340\,\mathrm{km\,s^{-1}}$ and $f = 32.76\,\mathrm{Hz}$, this limits T_{obs} to 27 s. Consequently, to reach the same flux limit as a single day 8 Mpt transform and maintain sensitivity to PSR 2127+11C in its orbit, would require 18 days of observations, stacked as 18×256 32 kpt transforms (to reach a similar flux limit for a 1 ms pulsar would require 390 days).

4.3.3 Coherent Multiple Day Search

By including pulse phase information in a coherent multiple day search, it is possible to detect fainter pulsars. PSR 2127+11F,H were detected in a coherent search of seven consecutive observations. We acknowledge the independent discovery of PSR 2127+11F,H by J. Middleditch—with his similar search effort on an independent data set detecting these two pulsars 1–2 weeks prior to our analysis (Middleditch, private communication). PSR 2127+11G was discovered in a coherent search of 16 observations over a 25 day period, that were resampled down to 2 ms samples to readily fit into available computer memory.

This coherent search technique differs from the incoherent search described in Section 4.3.2 in that both the amplitude and phase of the Fourier transforms are used. This necessitates a search for pulsations at a much finer frequency resolution than the individual observation Fourier bin spacing, since the search algorithm is now effectively timing the putative pulsar, i.e., keeping track of pulse phase, over the full span of the observations rather than a single observation. The required frequency resolution is determined by the same criteria for independent Fourier bin spacing as in the single day transform, i.e., that adjacent frequency trials result in a change of one pulsation period over the complete span of the data. Theoretically, one must search over the $n_{day}(24\,\mathrm{hr}\,/T_{obs})$ independent frequency bins between adjacent single day Fourier bins. In practice, the simplest and most efficient

algorithm to accomplish this is a large "gigapoint" transform spanning all of the data. To avoid introducing additional noise in the power spectrum of such a transform, the inter-observation gaps should be filled with the mean value of the time series, as is readily seen by considering Parseval's theorem, which states that the total power in the frequency domain must equal the total power in the time domain.

As in the incoherent stack, the coherent search is susceptible to several selection effects against millisecond signals. The modification to Equation 4.1 for phase coherence over the n_{day} observation is,

$$\left|\frac{\partial f}{\partial t}\right| T_{run} < \frac{1}{T_{run}} \qquad \text{or} \qquad \left|\dot{P}\right| T_{run} < \frac{P^2}{T_{run}}, \tag{4.2}$$

where T_{run} is the time span of the observations to be coherently searched. The same four sources of frequency/period drift need to be considered: (1) intrinsic pulsar spin evolution, (2) acceleration in a GC gravitational field, (3) positional offset from the center of the telescope beam, and (4) orbital motion in a binary system.

Intrinsic $\dot{P}$ in Coherent Search

The limitation from intrinsic pulsar spin evolution on the number of days observations that may be coherently transformed follows directly from Equation (4.2). To maintain sensitivity to millisecond periods the requirement is $\dot{P} < 1.34 \times 10^{-16}\,\mathrm{s\,s^{-1}}/n_{day}^2$, or expressed in terms of the characteristic age of the putative pulsar, $\tau_c > n_{day}^2\,(1.2\times10^5\,\mathrm{yr})$. Consequently, transforms of up to 29 d may be performed before selecting against millisecond pulsars in the population of old recycled pulsars, $\tau_c \gtrsim 10^8\,\mathrm{yr}$.

Globular Cluster Acceleration in Coherent Search

As in the incoherent stack the effects of cluster acceleration are similar to intrinsic period evolution. The requirement for the cluster acceleration component of $\dot{P}_{obs}$ to satisfy equation (4.2) is,

$$\frac{|a_l|}{c}P < \frac{P^2}{T_{run}^2} \qquad \longrightarrow \qquad |a_l| < \frac{4.0 \times 10^{-3}\,\mathrm{cm\,s^{-2}}}{n_{day}^2}.$$

For a typical cluster with $|a_l| < 3 \times 10^{-7}\,\mathrm{cm\,s^{-2}}$ (cf. § 4.3.2), this places a limit of 115 days on the length of a multiple day transform before the cluster acceleration will spread a 1.0 ms signal over multiple Fourier bins. In the core of the cluster M15, with $|a_l| < 1.2\times10^{-5}\,\mathrm{cm\,s^{-2}}$ (see § 4.6.2), the requirement is $n_{day} < 18$.

Position Offset in Coherent Search

The effect of a position offset from the fiducial position at the telescope beam center is derived from the transformation of TOAs from the observatory to the solar system barycenter (SSB), where the putative pulsar appears to be periodic. At the level of accuracy required here, only the Roemer delay, corresponding to the light propagation time across the Earth's orbit, need be considered: $t_b = t_{obs} + \vec{r}_{obs} \cdot \vec{n}$, where t_b is the SSB arrival time of a pulse originating from direction $\vec{n}$ that passes through the space time event $(t_{obs}, \vec{r}_{obs})$. Consequently, any error in the presumed position of the pulsar will result in an "incorrect" time series in which the pulse signal is no longer periodic and will spread the signal over multiple Fourier bins, with a concomitant loss in sensitivity.

The conversion of topocentric TOAs to the SSB is done in three stages (Backer and Hellings 1986): from the observatory to the Earth center, from the Earth center to the Earth-Moon barycenter (EMB), and from the EMB to the SSB. The correction to the center of mass of the earth has a periodicity of $P_\oplus = 1$ sidereal day, and an amplitude of $T_\oplus \simeq 21\,\mathrm{ms}$. Similarly, we have $P_{EMB} = 27.3\,\mathrm{d}$, $T_{EMB} \simeq 17\,\mathrm{ms}$; and $P_{SSB} = 1\,\mathrm{yr}$, $T_{SSB} \simeq 500\,\mathrm{s}$. For a small angle error in the assumed position of the pulsar, ϵ, the ephemeris error will be a sum of three sinusoidal terms with period $P_{\{\oplus,EMB,SSB\}}$ and amplitude $\leq \epsilon T_{\{\oplus,EMB,SSB\}}$. For our observations, ϵ is limited by the telescope beam size to $\lesssim 5'$, implying maximum ephemeris amplitudes of $31\,\mu\mathrm{s}$, $25\,\mu\mathrm{s}$, and $730\,\mathrm{ms}$. Given our $500\,\mu\mathrm{s}$ sample time, only the final SSB correction pertains for detection. As an example, Figure 4.3 demonstrates the pulse phase error for PSR 2127+11F over a 6 day period, for an assumed position in the core (PSR 2127+11F is $16''.7$ from the core of M15).

Approximating the motion of the observatory as a circular orbit about the SSB leads to an ephemeris correction of $\delta t \equiv t_{ssb} - t_{obs} = R_\oplus \cos\beta \cos\phi$, where β is the ecliptic latitude of the pulsar and $\phi \equiv \lambda_{psr} - \lambda_\oplus$ is the relative heliocentric longitude of the pulsar. If one parametrizes the pulsar position relative to the beam center (λ, β), by a direction angle γ, and a small angular displacement ϵ, one obtains:

$$\left.\begin{aligned} \lambda &\rightarrow \lambda + \epsilon \frac{\cos\gamma}{\cos\beta} \\ \beta &\rightarrow \beta + \epsilon \sin\gamma \end{aligned}\right\} \quad \Rightarrow \quad \delta t \rightarrow \delta t - \epsilon R_\oplus (\sin\beta \cos\phi \sin\gamma + \sin\phi \cos\gamma),$$

or

$$\left.\begin{aligned} A^2 &= \cos^2\gamma + \sin^2\beta \sin^2\gamma \\ \phi_0 &= \tan^{-1}\left[\frac{\cos\gamma}{\sin\beta \sin\gamma}\right] \end{aligned}\right\} \quad \Rightarrow \quad \delta t_{err} = -\epsilon R_\oplus A \cos(\phi - \phi_0).$$

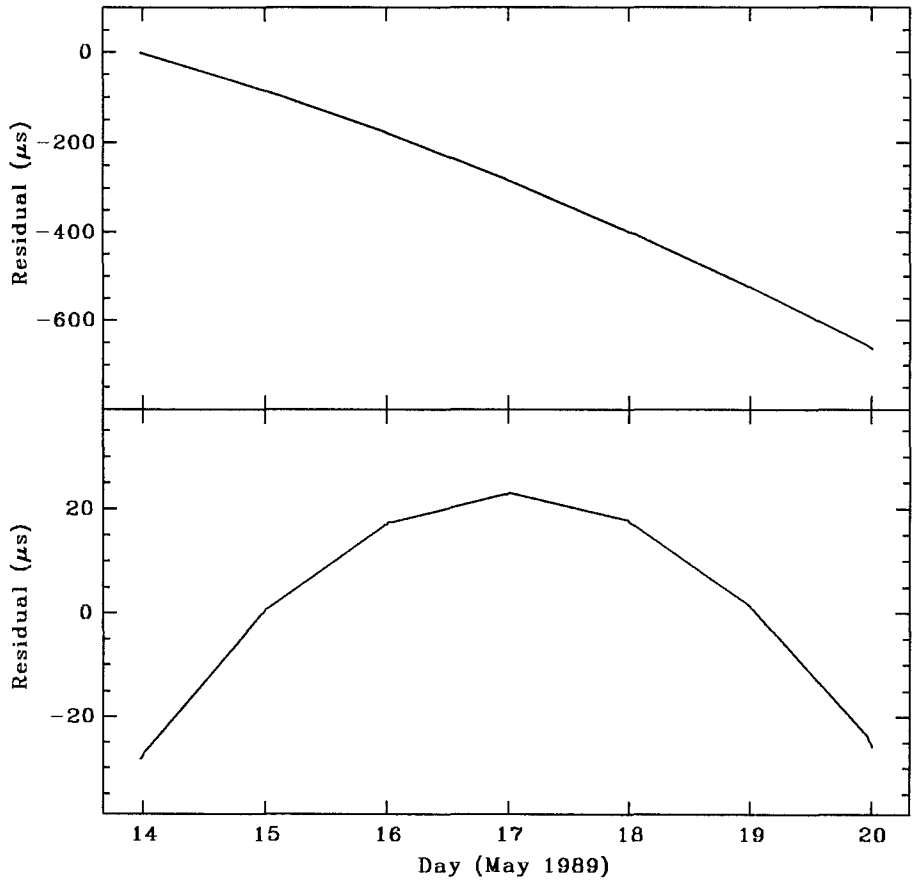

Figure 4.3: Example ephemeris error in constructing a one week time series for PSR 2127+11F assuming a core position rather than the actual 16″.7 displacement from the core. The linear term in the top panel results in a frequency shift which when subtracted leaves the residuals in the bottom panel.

While the amplitude of the ephemeris error is a function of the telescope beam position as well as the positional offset of the pulsar, if one considers position offsets along the ecliptic, i.e., $\gamma = \{0, \pi\}$, then the extreme case, $\delta t_{err} = \epsilon R_{\oplus} \sin\phi$, occurs for all ecliptic latitudes. Consequently, to maintain maximum sensitivity over the telescope beam it is sufficient to require $\epsilon R_{\oplus} < T_{sample}/2$. However, it is worth noting that the necessary condition to maintain sensitivity is strongly dependent on $\phi - \phi_0$. For example, transforms of less than 52 days have a maximum ephemeris error that is an order of magnitude less at $\lambda_{\oplus} = \lambda_{psr} + \phi_0 \pmod{\pi}$ than at $\lambda_{\oplus} = \lambda_{psr} + \phi_0 + \pi/2 \pmod{\pi}$. In Figure 4.4 we show the minimum and maximum one-sided deviation of the ephemeris error from a linear phase drift.

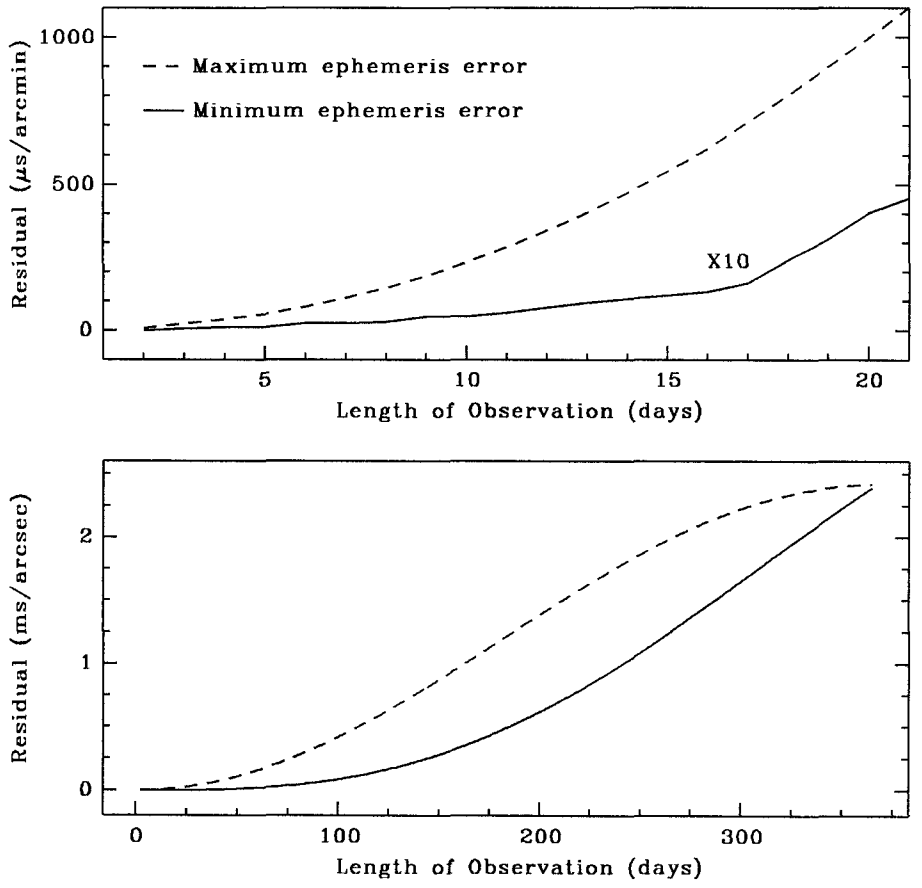

Figure 4.4: Ephemeris error in searching for a millisecond pulsar that is not located at the beam center. Both the minimum and maximum effect are shown, the large difference reflecting a strong dependence on the relative heliocentric longitude of the putative pulsar.

Binary Motion in Coherent Search

There are three types of binary systems that can be detected without loss of sensitivity in a multiple day transform. The first case is when the reflex motion is less than half a pulse period (150 km for $P = 1$ ms), e.g., planetary systems like PSR 1257+12 (Wolszczan 1992). The second case is when the orbit is sufficiently wide that the constraint in § 4.3.3 is satisfied, i.e., $|a_l| < 4.0 \times 10^{-3}\,\mathrm{cm\,s^{-2}}/n_{day}^2$. The third case is where the Keplerian orbital parameters of the companion star are known *a priori*, as is the case in searching for pulsations from the companion star to PSR 2127+11C (see § 4.3.4). While not attempted yet, the second case may be extended to search for more realistic binary systems,

such as the 256 day binary pulsar 1310+18A, by extending the constant acceleration search used to discover PSR 2127+11C to the gigapoint transforms necessary for a multiple day search.

4.3.4 PSR 2127+11C Companion Search

As argued in Prince *et al.* (1991) (see Chapter 3), and indicated by the large mass found in § 4.5, the companion to PSR 2127+11C is most probably another neutron star. Consequently, we have searched for radio emission from the companion star. Our flux limit for pulsed radiation beamed towards Earth at 430 MHz is 250 μJy for $P > 10$ ms (the drop off in sensitivity for 1 ms $< P <$ 10 ms may be found in Figure 4.15). The *a priori* probability of a neutron star companion being a detectable pulsar is $\sim 4/N_{\rm ns}$, where 4 is the number of pulsars in M15 that are above our single day detection threshold and beamed towards Earth, i.e., PSR 2127+11A–D, and $N_{\rm ns}$ is the number of neutron stars in M15 when the binary system 2127+11C was formed. While this probability is only $\mathcal{O}(10^{-3}$–$10^{-4})$, the wealth of information provided by such a system makes a search worth the effort. For example, the measurement of a single relativistic parameter, $\dot{\omega}$, would determine both the stellar masses, leaving the second readily measured relativistic parameter, γ, as a precise check on general relativity. This method has the advantage of not relying on an orbital period decay measurement, $\dot{P}_b$, which can be corrupted by acceleration of the binary system in the cluster potential, or as in the case of PSR 1913+16, acceleration in the Galactic potential (Damour and Taylor 1991).

There are three basic approaches to searching for the companion "pulsar": 1) a general acceleration search (see § 4.3.1); 2) a "stack" search (see § 4.3.2); and 3) a "Keplerian" orbit search described below. An initial flux limit for the companion star was established by the acceleration search which discovered PSR 2127+11C (Anderson *et al.* 1990b, see Chapter 2). Since the instantaneous orbital acceleration of the companion star is opposite in sign and within 50% of the magnitude of that observed for PSR 2127+11C (as determined from the mass limits in § 4.5), a flux limit slightly less than the flux of PSR 2127+11C may be placed on pulsations with periods similar to or larger than PSR 2127+11C. However, that acceleration search was significantly less sensitive to millisecond pulsations. To extend the search down to millisecond periods requires the use of either of the other two search strategies mentioned above. However, given the *a priori* knowledge of the orbit being searched,

which the stack search may only partially utilize, the Keplerian search is significantly more sensitive (see Appendix C).

To perform a search that reaches the flux limit imposed solely by the amount of observing time and maintain sensitivity to millisecond pulsations requires a precise timing model for the companion star. In particular, it is necessary to know the five Keplerian parameters governing its orbital motion. Of these, four are determined directly from the orbit of PSR 2127+11C: $\{T_0, P_b, e, \omega_0\}_{psr} \rightarrow \{T_0, P_b, e, \omega_0 - \pi\}_{companion}$, however, the size of the companion orbit is determined by the relative stellar masses, $a_c \sin i = (m_p/m_c)\, a_p \sin i$. Consequently, a one-dimensional search over assumed $a_c \sin i$ was performed. Using the constraints on the mass ratio found in § 4.5 we generated 450 trial time series in the rest frame of the companion star for the range $1.56\,\mathrm{ls} < a_c \sin i < 3.22\,\mathrm{ls}$, and subjected them to a standard isolated pulsar search algorithm. This extends the flux limit for pulsed radiation beamed towards earth down to rotation periods of a few milliseconds at a level approximately that shown for a single day transform in Figure 4.15.

4.3.5 Halo Search

Based on the discovery that PSR 2127+11C had been ejected from the core of M15 to a radius of $\sim 1'$ (Prince *et al.* 1991, see Chapter 3) a search was performed in collaboration with S. Kulkarni, T. Prince, and A. Wolszczan for additional ejected binaries pulsars by observing two concentric hexagonal rings around the core of M15. The first ring consists of 6 pointings at a radius of $\sim 5'$ from the core. The second ring consists of 9 pointings at a radius of $\sim 15'$. This corresponds to coverage out to the $20'$ tidal radius of M15, with no more than a 50% reduction in sensitivity at any one point. Each of these 15 pointings was observed at least once for between 69 and 138 minutes. Currently, slightly more than half of these beams have been searched for isolated and binary pulsars by performing a sweep over the observed dispersion measure range of the core pulsars orthogonal to a constant acceleration parameter search for binary pulsars (and a limited second order binary search to follow up on candidate signals). No significant detections have been made beyond the attenuated signals of the core pulsars. See Figure 4.15 for the resulting flux limit from isolated pulsars. The corresponding limits for binary pulsars is not well determined; however, we note that PSR 2127+11C would have been readily detected in any of the beams searched.

4.3.6 Optical Pulsation Search

As part of a more general search for optical variables in M15 carried out in collaboration with P. Gorham, S.R. Kulkarni, and T.A. Prince, the core region was observed with the 60″ Palomar telescope using a photon-counting camera capable of time tagging individual photon arrival times to 1 μs. To verify the time resolution and imaging capabilities of the camera, a 75 minute observation of the crab pulsar was made at 11:17 UT on 3 October 1991 through a Schombert B filter. For 210 s integrations a clean profile was generated with TOA rms residuals of 22 μs.

The data considered here consists of a 6.2 hr integration thru a Schombert U filter taken on 11 July 1991. A 1″.5 radius area was extracted for each of the 8 pulsar radio positions (Table 4.3). The topocentric photon arrival times were corrected to corresponding arrival times at the SSB and synchronously folded according to the 8 separate timing models in § 4.4 and § 4.5. No significant pulsed emission was seen, implying a magnitude limit of $U = 24$ for optical emission from the 8 pulsars 2127+11A–H.

4.4 Timing of the Isolated Pulsars: PSR 2127+11A,B,D–H

In this section we discuss the results of pulse time of arrival (TOA) measurements for the 7 isolated pulsars in M15. The pulsar spin parameters (Table 4.2) and timing positions (Table 4.3) are generated using the TEMPO pulsar timing program to convert topocentric pulse time of arrival (TOA) measurements into a timing model for the pulsar in the solar system barycenter (SSB). Individual pulse profiles are formed by folding the observed autocorrelation functions according to an initial timing model. Various filters were applied to maximize the signal to noise, including: radar interference rejection, zenith angle weighting to account for the significant ground illumination of the Arecibo telescope at high zenith angles (both a drop in sensitivity and a gain in noise), and radio frequency weighting according to the measured signal to noise squared variation across the observed 10 MHz band pass (as determined from PSR 2127+11A). The frequency dependent arrival time delays due to propagation through the free electrons in the interstellar medium were removed using the dispersion measure values given in Table 4.2 by Fourier interpolation to avoid resampling the data.

Integration times were empirically determined by requiring sufficient signal to noise

TABLE 4.2

Observed Parameters for PSR 2127+11A–H

Pulsar	Pulse Period† P (ms)	Period Derivative $\dot{P}$ (10^{-18} s s^{-1})	DM‡ (cm^{-3} pc)	Flux* (mJy)
A	110.6647087715 (6)	−21.07 (3)	0.06 (5)	1.70
B	56.1330335727 (12)	9.56 (6)	0.44 (12)	1.00
C	30.5292951283 (6)	4.991 (25)	−0.12 (5)	.64
D	4.8028043457 (3)	−1.075 (12)	0.03 (21)	.34
E	4.65143521539 (13)	0.178 (7)	−0.74 (12)	.24
F	4.02704270710 (15)	0.032 (8)	−1.73 (15)	.14
G	37.660166953 (8)	1.95 (45)	−0.82 (24)	.13
H	6.7433942397 (3)	0.024 (13)	−0.10 (12)	.16

Numbers in parentheses are the formal 3σ uncertainties in the last digit quoted.

† Periods measured at epoch JD = 2447633.02 in the Ephemeris DE 200.

‡ Dispersion measure relative to the nominal cluster value defined to be 67.25 cm^{-3} pc.

* The mean 430 MHz flux densities are scaled relative to PSR 2127+11A with an assumed value of 1.7 ± .4 mJy (Wolszczan *et al.* 1989b). The estimated precision is 10% for PSR 2127+11B–E and 20% for PSR 2127+11F–H.

to enable a TOA measurement by shifting the 65 hr integration template profiles (see Figure 4.1) with a Fourier interpolation algorithm to maximize the correlation with the observed profiles. The integration times selected are: 11.5 m for PSR 2127+11A,C; 23 m for PSR 2127+11B,E; and complete observation (average 62 m) for PSR 2127+11D,F,G,H.

The precision of arrival time measurements for complete observation integrations varies from 15 μs for PSR 2127+11A to 560 μs for PSR 2127+11G. It is interesting to note that if the pulse period of PSR 2127+11G where much lower ($P \lesssim 4$ ms) multiple observation integrations would be required to avoid random pulse numbering errors. As a test for systematic timing errors we show the decrease in post-fit TOA residuals as a function of integration time in Figure 4.6. The data follow the expected $t^{-1/2}$ behavior of statistically independent measurements.

The spin parameters for the 8 pulsars in Table 4.2 are calculated in the Jet Propulsion Laboratory DE200 planetary ephemeris and J2000 coordinate system. In Table 4.3 we present both the B1950 positions (using the Center for Astrophysics PEP740R ephemeris) and the J2000 positions (using the DE200 ephemeris). The determination of relative posi-

TABLE 4.3

Timing Positions for PSR 2127+11A–H

PSR	PEP740R/B1950		DE200/J2000		Cluster Position†			Radius‡
	$21^h\,27^m+$	$11^\circ\,56'+$	$21^h\,29^m+$	$12^\circ\,09'+$	α	δ	R_c	(pc)
A	$33^s.225\,(1)$	$49''.48\,(2)$	$58^s.247\,(1)$	$61''.30\,(2)$	$-0''.92$	$+0''.57$	$1''.08$	0.053
B	33.608 (3)	48.49 (6)	58.630 (3)	60.33 (6)	+4.69	−0.40	4.71	0.231
C	36.188 (3)	86.27 (4)	61.205 (3)	98.22 (4)	+42.45	+37.49	56.63	2.770
D	33.251 (7)	47.92 (13)	58.274 (7)	59.74 (13)	−0.53	−0.99	1.12	0.055
E	33.166 (4)	56.81 (8)	58.187 (4)	68.63 (8)	−1.80	+7.90	8.10	0.397
F	32.157 (5)	51.14 (10)	57.178 (5)	62.91 (10)	−16.60	+2.18	16.74	0.820
G	32.926 (30)	45.45 (60)	57.948 (30)	57.26 (60)	−5.31	−3.47	6.34	0.311
H	33.161 (5)	47.61 (10)	58.184 (5)	59.43 (10)	−1.85	−1.30	2.26	0.111

Note: Numbers in parentheses are uncertainties in the last digit quoted.

† Positions and radii relative to the cluster core (see text): $21^h\,29^m\,58^s.310$, $12^\circ\,10'\,00''.73$ (J2000).

‡ Projected radial position for the 10.0 kpc($1'' \rightarrow .049$ pc) distance estimate to M15 in Phinney (1992b) derived from Fahlman, Richer, and VandenBerg (1985)—Phinney (1992b) notes that the 12.8 kpc distance estimate in Lauer *et al.* (1991) from the same reference does not correct the apparent distance modulus for optical extinction.

tions to the cluster core is discussed in § 4.6.1. In Figure 4.5 we show the post-fit timing residuals for PSR 2127+11A–H as a function of observation epoch.

4.5 Timing of the Binary Pulsar: PSR 2127+11C

4.5.1 Doppler Fitting

In the case of binary pulsars, it is necessary to have an initial model of the orbit before precise pulse time of arrival analysis may be attempted. As an example, consider the parameter $a_1 \sin i$ which measures the projected semi-major axis of the orbit. In the case of PSR 2127+11C, the propagation time across the projected orbit is 144 radio pulses. Consequently, one needs to know $a_1 \sin i$ to $\sim$ 1:100 to unambiguously number the pulses. The initial Keplerian parameters are determined by a fit to the Doppler shifted pulse periods, i.e., a fit to pulsar velocity, while the more accurate relativistic orbit is determined from a fit to observed pulse arrival times, i.e., a fit to pulsar position.

The initial Doppler fitting for PSR 2127+11C was reported in Anderson *et al.* (1990b) (see Chapter 2) and is similar to the analysis of single line spectroscopic binaries.

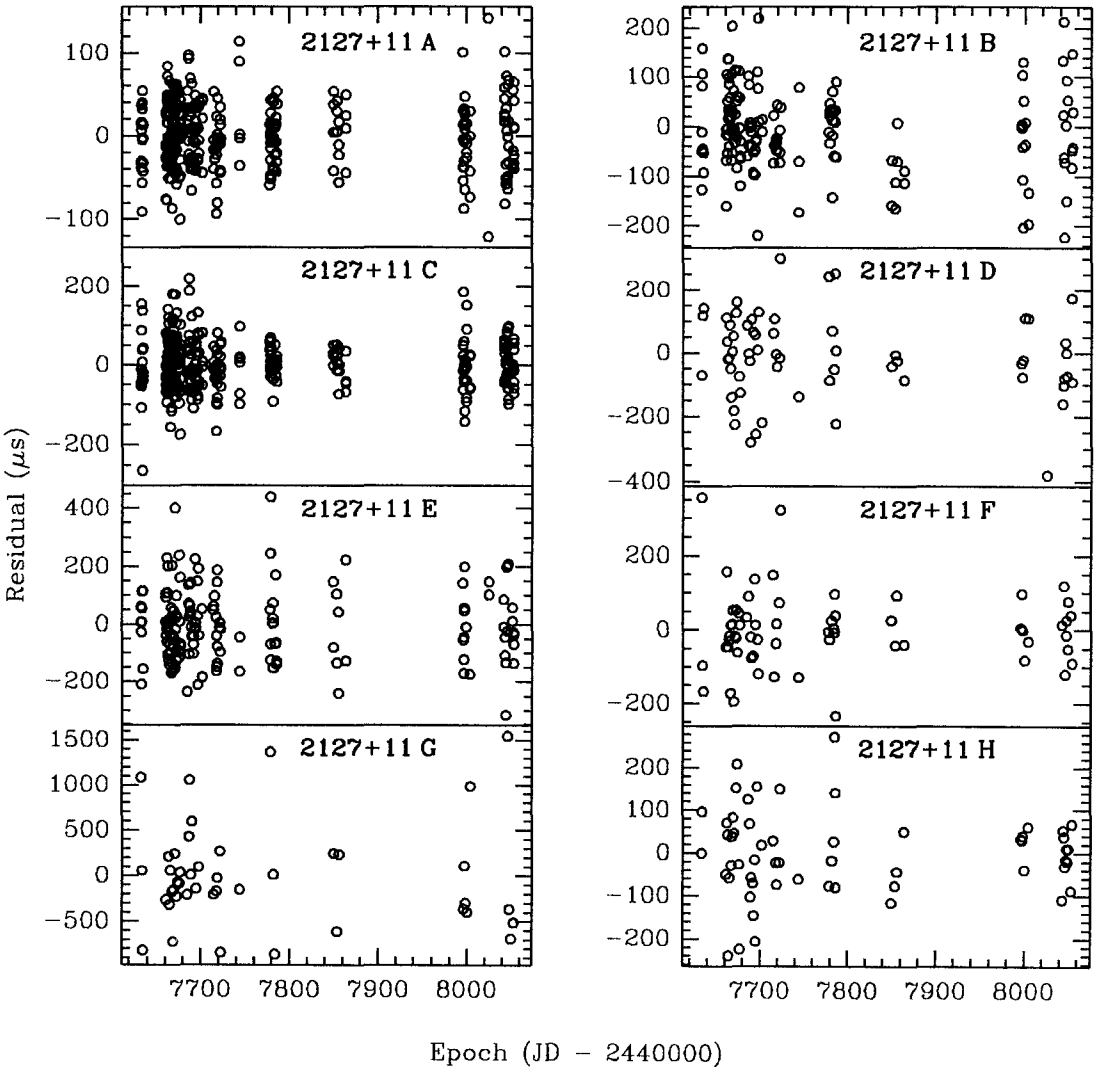

Figure 4.5: Timing residuals for PSR 2127+11A–H as a function of observation epoch. Integration times are 11.5 m for PSR 2127+11A,C; 23 m for PSR 2127+11B,E; complete observation (average 62 m) for PSR 2127+11D,F,G,H.

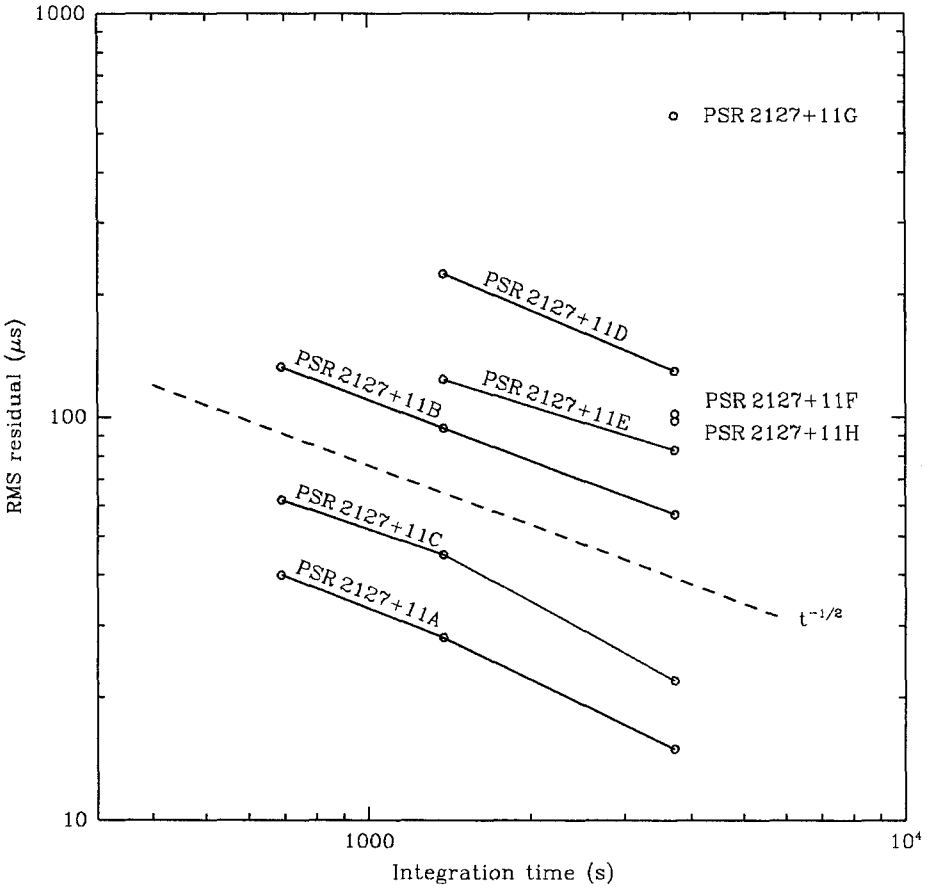

Figure 4.6: Timing residuals for PSR 2127+11A–H as a function of integration time.

Individual period/velocity measurements are obtained by searching for a Doppler shifted signal near the nominal pulse period in a sequence of short time segments. For PSR 2127+11C the signal detection was complicated by the long integration times (524 s) required to make a reliable detection. This is a large enough fraction of the orbit that the pulsar can no longer be treated as a periodic signal in the SSB. To obtain the data points in Figure 4.7 it was necessary to perform a one-dimensional search (higher dimensions are required near periastron) for a linearly drifting Doppler frequency, or equivalently a constantly accelerating signal source (see § 4.3.1).

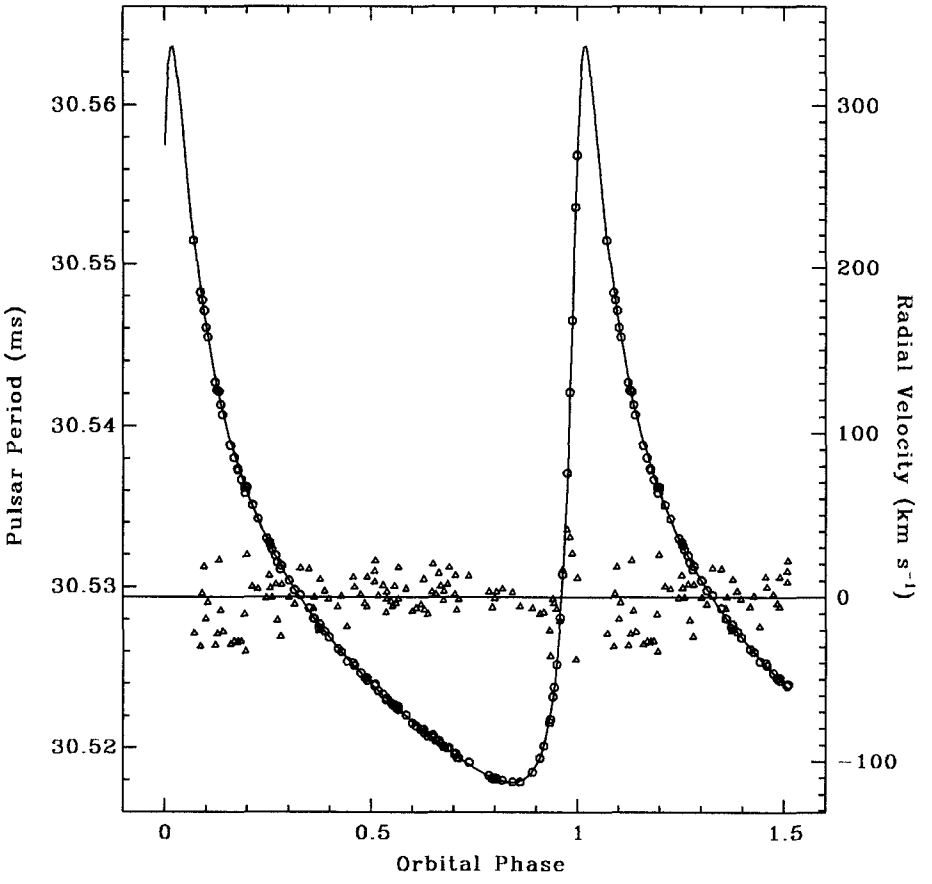

Figure 4.7: Doppler fit to the Keplerian parameters of PSR 2127+11C. Triangles denote post-fit residuals multiplied by 10.

4.5.2 Relativistic Orbit

The basic model used in our timing analysis of PSR 2127+11C is the highly theory-independent solution to the relativistic two point-mass orbit derived by Damour and Deruelle (1986), hereafter DD. In addition we calculate a timing solution using a variation of the DD model that explicitly assumes general relativity is the correct theory of gravity (Taylor and Weisberg 1989), hereafter DDGR. The relationship between solar system barycentric time and pulsar proper time is given by

$$t_b - t_0 = T + \Delta_R + \Delta_E + \Delta_S + \Delta_A.$$

Where the Roemer delay Δ_R refers to the geometrical propagation time across the binary orbit, the Einstein delay Δ_E refers to the effects of gravitational redshift and transverse Doppler shift, the Shapiro delay Δ_S refers to the excess time delay in propagating through the curved space around the companion star, and the aberration delay Δ_A refers to rotation effects of the pulsar. Of these, only Δ_R and Δ_E are observed for PSR 2127+11C. The expected magnitudes of the Δ_S term is $7\,\mu$s, well below the $62\,\mu$s individual TOA measurement precision for PSR 2127+11C.

Figure 4.8 shows the timing residuals for the DDGR timing model with parameters listed in Table 4.4. Figure 4.9 shows the resulting constraints on the pulsar and companion masses.

TABLE 4.4

Orbital Parameters for PSR 2127+11C

Keplerian		
Orbital period	P_b	28968.3697(3) s
Projected semi-major axis	$a_1 \sin i$	2.5183(12) ls
Eccentricity	e	0.681386(16)
Epoch of periastron	T_0	2447632.4672049(15) JD
Longitude of periastron	ω_0	316°.36(3)
Relativistic		
Apsidal motion	$\dot{\omega}$	4°.460 yr^{-1} §
		4°.463(5) yr^{-1}
Einstein delay	γ	4.859 ms §
		4.9(1.1) ms
Orbital period decay	$\dot{P}_b$	-3.937×10^{-12} s s^{-1} §
		$< 20 \times 10^{-12}$ s s^{-1}
Total mass	$M \equiv m_p + m_c$	2.712(5) $M_\odot$
		2.712 $M_\odot$ §
Companion mass	m_c	1.37(23) $M_\odot$
		1.37 $M_\odot$ §

The Keplerian parameters are the timing solution for the DDGR timing model with the JPL DE200 planetary ephemeris in J2000 coordinates. Numbers in parenthesis are the formal 3σ error in the last digit(s). The two values for the relativistic parameters correspond to the DDGR and DD timing models, respectively.

§ Parameter not fit for—determined from timing solution.

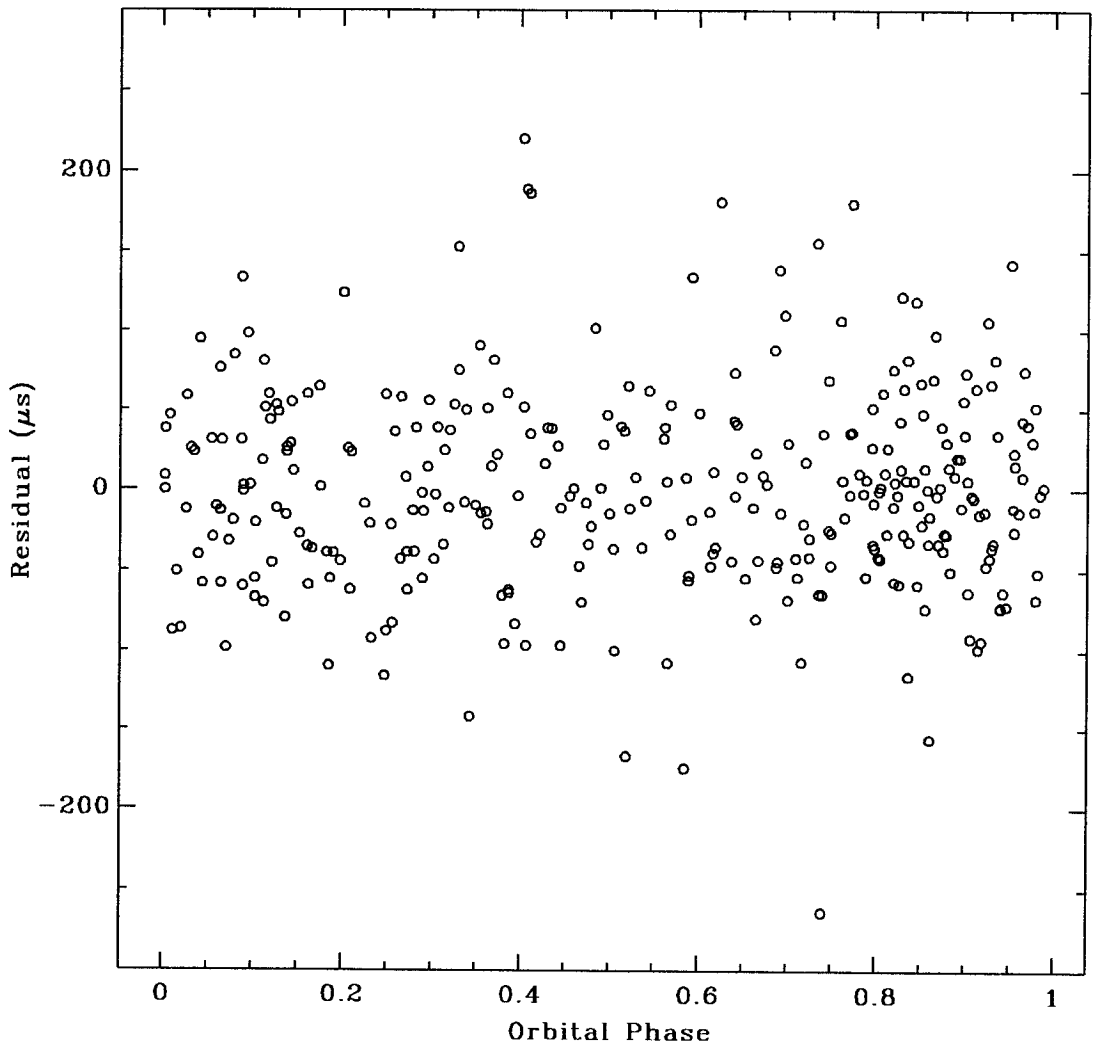

Figure 4.8: Post-fit timing residuals from the DDGR timing model of PSR 2127+11C as a function of orbital phase for 689 s integrations.

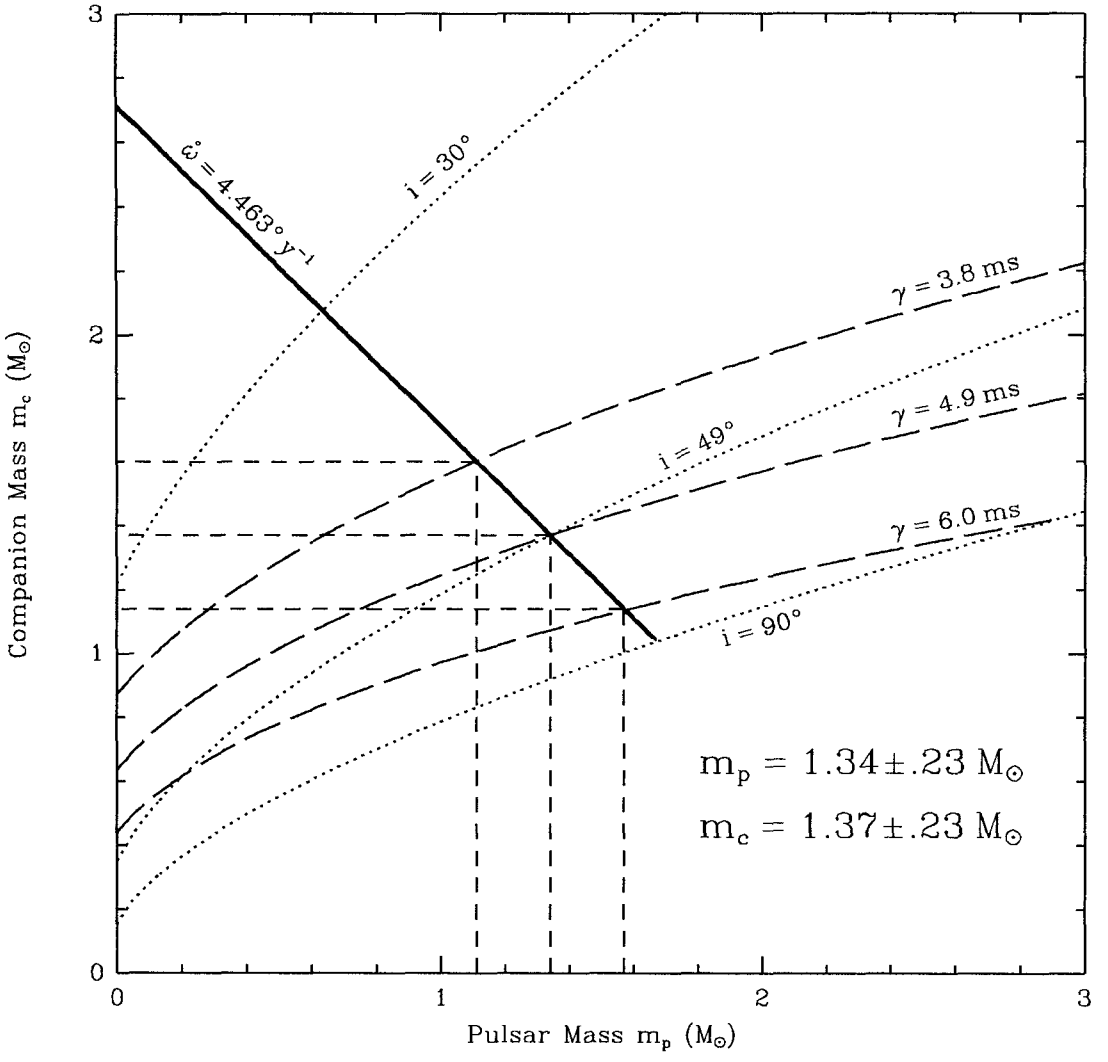

Figure 4.9: Constraints on the pulsar and companion masses in the 2127+11C system.

4.6 Discussion

4.6.1 Pulsar Positions

To use the precise timing information of PSR 2127+11A–H to probe the internal structure of the globular cluster M15, it is necessary to have an accurate frame-tie between the optical measurement of the core position and the timing positions of the pulsars. Since the 8 pulsars in M15 are not optically visible (§ 4.3.6) a direct comparison may not be made. However, the optical counterpart of the X-ray binary, AC211 (Aurière, Le Fèvre, and Terzan 1984), offers an indirect frame-tie—being visible in both the optical and radio bands. An image of M15 taken with the Hubble Space Telescope (HST) has been analyzed to determine the cluster core radius ($r_c = 2''.2$) and relative position of AC211 to within $0''.06$ (Lauer *et al.* 1991). Two measurements of the position of AC211 have been made with the Very Large Array (VLA) (Kulkarni *et al.* 1990; Johnston, Kulkarni, and Goss 1991). The frame-tie between pulsar timing positions and VLA imaging positions has been extensively studied. See Fomalont *et al.* (1992) for a recent study of 40 pulsars positions with the VLA, and Backer *et al.* (1985) for a detailed comparison of VLA and timing positions for PSR 1913+16 and PSR 1937+21. The core position of M15 was found by rotating the average VLA position of AC211 in the FK4 B1950 coordinate system to epoch J2000 according to the prescription in Appendix 2 of Aoki *et al.* (1983). This position may be directly compared with the pulsar timing positions based on the DE200 ephemeris in J2000.0 coordinates. See Backer *et al.* (1985) and Bartel *et al.* (1985) for a discussion of the relative orientations of planetary ephemerides. The resulting M15 core position is $21^h\,29^m\,58^s.310$, $12^\circ\,10'\,00''.73$ (J2000), with an estimated uncertainty of $\sim 0''.3$ from the $0''.23$ difference between the two VLA measurements of AC211 and the HST uncertainty of $0''.06$.

In Figure 4.10 we show the positions of the eight pulsars in M15 superimposed on B-band CCD image of M15 taken with the $60''$ Palomar telescope. In Figure 4.11 we show the positions of PSR 2127+11A,B,D,G,H superimposed on the HST U-band optical image of the core of M15 (Lauer *et al.* 1991).

From the observed radial distribution of isolated pulsars it is possible to estimate the number of neutron stars and white dwarfs formed in M15, as well as statistically determine the mass of the isolated recycled neutron stars. In Figure 4.12 we show the observed radial position histogram, where the dashed line denotes an empirical fit to a pulsar density distribution, $n_p \propto r^{-3}$, corresponding to $N_p(< r)$ linear in $\log r$.

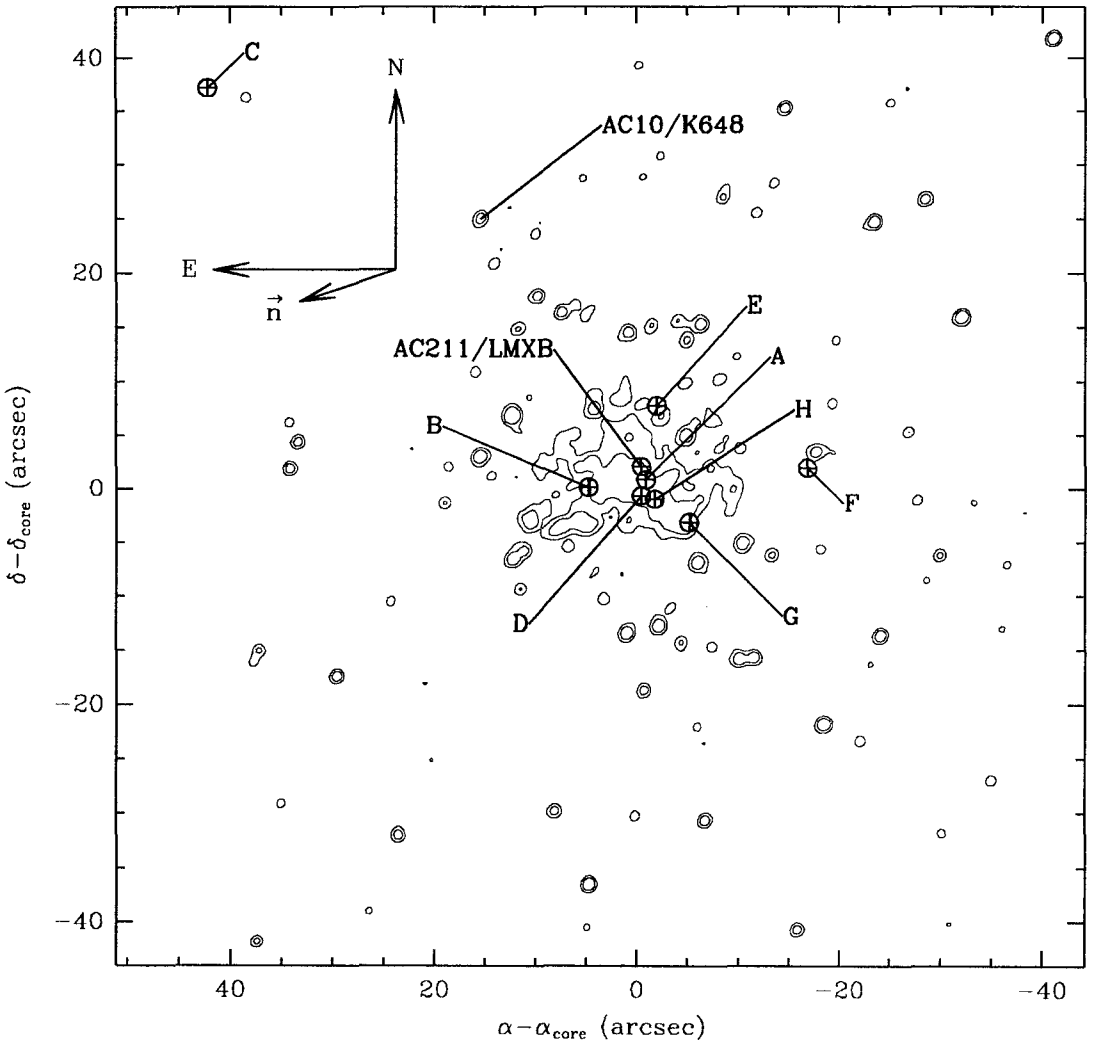

Figure 4.10: CCD image of M15 taken with the 60″ Palomar telescope at B-band with the timing positions of the 8 pulsars superimposed. The direction $\vec{n}$ is parallel to an observed dispersion measure gradient (see §4.6.5). The positions of the planetary nebula (AC10/K648) and low-mass X-ray binary (AC211) are also shown.

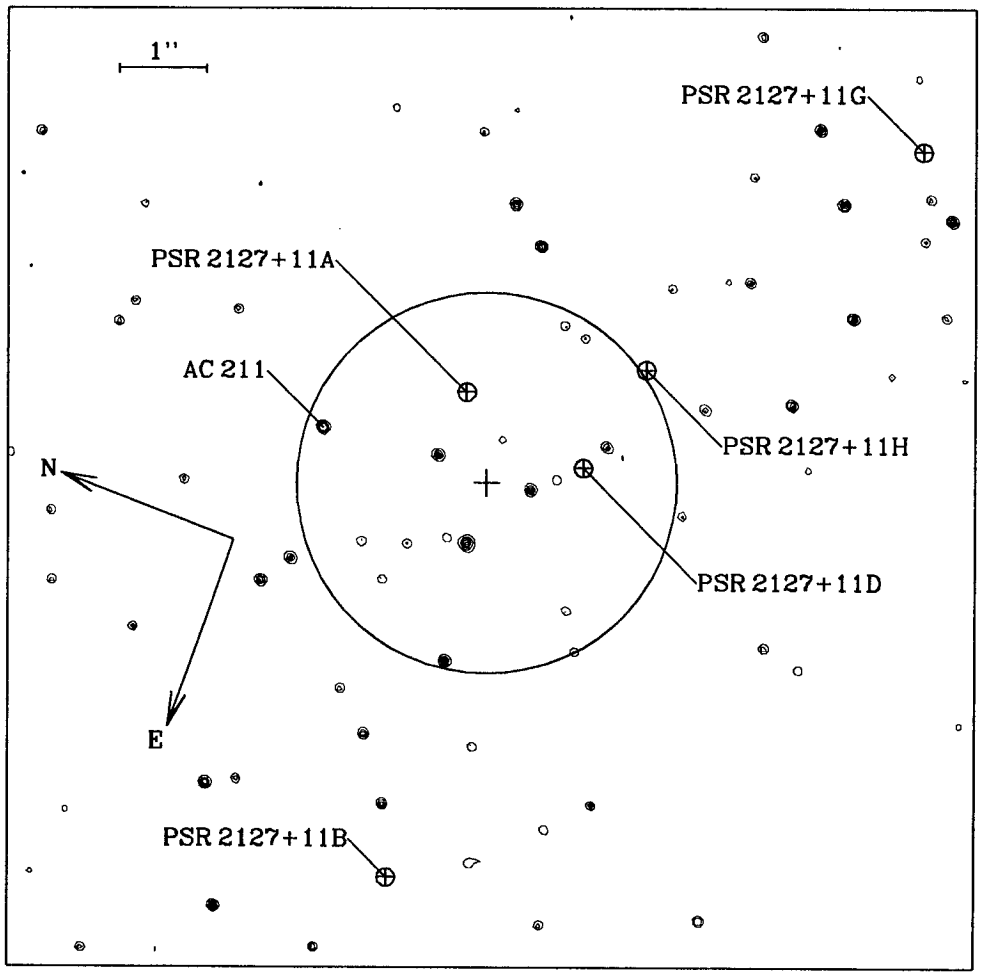

Figure 4.11: Hubble Space Telescope image of the central region of M15 (Lauer *et al.* 1991) taken at U-band with the positions of PSR 2127+11A,B,D,G,H, the low-mass X-ray binary (AC211), and the core radius of 2″.2 superimposed.

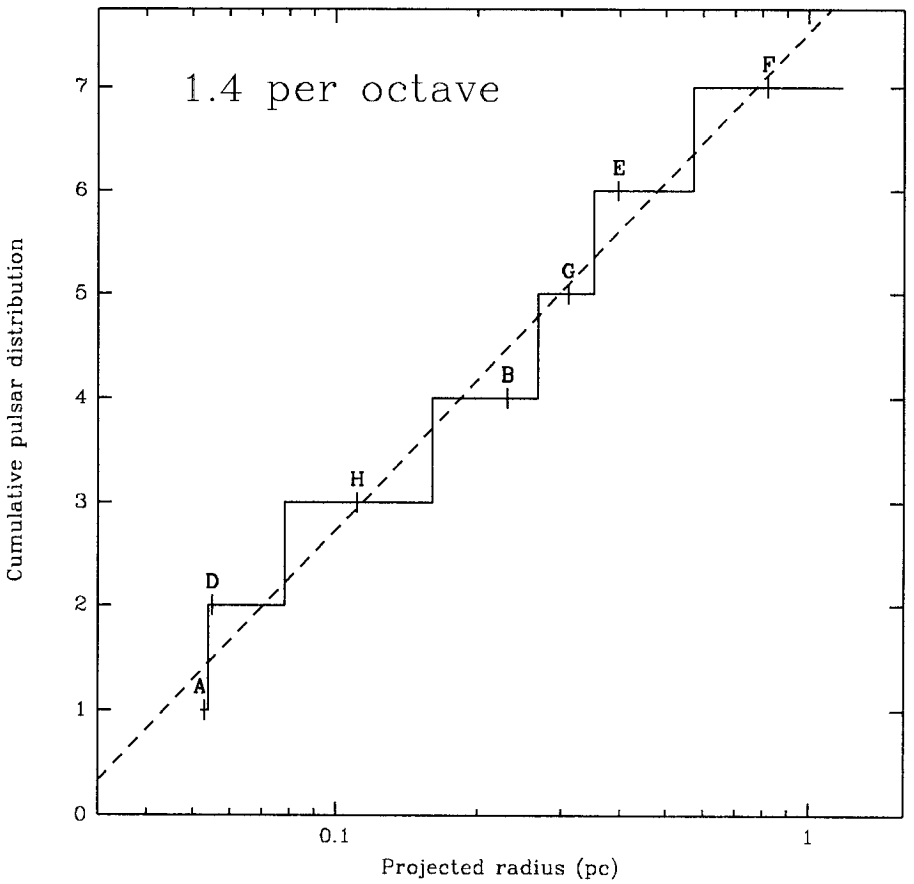

Figure 4.12: Radial position histogram for the seven "core" pulsars 2127+11A,B,D–H. The dashed line is an empirical fit to an equal population of pulsars per logarithmic interval of projected radius.

Such an observed distribution is in good agreement with stellar dynamics and provides the first mass measurement of isolated recycled pulsars, albeit a statistical one, similar to the measurement of globular cluster X-ray source masses by Grindlay *et al.* (1984). Since these core pulsars all have minimum characteristic ages in excess of 5×10^7 yr (Table 4.2) they should be in statistical equilibrium with the other mass species in the core of M15, where the two-body gravitational relaxation time is $\lesssim 10^7$ yr (Webbink 1985). Under the assumption that the core is in isothermal equilibrium, the spatial density of any such equilibrated mass species scales like $e^{-\Phi/\sigma^2}$, where Φ is the gravitational potential and σ is the velocity dispersion (Binney and Tremaine 1987). The equipartition of kinetic

energy implies that $\sigma_p^2/\sigma_t^2 = m_t/m_p$, consequently, the pulsar density should scale like $n_p \propto n_t^{m_p/m_t}$, where n_t, m_t refer to the current main sequence turnoff stars ($0.7\,M_\odot$) that are dominating the light profile of M15. From the observed optical light profile, indicating $n_t \propto r^{-\nu}$ with $\nu = 1.56+0.043(\ln\theta)^2$ (Phinney 1992a, and references therein), it follows that the pulsar density near the core should scale as $n_p \propto r^{-\alpha}$, where $\alpha = 1.56(m_p/m_t)$. The observed $\alpha = 3$ implies that $m_p \simeq (3/1.56)0.7\,M_\odot = 1.35\,M_\odot$, a value consistent with most theories of recycled pulsar formation, and remarkably similar to the other two neutron star mass determinations in M15—$(1.34, 1.37) \pm .23\,M_\odot$ for PSR 2127+11C and its companion (see § 4.5).

As discussed in Phinney (1992a) and Phinney (1992b), for the central region of M15 under the assumption of isothermal equilibrium, the dominant mass species should scale as $n_d \propto r^{-2}$, with lighter species having a shallower distribution, and more massive species a steeper one. Consequently, with the observed $n_p \propto r^{-3}$ and $n_t \propto r^{-1.56}$ in the core region (with n_t not rising to the dominant mass species until $\theta \simeq 25''$) there must be an intermediate dark mass component, presumably massive white dwarfs. Phinney (1992b) concludes that the initial mass function (IMF) in M15 must have been at least as flat as the Salpeter IMF ($dN/dm \propto m^{-2.35}$) and consequently, that at least 10^4 neutron stars were formed in M15—with some unknown fraction being ejected from the cluster at birth. The difference between this estimate and the estimated $\mathcal{O}(100)$ currently observable isolated pulsars in M15 (see § 4.6.4) gives an indication of the pulsar recycling efficiency in M15—subject to one or more of the following poorly understood effects: luminosity cutoff, fraction of neutron stars ejected from the cluster at birth, beaming fraction, and binary fraction.

4.6.2 Pulsar Accelerations

From the observation of anomalous pulsar spin down rates of PSR 2127+11A,D it is possible to place distance independent limits on the central density and mass-to-light ratio in the core of M15. The analysis of the observed period derivatives follows closely the analysis in Phinney (1992a) and Phinney (1992b), where similar limits are inferred from the negative period derivatives of PSR 2127+11A,D. In Appendix D we calculate the line of sight acceleration probability distribution for the observed pulsar spatial density, $n_p \propto r^{-3}$ (see § 4.6.1), and note that it agrees to within a few percent with the "rule of thumb" calculated in Phinney (1992a) for $n_p \propto r^{-2}$. Consequently, either distribution gives similar

results in the following discussion.

Phinney (1992a) established the "rule of thumb" that to within 10% for reasonable cluster models,

$$\frac{\max|a_l(R_\perp)|}{c} \simeq 1.1\frac{GM(<R_\perp)}{c\pi R_\perp^2} = 5.1\times10^{-16}\left(\frac{\bar{\Sigma}(<R_\perp)}{10^6\,M_\odot\,\mathrm{pc}^{-2}}\right)\mathrm{s}^{-1}, \tag{4.3}$$

where $\max|a_l(R_\perp)|$ is the maximum line of sight acceleration at a projected distance $R_\perp$ from the cluster center and $\bar{\Sigma}(<R_\perp)$ is the mean surface density within $R_\perp$. From the observed negative spin period derivative ($\dot{P}$) of PSR 2127+11D at a radius of 1.″1 (and the assumption of an intrinsic positive $\dot{P}$) it follows that maximum line of sight acceleration ($\max|a_l|/c$) at $R_\perp = 0.055\,\mathrm{pc}$ is at least as large as $2.24\times10^{-16}\,\mathrm{s}^{-1}$. Consequently, Equation 4.3 implies that $\bar{\Sigma} > 4.4\times10^5\,M_\odot\,\mathrm{pc}^{-2}$ and Equation D.1 implies that $M(<.055\,\mathrm{pc}) > 1.9\times10^3\,M_\odot$, or a central density of $\rho_c > 2.7\times10^6\,M_\odot\,\mathrm{pc}^{-3}$. From the observation of the core region with the Hubble Space Telescope (Lauer *et al.* 1991) a central surface brightness in the U-band of $\Sigma_{c,U} = 2.3\times10^5\,L_{\odot,U}\,\mathrm{pc}^{-2}$ may be inferred (Phinney 1992b). Consequently a lower limit to the central mass-to-light ratio at U-band may be set at $M/L_U > 1.9\,M_\odot\,/\,L_{\odot,U}$ (since the U-V color of M15 is similar to the Sun this should also apply in V-band).

The expected value of $\max|a_l(R_\perp)|$ at the 1.″1 radius of PSR 2127+11A,D is 1.5 times the average observed magnitude of acceleration (see Appendix D). Consequently, the estimates for core parameters in M15 are: $\bar{\Sigma} \simeq 6.1\times10^5\,M_\odot\,\mathrm{pc}^{-2}$, $M(<.054\,\mathrm{pc}) \simeq 2.6\times10^3\,M_\odot$, $\rho_c \simeq 3.7\times10^6\,M_\odot\,\mathrm{pc}^{-3}$, and $M/L_U \simeq 2.7\,M_\odot\,/\,L_{\odot,U}$.

To extend these core estimates out to the larger radii of the other pulsars Equation 4.3 is related to the observed visual surface brightness of M15 in Phinney (1992a),

$$\frac{\max|a_l(\theta)|}{c} = 8\times10^{-17}\,\theta^{-0.56}\,10^{-0.076(\log_{10}\theta)^3}\,\frac{M_{cyl}}{L_{cyl,V}}, \tag{4.4}$$

where θ is the observed pulsar angular displacement from the cluster core in units of arcsec, and M_{cyl}, $L_{cyl,V}$ are the total mass and visual luminosity in solar units ($M_\odot$, $L_\odot$) within the cylinder centered on the cluster core and extending out to θ. In Table 4.5 we present the maximum line of sight acceleration and implied constraints on magnetic field strength and characteristic ages of PSR 2127+11A–H by assuming the mass-to-light ratio of $2.7\,M_\odot\,/\,L_\odot$ inferred from PSR 2127+11A,D.

The young characteristic ages of PSR 2127+11B,C ($\sim 10^8\,\mathrm{yr}$) are suggestive of a recent surge in recycling activity, as might be expected from the large central density

TABLE 4.5

Acceleration Limits for PSR 2127+11A–H

Radius ($''$)	PSR	$\max \lvert a_l \rvert / c$ ($10^{-16}\,\mathrm{s}^{-1}$)	$\dot{P}/P$ ($10^{-16}\,\mathrm{s}^{-1}$)	B (10^9 G) min	B (10^9 G) max	τ_c(10^8 yr) min	τ_c(10^8 yr) max
1.08	A	3.1	−1.90	—	38	1.3	—
1.12	D	3.1	−2.24	—	1.4	1.8	—
2.26	H	1.4	0.04	—	2.6	1.1	—
4.71	B	.86	1.70	16	28	.62	1.9
6.34	G	.70	0.52	—	13	1.3	—
8.10	E	.59	0.38	—	1.4	1.6	—
16.74	F	.32	0.08	—	0.8	4.0	—
56.63	C	.04	1.63	12.2	12.5	.95	1.0

For PSR 2127+11A,D the maximum line of sight acceleration, $\max \lvert a_l \rvert / c$, is the expected value for the distribution in Appendix D, i.e., 1.5 times their average value. For PSR 2127+11B,E,F,G,H the maximum line of sight acceleration is computed from Equation 4.4 with the estimate of the mass to light ratio of $2.7\,M_\odot / L_\odot$ inferred from the negative $\dot{P}$ of PSR 2127+11A & D at a radius of $1''.1$. For PSR 2127+11C Equation A.6 in Phinney (1992a) is used.

enhancement during an episode of core collapse. Since PSR 2127+11B is a slowly rotating isolated pulsar, it must have undergone at least one close stellar encounter in the last 10^8 yr to remove the presumed mass donor. It is argued in Prince *et al.* (1991) (see Chapter 3) that the current companion of PSR 2127+11C was not the mass donor which recycled the pulsar $\sim 10^8$ yr ago. Consequently, PSR 2127+11C has also undergone at least one collisional interaction in the last 10^8 yr. The remaining six isolated pulsars are consistent with belonging to an old population ($\tau_c \gtrsim 10^9$ yr) of pulsars, indicating that with a large enough detected population, the effects of cluster acceleration may be deconvolved from the intrinsic spin evolution to measure the cluster mass profile.

One diagnostic for interpreting the observed $\dot{P}$'s is the cumulative distribution function of $(\dot{P}/P)/a_{max}(R_\perp)$. The two major components of any such model are $a_{max}(R_\perp)$ and the intrinsic distribution of $\dot{P}/P$. Since,

$$\left(\frac{\dot{P}}{P}\right)_{obs} = \frac{a_l}{c} + \left(\frac{\dot{P}}{P}\right)_{int},$$

the observed distribution of $\dot{P}/P$ is the convolution of the intrinsic distribution with the

distribution of a_l/c (Phinney 1992a). Consequently, if

$$\left\langle \left(\frac{\dot{P}}{P} \right)_{int} \right\rangle \sim \left\langle \frac{a_l}{c} \right\rangle ,$$

corresponding to a characteristic age $\tau_c \sim 10^8\,\mathrm{yr}$ in the core, the two unobserved distributions will have support over the same "length" scale ($\sim 2 \times 10^{-16}\,\mathrm{s}^{-1}$), generating an observed distribution that may not be accurately deconvolved. There are two physical phenomena capable of generating an intrinsic $\dot{P}$ distribution at this length scale: a recent burst of recycling (as might be speculated given the post core collapse nature of M15 and the small $\tau_c \sim 10^8\,\mathrm{yr}$ of PSR 2127+11B,C), or an observational selection effect against old pulsars (as might be expected given the evidence for a correlation between luminosity and $\dot{P}/P^3$ found for recycled pulsars in Kulkarni, Narayan, and Romani (1990)). However, it appears that the six pulsars excluding PSR 2127+11B,C are consistent with a constant birthrate of pulsars in M15 over the $\sim 10^{10}\,\mathrm{yr}$ lifetime of the cluster, and consequently, that it is possible to infer information about a_l directly from the observed $\dot{P}$'s.

In Figure D.1 we show the probability density and cumulative distribution for a_l. In the absence of any intrinsic $\dot{P}$, the distribution of observed $\dot{P}$'s scaled to a model prediction of $a_{max}(R_\perp)$ would follow this distribution. However, as noted above, the actual observed distribution is the convolution of the two probability distributions $\Pr(a_l/c)$ and $\Pr(\dot{P}/P)$. In Figure 4.13 we show the observed distribution as compared to a constant birthrate model during the last $10^{10}\,\mathrm{yr}$. In Figure 4.14 we show the observed distribution as compared to a constant birthrate model during the last $10^9\,\mathrm{yr}$. It is concluded that while two of the eight pulsars in M15 have undergone a recent stellar interaction, the remaining population is consistent with a mass to light ratio of $2.7\,M_\odot\,/\,L_\odot$ and an old population formed uniformly over the age of the cluster.

It is noted, however, that in full cluster models the central mass to light ratio does not remain constant over the range of observed $R_\perp$ for these 7 pulsars. For example, in the model presented in Phinney (1992b) which comfortably explains the radial distribution of observed pulsars and the negative $\dot{P}$'s of PSR 2127+11A,D, the maximum acceleration for PSR 2127+11E,F,G is decreased by $\sim 50\%$ (35% for PSR 2127+11B and 25% for PSR 2127+11H) from that in Table 4.5 and Figures 4.13, 4.14. The result of this is that PSR 2127+11E–H move to the right in Figures 4.13, 4.14 and more closely follow the theoretical curve, while PSR 2127+11B is pushed further out on the tail.

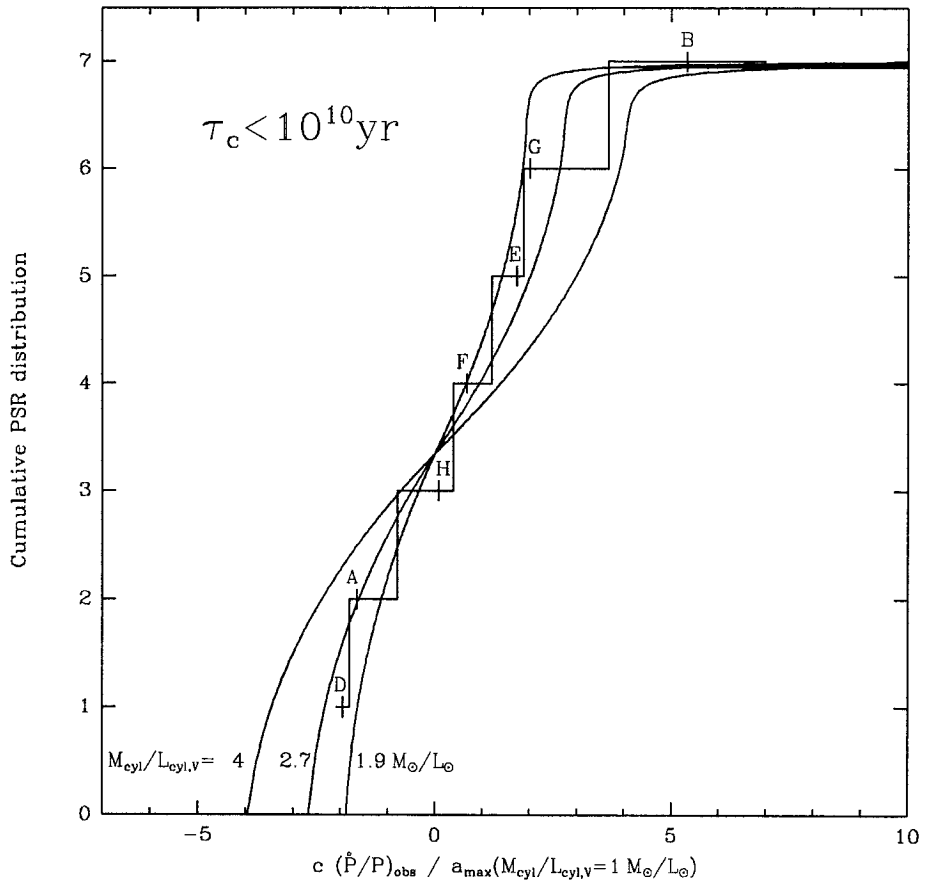

Figure 4.13: Histogram of normalized apparent spin-down rates ($\tau_c < 10^{10}$ yr).

4.6.3 Search Sensitivities and Flux Measurements

Figure 4.15 shows the mean flux densities for PSR 2127+11A–H and the estimated flux limits of our search. The minimum detectable flux may be expressed as (Dewey *et al.* 1984),

$$S_{min} = \beta \left(\frac{T_{rec} + T_{sky}(l,b) + T_{sp}(Z)}{G\sqrt{N_p B t}} \right) \times \sqrt{\frac{w_e}{P - w_e}},$$

where T_{rec} is the receiver excess noise temperature, T_{sky} is the sky background temperature at Galactic longitude l and latitude b, T_{sp} is the spill-over temperature from the fraction of the telescope beam illuminating the ground as a function of zenith angle Z, G is the telescope gain in K/Jy, N_p is the number of polarizations observed, B is the bandwidth of the observations, t is the integration time, and β is the detection threshold. The effective

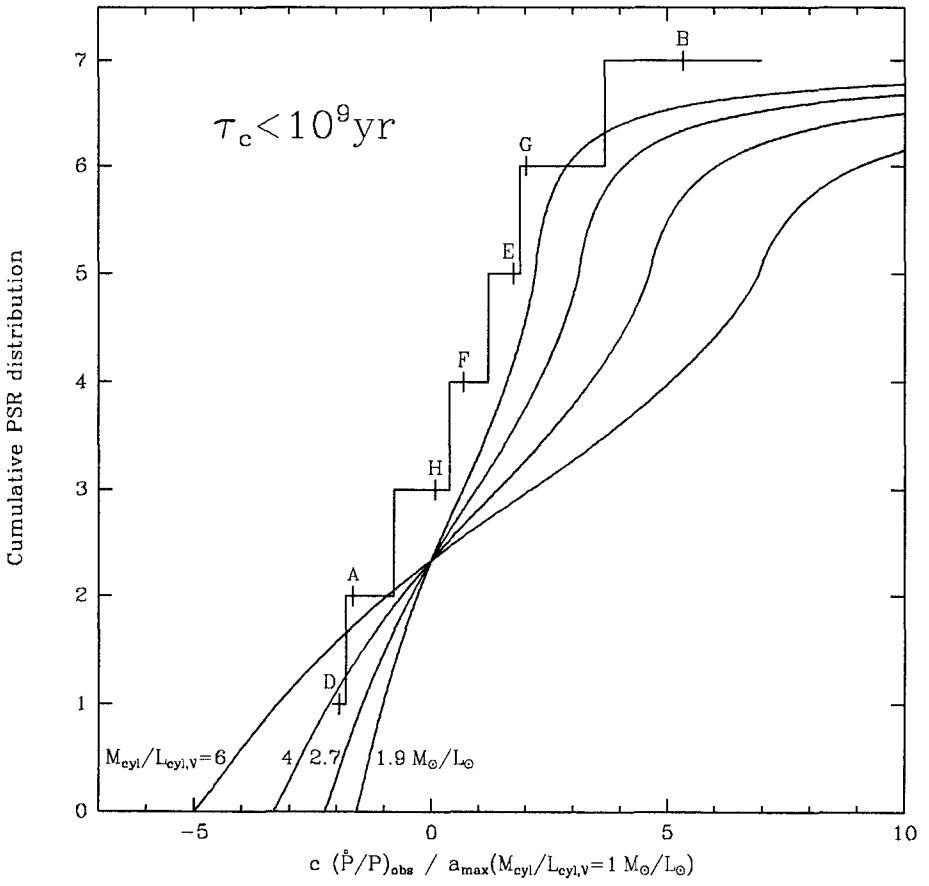

Figure 4.14: Histogram of normalized apparent spin-down rates ($\tau_c < 10^9$ yr).

width, w_e, of a pulse of period P, is given by,

$$w_e^2 = w_0^2 + \tau_{samp}^2 + \tau_{DM}^2 + \tau_{scatt}^2,$$

where w_0 is the intrinsic pulse width, τ_{samp} is the broadening due to the finite sampling time, τ_{DM} is due to dispersion smearing, and τ_{scatt} is due to scattering effects.

In Figure 4.15 we estimate the sensitivity of three separate search strategies, single observation searches, week long, and month long transforms from the following set of observational parameters: $T_{rec} = 80\,\mathrm{K}$, $T_{sky} + T_{sp} = 90\,\mathrm{K}$, $G = 13.5\,\mathrm{K}/Jy$, $N_p = 2$, $B = 10\,\mathrm{MHz}$, $\beta = 10$, $\tau_{samp} = 506\,\mu\mathrm{s}$, $\tau_{DM} = 550\,\mu\mathrm{s}$, $\tau_{scatt} = 50\,\mu\mathrm{s}$, and $w_0 = .2P$.

The reduced sensitivity to short period signals in the month long transform is the result of resampling the data to fit into available computer memory, see Appendix E.

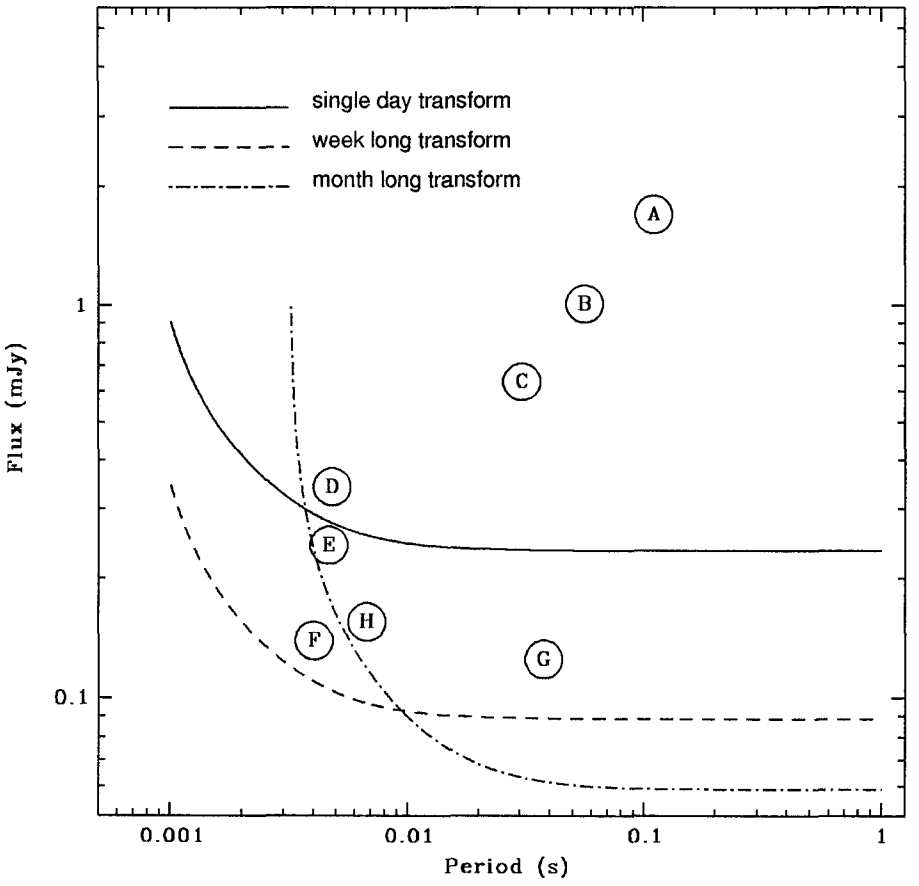

Figure 4.15: Flux limits for three searches.

4.6.4 Radio Luminosities

We find that the radio luminosities of the 8 pulsars in M15 may be described by a luminosity function $\Phi(L) \propto L^{-n}$, where L is the radio "luminosity" estimated in the usual fashion from the average flux density at 430 MHz, $S_{430} \times D^2$, and $\Phi(L)$ is the number of pulsars per logarithmic interval of L. The mean flux densities for the eight pulsars were estimated from the profiles in Figure 4.1, resulting from 65 hr of integration during the 1.2 yr period shown in Figure 4.5. The flux values for PSR 2127+11B–H were scaled relative to an assumed flux of 1.7 mJy for PSR 2127+11A (Wolszczan *et al.* 1989b) and are given in Table 4.2. The resulting luminosity function, which apart from a horizontal shift is independent of distance, is shown in Figure 4.16.

The estimation of the power-law exponent n, in $\Phi(L) \propto L^{-n}$, is readily accom-

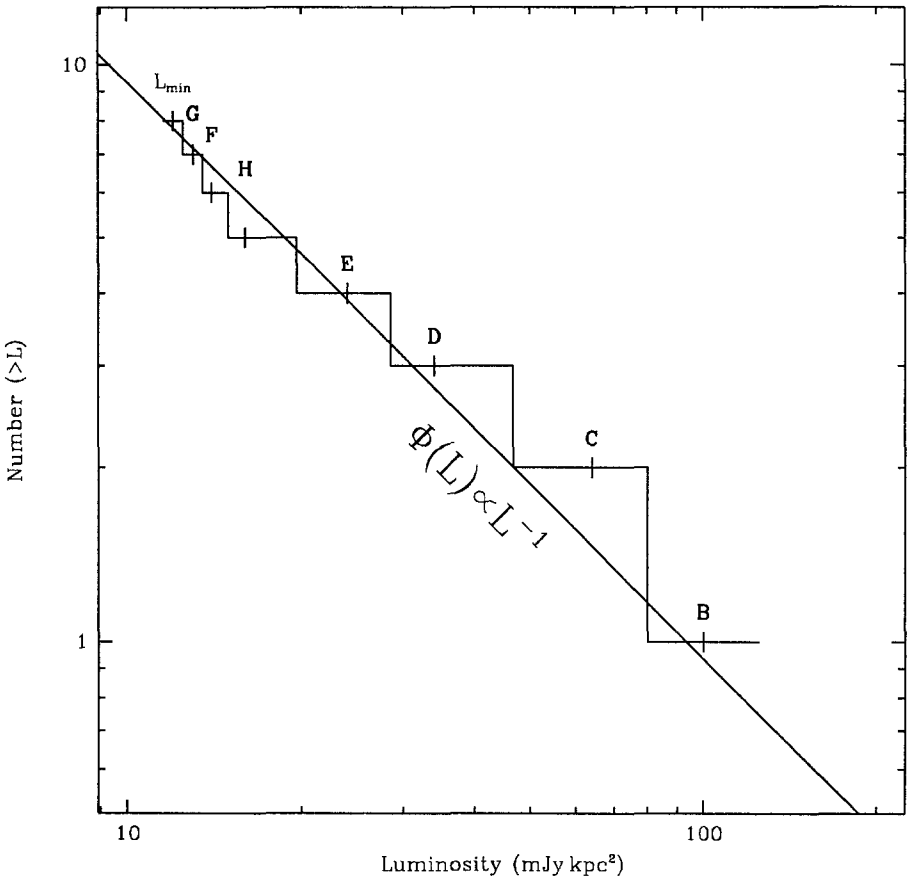

Figure 4.16: Luminosity function of the pulsars in M15. The seven pulsars PSR 2127+11B–H are scaled relative to an assumed flux of 1.7 mJy for m15A (Wolszczan *et al.* 1989b) and an assumed distance of 10 kpc to M15 (Fahlman, Richer, and VandenBerg 1985).

plished via the maximum likelihood method. The probability per unit luminosity is written,

$$\Pr(L)\,dL = \frac{\Phi(L)\frac{d\log L}{dL}}{N(>L_{min})}\,dL; \quad L_{min} < L < \infty,$$

where $N(>L_{min})$ is the number of observed pulsars with luminosity greater than L_{min}. The likelihood function may be written,

$$\mathcal{L}(n) \propto \prod_{i=1}^{N} \Pr(L_i), \tag{4.5}$$

$$\mathcal{L}(n) \propto \exp\left[N\log n + nN\log L_{min} - (n+1)\sum_{i=1}^{N}\log L_i\right], \tag{4.6}$$

$$\frac{\partial \mathcal{L}}{\partial n} = 0 \quad \Rightarrow \quad \frac{1}{n} = \frac{1}{N}\sum_{i=1}^{N} \log(L_i/L_{min}), \tag{4.7}$$

i.e., the exponent n is simply the inverse of the logarithmic average of the observed luminosities scaled by L_{min}. The error on this estimate may be obtained by applying the central limit theorem to the random variable $\Lambda \equiv \log(L/L_{min})$:

$$\sigma^2_{1/n} = \left[\left\langle \Lambda^2 \right\rangle - \langle \Lambda \rangle^2\right], \tag{4.8}$$

$$\langle \Lambda \rangle \equiv \int_{L_{min}}^{\infty} \Pr(L)\Lambda \, dL = \int_{L_{min}}^{\infty} n \frac{L^n_{min}}{L^{n+1}} \log\left(\frac{L}{L_{min}}\right) dL = \frac{1}{n}, \tag{4.9}$$

$$\left\langle \Lambda^2 \right\rangle = \frac{1}{n^2}, \tag{4.10}$$

$$\sigma^2_n = n^2 \sigma^2_{1/n} = \frac{n^2}{N}. \tag{4.11}$$

If one includes all 8 pulsars with $L_{min} = 12\,\mathrm{mJy\,kpc^2}$, the maximum likelihood solution is $\Phi(L) \propto L^{-1.0\pm.35}$. However, since the detection of PSR 2127+11C,G involve significant selection effects we also compute an estimate of the isolated pulsar luminosity function from PSR 2127+11A,B,D,E,F,H. Assuming $L_{min} = 13\,\mathrm{mJy\,kpc^2}$ these six pulsars yield, $\Phi(L) \propto L^{-0.93\pm0.38}$. This luminosity function is in agreement with that observed for field pulsars, $\Phi(L) \propto L^{-1.1}$ (Manchester and Taylor 1977; Lyne, Manchester, and Taylor 1985). For both luminosity function estimates, L_{min} was chosen to be $1\,\mathrm{mJy\,kpc^2}$ (an estimate of the pulsar luminosity spacing from Table 4.2) below the faintest pulsar considered. Extrapolating the observed luminosity function down to an intrinsic cutoff luminosity of $1\,\mathrm{mJy\,kpc^2}$ (Dewey *et al.* 1985) we estimate the current total population of observable isolated pulsars in M15 to be approximately 25–175, a number slightly higher than the 21 estimated in Kulkarni, Narayan, and Romani (1990). To estimate the total number of pulsars in M15 from the observed luminosity function, would require knowledge of the fraction of pulsars beamed away from Earth, and the fraction of pulsars in binary systems in addition to the assumed intrinsic cutoff luminosity—quantities that are poorly understood.

4.6.5 Dispersion Measures

By coherently folding the 128 separate correlator channels over our complete set of observations according to the 8 timing models in § 4.4 and § 4.5, it is possible to accurately measure the frequency dependence of pulse arrival time across the 10 MHz bandwidth of our observations, and hence, obtain the dispersion measure (DM) values in Table 4.2. The

three most likely sources for the observed range of *DM* values are: 1) a uniform distribution of free electrons that follows either the cluster gravitational potential, or a particular class of stars; 2) a small number of exotic objects, such as the low-mass X-ray binary or planetary nebula in M15; or 3) a distribution of inhomogeneities in the intervening interstellar medium (ISM). We consider these three cases in turn.

From the negative $\dot{P}$ of PSR 2127+11A,D it is known that these two pulsars lie behind the cluster core. Consequently, the lack of any increase in the *DM* towards these two pulsars relative to PSR 2127+11H which is probably near the middle of the cluster ($|l| \ll R_\perp$ in Figure D.2), places a limit of $5\,\mathrm{cm}^{-3}$ on the density of free electrons in the core. The observation of the highest *DM* being associated with PSR 2127+11B a pulsar that is most probably being accelerated away from Earth, i.e., is located near $l \simeq -R_\perp$, and that the *DM* of PSR 2127+11C (the binary pulsar ejected out of the cluster core to $R_\perp = 2.78\,\mathrm{pc}$) is equal to that of the inner core pulsars, indicate that a centrally condensed cluster component is not the dominant source of the observed spatial *DM* variations.

The two obvious choices for exotic objects in M15 that might be creating a wind of ionized particles responsible for the observed *DM* distribution, are the low-mass X-ray binary X2127+11 associated with the star AC211 (Aurière, Le Fèvre, and Terzan 1984), and the planetary nebula K648 associated with the star AC10 (Adams *et al.* 1984). However, as can be seen in Figures 4.10 and 4.11 there is no observed correlation of observed *DM* with distance from either of these two objects.

The lack of a radial dependence from any of the three obvious sources: cluster core, X-ray binary, planetary nebula, strongly suggests that the observed distribution is due to the intervening ISM. Inhomogeneities in the ISM are typically modeled as a power law spectrum of the form

$$P_{\delta n_e}(q) = C_n^2\, q^{-\beta}, \qquad \frac{2\pi}{l_o} \leq q \leq \frac{2\pi}{l_i}$$

where q is the wavenumber of the fluctuations, l_i and l_o are the inner and outer length scales—see Rickett (1990) for a recent review. Length scales of $10^{9-11}\,\mathrm{cm}$ are probed by diffractive interstellar scintillation (Cordes, Weisberg, and Boriakoff 1985), while length scales of $10^{11-13}\,\mathrm{cm}$ are probed by refractive interstellar scintillation (Kaspi and Stinebring 1992). Phillips and Wolszczan (1991) have shown that $3.7 < \beta < 3.9$ for length scales up to $10^{15}\,\mathrm{cm}$ by considering the *DM* time variability of three pulsars. All three of these regimes show β to be in the range $11/3 \pm 0.3$, consistent with a Kolmogorov turbulent spectrum of

$\beta = 11/3$ (Cordes *et al.* 1992, and references therein). We show that the observed spatial structure of the seven M15 "core" pulsar dispersion measurements are consistent with a $\beta \sim 3$ spectrum at 10^{17} cm, with an indication of cut-off around 10^{18} cm.

To first order in angular displacement from the cluster center the dispersion measure toward the seven "core" pulsars may be written $DM(\vec{r}) - DM_0 = \vec{r} \cdot \nabla\rho(x,y) + \delta$, where $DM_0 \equiv 67.25\,\mathrm{cm}^{-3}\,\mathrm{pc}$, $\nabla\rho(x,y)$ is the ISM column density gradient ($\mathrm{cm}^{-3}\,\mathrm{pc}\,/\mathrm{arcsec}$), and δ is the dispersion offset from the nominal value DM_0 at the cluster center. Parameterizing $\nabla\rho(x,y)$ as a magnitude g and unit vector $\vec{n}$ with position angle θ (measured east of north), a 3 parameter least-square fit to the 7 "cluster" pulsars yields: $g = 0.1\,\mathrm{cm}^{-3}\,\mathrm{pc}\,/\mathrm{arcsec}$, $\theta = 108°$, and $\delta = -0.10\,\mathrm{cm}^{-3}\,\mathrm{pc}$. In Figure 4.17 we compare this gradient fit to the data ($\vec{n}$ is shown in Figure 4.10).

This observed linear dependence may be related to the ISM power law exponent, β. The analysis in Phillips and Wolszczan (1991) may be carried out directly on the observed spatial distribution, with the electromagnetic phase structure function written as,

$$D_\phi(\vec{b}) \equiv \left\langle [\delta\phi(\vec{x}) - \delta\phi(\vec{x}+\vec{b})]^2 \right\rangle,$$

where $\vec{x}$ and $\vec{b}$ are vectors perpendicular to the line of sight, and the brackets denote an ensemble average. The phase fluctuations may be directly related to DM fluctuations,

$$\delta\phi(\vec{x}) = \lambda r_e \int_0^D \delta n_e(\vec{x},z)\,dz = 6.07 \times 10^7\,\delta DM(\vec{x}).$$

For the above power law spectrum, the structure functions may be expressed as

$$D_\phi(b) \propto \begin{cases} b^2 & \text{if } b \ll l_i, \\ b^{\beta-2} & \text{if } l_i \ll b \ll l_o, \\ b^0 & \text{if } b \gg l_o. \end{cases}$$

From the observation of a simple spatial gradient in DM it follows that $D_\phi(\vec{b}\cdot\vec{n}) \sim (\vec{b}\cdot\vec{n})^1$. Consequently, if the observations are attributed to a spectrum of inhomogeneities, β is ~ 3 for length $\lesssim 10^{17}$ cm. That the DM fluctuations do not appear to continue out to the radius of PSR 2127+11C may be taken as an initial indication that at length scales of 10^{18} cm, the outer length scale (l_o) has been reached. Obviously, the detection of several more pulsars would help test this hypothesis and determine whether $l_o \ll 10^{17}$ cm and rather than a spectrum of inhomogeneities, a single "cloud" is being observed. It is also interesting to note, that a fifth and rather unconventional explanation that the observations are due to a pulsar specific DM contribution is ruled out by the observed spatial coherence.

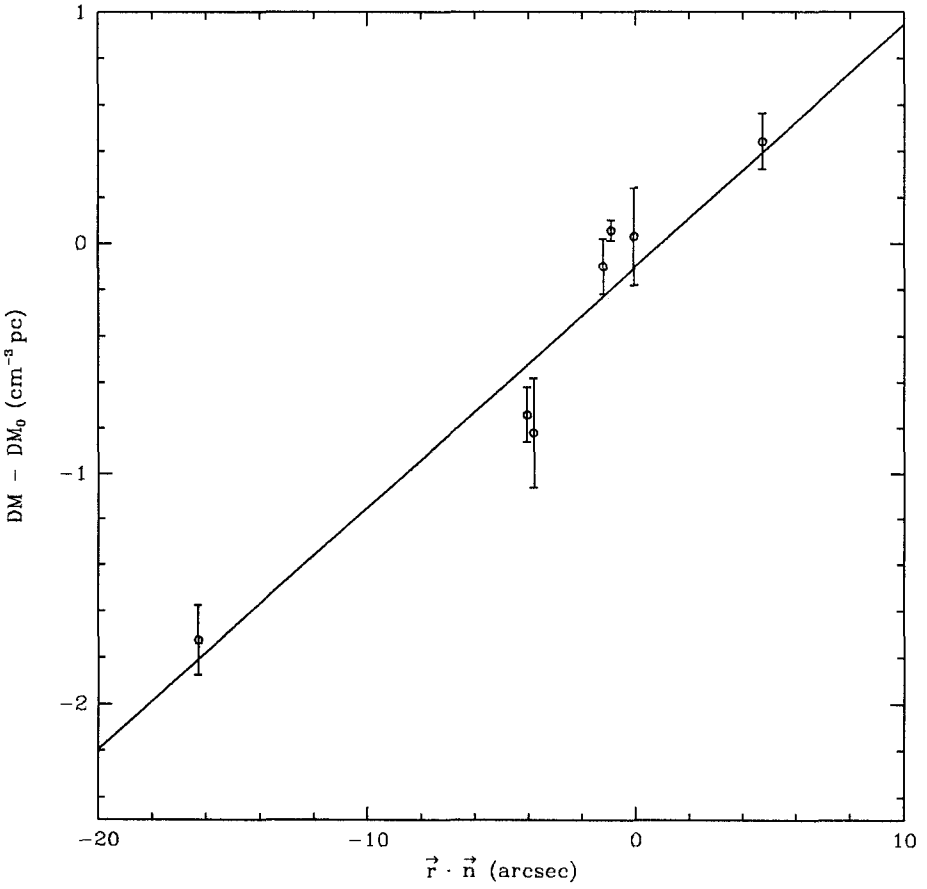

Figure 4.17: Dispersion measure relative to the nominal value, $DM_0 = 67.25\,\mathrm{cm}^{-3}\,\mathrm{pc}$, as a function of angular distance along the direction $\vec{n}$ (see Figure 4.10).

4.7 Conclusion

We have successfully detected and determined timing models for 8 pulsars in the globular cluster M15. Two relativistic parameters for the binary pulsar 2127+11C have been measured, constraining the two stellar masses to be $m_p = 1.34 \pm .23\,M_\odot$ and $m_c = 1.37 \pm .23\,M_\odot$. The remaining seven pulsars are single systems with PSR 2127+11A,D showing direct evidence of acceleration in the gravitational field of the cluster through their apparent rate of spin-up.

From the observed radial distribution and accelerations of the seven isolated pulsars in the core region of M15 lower limits on the central mass-to-light ratio ($M/L_U > 1.9\,M_\odot\,/\,L_{\odot,U}$), average surface density ($\bar{\Sigma} > 4.4 \times 10^5\,M_\odot\,\mathrm{pc}^{-2}$), and central density ($\rho_c >$

$2.7 \times 10^6\, M_\odot\, \mathrm{pc}^{-3}$) have been inferred.

The observed luminosity function $\Phi(L) \propto L^{-0.93\pm0.38}$ for the isolated pulsars in m15 lead to an estimate of $\mathcal{O}(100)$ currently observable isolated pulsars in M15.

ACKNOWLEDGEMENTS

This work was done in collaboration with S. R. Kulkarni, T. A. Prince, and A. Wolszczan. We thank J. H. Taylor for supplying the TEMPO software package, E. S. Phinney for helpful discussions, and T. R. Lauer for supplying the Hubble Telescope image of M15. We also thank P. S. Ray for help in analyzing the radio observations and J. C. Chiu for reducing the optical PCC data.

Chapter 5

Discovery of PSR 1310+18A and PSR 1639+36A

"Old Pulsars in the Low-Density Globular Cluster M13 and M53"

S.R. Kulkarni, S.B. Anderson, T.A. Prince, and A. Wolszczan

Appeared originally in *Nature*, Vol. 349, No. 6304, pp. 47–49, 3rd January, 1991

OLD PULSARS IN THE LOW-DENSITY GLOBULAR CLUSTERS M13 AND M53

S.R. KULKARNI, S.B. ANDERSON, AND T.A. PRINCE
Division of Physics, Mathematics and Astronomy,
California Institute of Technology, 206-49, Pasadena, CA 91125 USA

A. WOLSZCZAN
Arecibo Observatory, Arecibo, Puerto Rico 00613

ABSTRACT

Millisecond pulsars are conventionally assumed to be spun up through the action of binary companions, although some subsequently lose their companions and appear as isolated pulsars. Such objects should therefore be more numerous in dense stellar systems. We report here the surprising discovery of two pulsars in low-density globular clusters: one is a single 10-ms pulsar (PSR 1639+36) in M13 (NGC 6205), the other a 33-ms pulsar (PSR 1310+18) in a 256-d binary in M53 (NGC 5024). Their ages, inferred from their luminosities and constraints on their period derivatives, seem to be $\sim 10^9$ years, significantly greater than previously reported ages ($\lesssim 10^8$ years) of cluster pulsars (Phinney and Kulkarni 1991). The implied birth rate is inconsistent with the conventional two-body tidal capture model (Verbunt 1988; Bailyn and Grindlay 1990), suggesting that an alternative mechanism such as tidal capture between primordial binaries and a reservoir of (hundreds of) primordial neutron stars may dominate the production of tidal binaries in such clusters (Phinney and Kulkarni 1991; Phinney and Sigurdsson 1991). The period derivative of PSR 1639+36 is surprisingly small, and may be corrupted by acceleration due to the mean gravitational potential of the cluster (Phinney 1992a).

5.1 Analysis

We discovered the pulsars during a survey of globular clusters with the Arecibo 305 m radio telescope (Anderson *et al.* 1989d; Anderson *et al.* 1989c, see Appendix B). The observations were conducted at a centre frequency of 430 MHz and bandwidth of 10 MHz using the observatory's digital correlator in a manner identical to that described in Wolszczan *et al.* (1989b). The data analysis was carried out on Caltech's 512-node nCUBE/10 supercomputer.

The pulse profiles of the two pulsars are shown in Figure 5.1. By comparison with PSR 2127+11A (Wolszczan *et al.* 1989b), we estimate S_{430}, the 430-MHz flux density, of PSR 1310+18 and PSR 1639+36 to be 1 mJy and 3 mJy, respectively. Owing to the declination dependent sensitivity of the Arecibo telescope, the signal-to-noise-ratio of PSR 1639+36 is no better than that of PSR 1310+18. The corresponding 430 MHz radio luminosities, $L \equiv S_{430}\, d^2$, are $\sim$ 340 and 150 mJy kpc^2; (d is the distance (kpc) to the cluster).

We obtained timing data using the same hardware as that used in the discovery. In the case of PSR 1639+36, the fast sampled data, recorded on magnetic tape, were synchronously folded using a workstation computer and the resulting profiles cross-correlated with a high quality template to yield times of arrival (Anderson *et al.* 1990b, see Chapter 2). The software package TEMPO was used to transform the topocentric times of arrival to the barycentre from which the usual pulsar parameters were obtained, Table 5.1. For PSR 1310+18, the pulsar and orbital parameters are based on a least-squares fit to the apparent barycentric periods (Figure 5.2), assuming that the pulsar is at the centre of the cluster.

PSR 1639+36 is located 6.8 arcsec west and 21.4 arcsec south of the optical centroid (Table 5.1), well within the 45 arcsec core of the cluster. In the absence of a timing position all we can say is that PSR 1310+18 is within 6 arcmin (the primary beam half-width at half maximum of the Arecibo telescope at 430 MHz) of the centre of the cluster. Given the rarity of pulsars with short periods, the spatial coincidences are strong circumstantial evidence that the two pulsars are associated with their respective clusters.

5.2 Discussion

Although large numbers of pulsars are being discovered in globular clusters, the discovery of pulsars in M13 and especially M53 was unexpected because the usual models (Verbunt 1988; Bailyn and Grindlay 1990) predict essentially no pulsars in such low-density clusters. This is not a statistical fluctuation because pulsars have been found in all but two clusters (M 3 and Pal 2) of the six low-density clusters searched from the Arecibo telescope. Indeed, in one of them, M5, two pulsars have been reported by Wolszczan *et al.* (1989a).

In the standard model, primordial neutron stars (those born in the earliest epoch of the cluster) tidally capture other cluster stars (of mass M and radius R and moving at

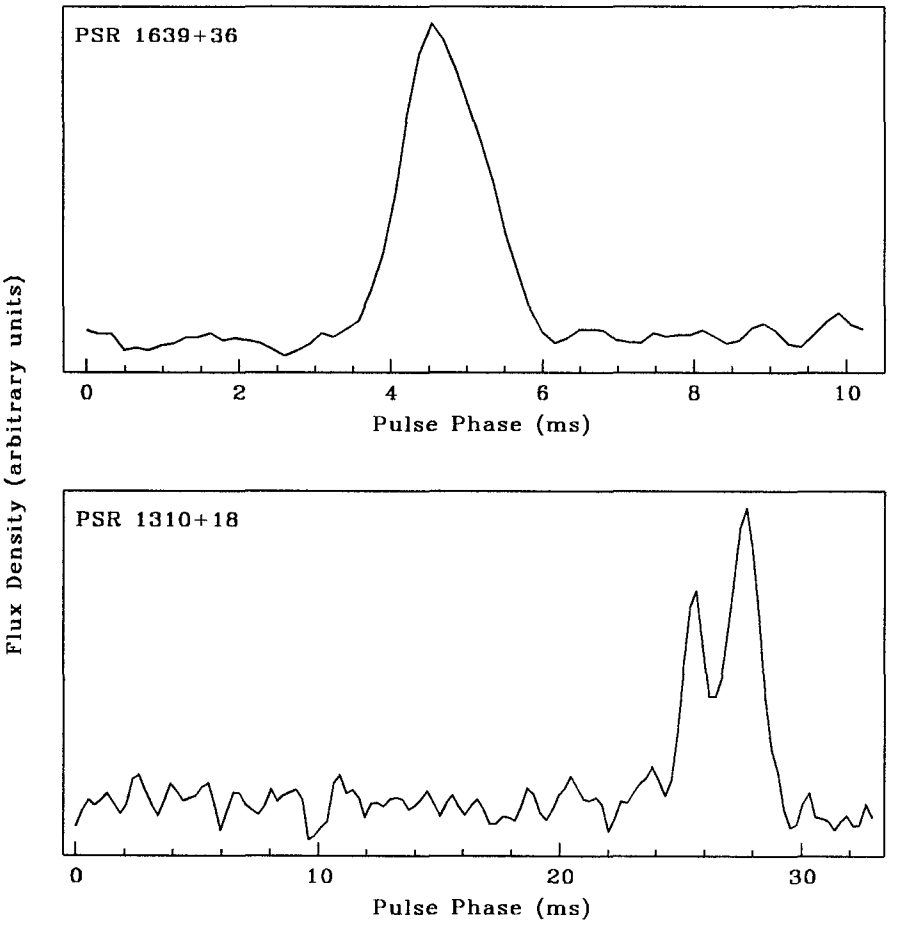

Figure 5.1: The pulse profile of PSR 1639+36 in M13 (top) and PSR 1310+18 (bottom) at 430 MHz. The temporal resolution is limited by the sampling interval of 506 μs.

a relative velocity v) at the volumetric rate (Lee and Ostriker 1986),

$$\Gamma = 3 \times 10^{-10} \kappa(M) \frac{R}{R_\odot} \frac{M}{M_\odot} \frac{n_{ns}}{10^2\,\mathrm{pc}^{-3}} \frac{n}{10^4\,\mathrm{pc}^{-3}} \frac{10\,\mathrm{km\,s}^{-1}}{v}\,\mathrm{yr}^{-1}\,\mathrm{pc}^{-3}\,. \tag{5.1}$$

Here n and n_{ns} are the volume densities of the non-degenerate cluster stars and the neutron stars and κ is essentially unity for $M \lesssim 0.8\,M_\odot$. Mass transfer then spins up the neutron star and the end product is a spun-up pulsar in orbit around a white dwarf star. In a competing model (Bailyn and Grindlay 1990; Michel 1987), a massive white dwarf is substituted for a neutron star. Copious mass transfer leads to the collapse of the accreting white dwarf into a neutron star after which the evolutionary path is the same as above. Main sequence captures lead to binaries with orbital periods of about 1 day. About 15% of the encounters are with giants (Verbunt 1988). However, only a quarter are expected to result in large orbital period

($\gtrsim$ 100 d) binaries, with the rest forming ultracompact binaries (Bailyn 1988; McMillan, McDermott, and Taam 1987).

PSR 1310+18 with an orbital period of 256 d and a mass function of 0.0098 $M_\odot$ appears to be an approximate twin of PSR 1620−26, the 11 ms, 191 d binary pulsar in the cluster M4 (Lyne *et al.* 1988). Both systems may be the result of a tidal capture of a giant star (but see discussion below). Assuming a mass of 1.4 $M_\odot$ for PSR 1310+18, the minimum mass of the companion is 0.3 $M_\odot$ which is quite consistent with the expectation that it is a white dwarf.

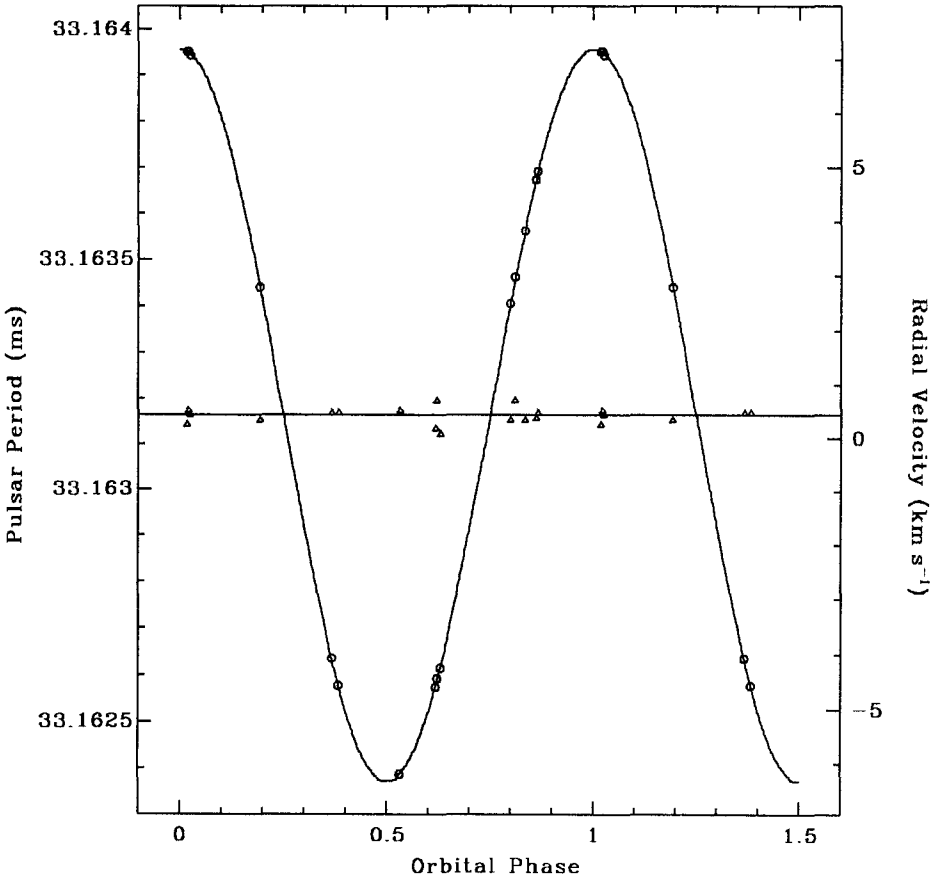

Figure 5.2: The apparent period of PSR 1310+18 as a function of the orbital phase. Triangles denote post-fit residuals multiplied by 10.

The formation of a single pulsar such as 1639+36 is something of a puzzle. The simplest version of the standard model requires that the white dwarf/pulsar binary be

disrupted by passing stars. In M28, a cluster that is denser than M13, this mechanism has already been found to be quite improbable (Rappaport, Putney, and Verbunt 1989). We must therefore consider alternative mechanisms. The preponderance of single pulsars in clusters has already been noted (Phinney and Kulkarni 1991; Kulkarni *et al.* 1990) and has been attributed (Phinney and Kulkarni 1991) to the expansion of the companion on capture (Ray, Kembhavi, and Anita 1987), followed by the neutron star spiralling in and destroying the companion.

Integrating equation (5.1) over the volume of the cluster (assumed to be described by a King model with parameters from Chernoff and Djorgovski (1989) and assuming $M \sim 0.6\,M_\odot$), we estimate N_t, the number of two-body tidal captures over a Hubble lifetime ($t_H \sim 10^{10}$ y) to be $4(N_{ns}/100)$ and $2(N_{ns}/100)$ in M13 and M53, respectively. Here N_{ns} is the number of primordial neutron stars in the cluster. To get one wide binary pulsar, we need $N_{ns} = 1{,}300$. Even so, the expected age of such a pulsar in M53 would be $t_H/2$ (assuming a constant formation rate over t_H) whereas below we argue for a smaller age, $\sim t_H/10$.

The birth rate of pulsars in these low density systems seems to be quite high. In the absence of reliable values of the period derivative $\dot{P}$, we need other age estimators. Empirically it appears that the radio luminosity of the disk millisecond pulsars decreases with the characteristic age (E. S. Phinney, S. R. K. and H. M. Johnston, manuscript in preparation) and using this relation, the luminosities of these two pulsars suggest ages of $\sim 10^9$ yr. This in turn increases the birth rate by a factor of about five and can be accommodated only by $N_{ns} \gtrsim 10^3$, as above. But this would result in the core being contaminated by degenerate stars, a result not consistent with dynamical studies (Meylan 1989). Thus our discovery offers strong support to models (Phinney and Kulkarni 1991; Sigurdsson and Phinney 1990) that invoke other mechanisms such as three-body tidal collisions involving primordial binaries and an N_{ns} of ~ 400. We also note that the giant binary in M53 has a natural explanation in this framework.

The observed period derivative of PSR 1639+36 is less than $4.5 \times 10^{-20}\,\mathrm{s\,s^{-1}}$, a 5σ upper limit. Thus the nominal lower limit to the characteristic age of the pulsar is 3.8×10^9 yr. However, like other pulsars in clusters, the $\dot{P}$ of PSR 1639+36 is expected to be corrupted by the line of sight acceleration, a, induced by the mean cluster gravitational

potential (Phinney 1992a),

$$a(r_\perp) = \frac{GM(<r)}{r^2}\frac{\sqrt{r^2 - r_\perp^2}}{r}. \tag{5.2}$$

Here r is the radial distance of the pulsar from the centre of the cluster, $r_\perp$ is the impact parameter and $M(<r)$ is the mass contained within radius r. This acceleration corrupts the intrinsic period derivative by an amount, $\dot{P}_c = a(r_\perp)P/c$.

For the observed $r_\perp$ we have calculated $a(r_\perp)$ assuming a King model to derive $M(<r)$, and by assuming (Phinney 1992a) that the neutron star volume density is proportional to ρ^q where $q \sim 2$ is the ratio of the mass of a neutron star to the mass of a typical star that contributes to the light distribution. The median and extreme accelerations are found to be $a = \pm 2.9 \times 10^{-7}$ cm s^{-2} and $\pm 4.0 \times 10^{-7}$ cm s^{-2} which will perturb the period derivative by $\pm 10 \times 10^{-20}$ s s^{-1} and $\pm 14 \times 10^{-20}$ s s^{-1}; the sign of the acceleration depends on whether the pulsar is located ahead or behind the centre of the cluster.

5.3 Conclusion

From the above discussion, we can draw one firm conclusion: the intrinsic period derivative, $\dot{P}_p = \dot{P} - \dot{P}_c$ is less than 19×10^{-20} s s^{-1}. Thus the pulsar is older than 0.9×10^9 yr, about equal to the rough estimate of the age from our empirical luminosity relation. This makes PSR 1639+36 the oldest known cluster pulsar. A subsidiary conclusion is that the dipole field strength of the pulsar, estimated the usual way, $B_9 \equiv (B/10^9\,\mathrm{G}) = 10^3\sqrt{P\dot{P}_{-15}}$, cannot be larger than 1.2 in which case the pulsar was spun up to no more than 4 ms, assuming that the equilibrium spin-up period is $3.45 B_9^{6/7}$ ms (Bhattacharya and van den Heuvel 1991).

The gradient of the mean gravitational field and the gravitational attraction due to the nearest neighbours will result in changes in the observed values of the higher period derivatives (Blandford, Romani, and Applegate 1987). Measurement of $\ddot{P}$, the largest effect, would unfortunately need six decade's of timing observations.

ACKNOWLEDGEMENTS

We thank A. S. Fruchter for donation of telescope time, J. H. Taylor for the TEMPO software package, and E. S. Phinney and S. Djorgovski for discussions. This work was supported by an NSF Presidential Young Investigator award and DOE DE-FG03-85ER25009 (TAP); an NSF Graduate Fellowship (SBA); and an NSF Presidential Young Investigator award and an Alfred P. Sloan Fellowship (SRK). Arecibo Observatory is part of the National Astronomy and Ionosphere Center, operated by Cornell University under contract with the NSF.

TABLE 5.1

Pulsar and Cluster Parameters

Timing Parameters: PSR 1639+36*	
Right ascension (B1950)	$16^h\,39^m\,53^s.626\,(3)$
Declination (B1950)	$36^\circ\,32'\,54''.94\,(6)$
Dispersion Measure	$30.36(4)\,\mathrm{cm}^{-3}\,\mathrm{pc}$
Barycentric Period	10.3775094520(6) ms
Period Derivative	$< 4.5 \times 10^{-20}\,\mathrm{s\,s}^{-1}$ (5σ)
Epoch	2447666.71 JD
Globular Cluster Parameters: M13	
Right ascension (B1950)	$16^h\,39^m\,54^s.19\,(5)$
Declination (B1950)	$36^\circ\,33'\,16''.3\,(6)$
Galactic Latitude	$59^\circ.0$
Galactic Longitude	$40^\circ.9$
Distance	7.1 kpc
Core Radius	$45''$
Timing Parameters: PSR 1310+18†	
Dispersion Measure	$24.0 \pm 1.5\,\mathrm{cm}^{-3}\,\mathrm{pc}$
Barycentric Period	33.163166 (3) ms
Orbital Period	255.8 (6) d
$a_1 \sin(i)$	84.2 (7) s
T_0	2447061.2 JD
e	< 0.01
Globular Cluster Parameters: M53	
Right ascension (B1950)	$13^h\,10^m\,28^s.27\,(5)$
Declination (B1950)	$18^\circ\,26'\,2''.3\,(6)$
Galactic Latitude	$332^\circ.9$
Galactic Longitude	$79^\circ.7$
Distance	18.5 kpc
Core Radius	$22''$

Numbers enclosed in parenthesis are the uncertainties in the last significant digit(s). Timing parameters are derived from the observed period data. The pulsar is assumed to be located at the centre of the cluster. T_0 is the time of ascending node passage; JD Julian day; $a_1 \sin i$, projected semi-major axis; e, eccentricity. The cluster positions are taken from Shawl and White (1986) while the distance and core radii estimates are from Chernoff and Djorgovski (1989).

* Based on 17 observations made between 20 May 1989 and 19 May 1990. The r.m.s. of the post-fit residuals is 52 μs for an individual integration time of 23 min.

† Based on 13 observations made between 20 May 1989 and 8 April 1990 and one observation point on 29 DEC 1987. The r.m.s after fitting to the velocity curve is $18\,\mathrm{m\,s}^{-1}$.

Appendix A

Doppler Orbit for PSR 1639+36B

In this appendix we present initial timing parameters for PSR 1639+36B—a 3.5 ms binary pulsar in the globular cluster M13. The existence of a second pulsar in M13 provides additional evidence that the birthrate of radio pulsars in low-density globular clusters is higher than allowed from two-body tidal interactions. This lends support to other formation scenarios such as three-body interactions involving primordial binaries (Phinney and Kulkarni 1991).

Figure A.1 shows a Keplerian orbit fit to the observed Doppler shifted pulse periods scattered over a 2 year period, with the parameters give in Table A.1. The observed mass function, $f = 0.001815\,M_\odot$, implies a lower limit to the companion mass of $0.16\,M_\odot$ (assuming a pulsar mass of $1.4\,M_\odot$). The pulse profile is shown in Figure A.2.

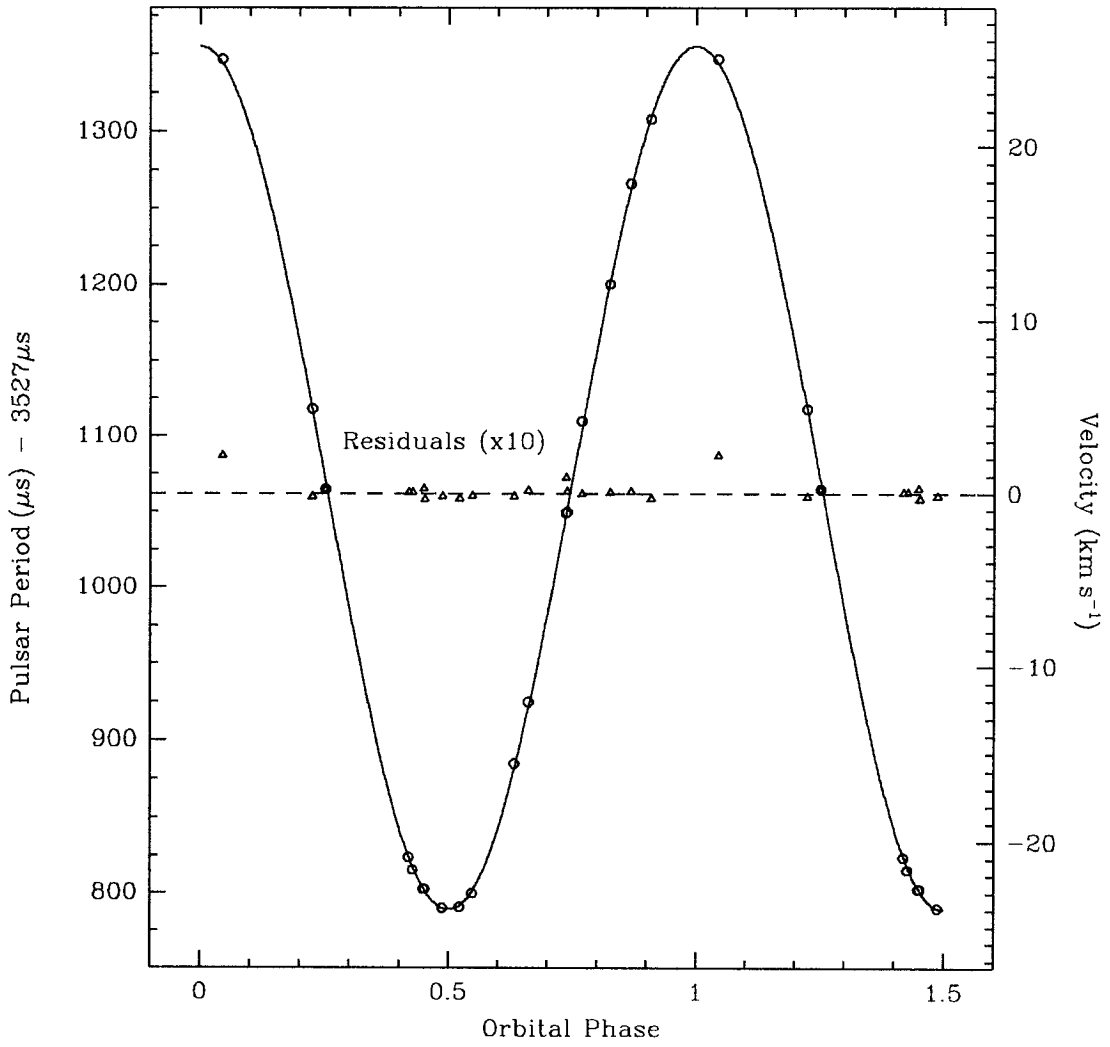

Figure A.1: Doppler fit to the Keplerian parameters of PSR 1639+36B. Triangles denote post-fit residuals multiplied by 10.

Figure A.2: Pulse profile of PSR 1639+36B

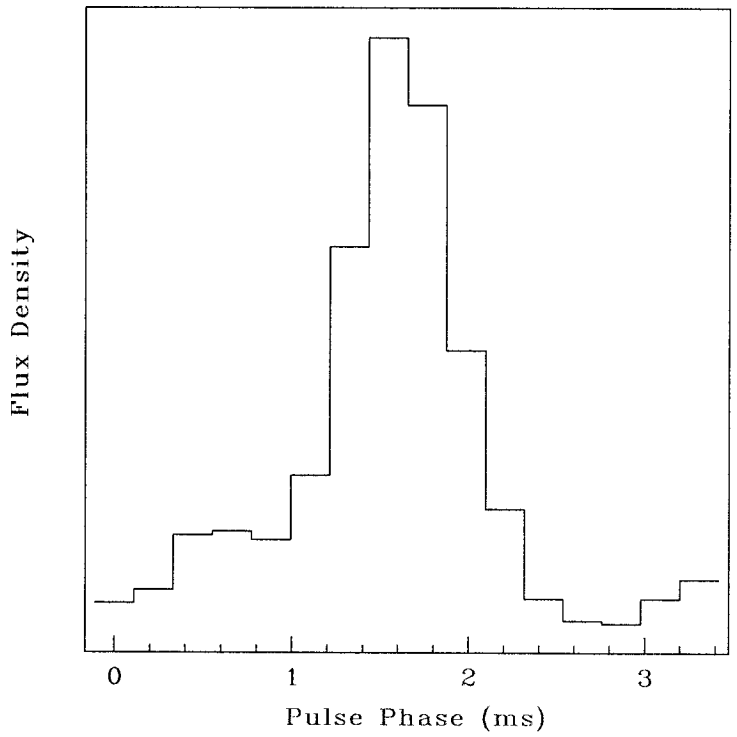

TABLE A.1

Keplerian parameters for PSR 1639+36B

Timing Parameters		
Pulsar period	P	3.528072 (5) ms
Dispersion measure	DM	$29.5 \pm 1.5\,\mathrm{cm}^{-3}\,\mathrm{pc}$
Right ascension*	α_{1950}	$16^{\mathrm{h}}\,39^{\mathrm{m}}\,54^{\mathrm{s}}.19 \pm 5'$
Declination*	δ_{1950}	$36^{\circ}\,33'\,16''.3 \pm 5'$
Orbital Parameters		
Orbital period	P_b	1.259113 (3) d
Projected semi-major axis	$a_1 \sin i$	1.389 (2) ls
Eccentricity	e	< 0.001
Epoch	T_0	2447149.6835 (18) JD
Mass function	f	0.001815 (8) $M_\odot$

* Assumed position is coincident with cluster center given in Shawl and White (1986) with errors corresponding to the beam size at 430 MHz.

Appendix B

IAU Circulars

B.1 Pulsar in Globular Cluster M15

(Anderson *et al.* 1989b, IAU Circular #4762)

S. Anderson, P. Gorham, S. Kulkarni, T. Prince, California Institute of Technology; and A. Wolszczan, Arecibo Observatory, write: "We report the discovery of a 56-ms pulsar in the globular cluster M15. Observations were made with the 305-m Arecibo reflector at 430 MHz on 1988 Dec. 26. A time series of 10E7 samples with a sample time 0.5 ms was padded to 2E24 samples and Fourier- transformed, using the Caltech nCUBE/10 hypercube supercomputer. The dispersion measure, 67.2 +/- 2.5 pc/cm3, is consistent with that of the 110-ms pulsar 2127+11 reported by Wolszczan et al. (1989, Nature 337, 531). The new pulsar is within 2' of the center of M15 (NGC 7078). In 1415-MHz Arecibo data taken one year earlier, the pulsar is detected with the identical barycentric period at the 5-sigma level. Based on these two observations, dP/dt < 5 x 10E-15 s/s. The flux density is 0.7 +/- 0.1 mJy at 430 MHz."

B.2 PSR 2127+11C

(Anderson *et al.* 1989a, IAU Circular #4772)

S. Anderson, P. Gorham, S. Kulkarni, and T. Prince, California Institute of Technology; and A. Wolszczan, Arecibo Observatory, write: "We report the discovery of a 30-ms binary pulsar in the globular cluster M15 (NGC 7078). Observations were made with the 305-m Arecibo reflector at 430 MHz on 1988 Dec. 26. A 2E24 sample time series representing 1.5 hr of observation was subject to a pulse search, assuming a range of constant accelerations on the Caltech nCUBE/10 supercomputer. The pulsar was best detected with an assumed constant acceleration of 9.4 m/s2. The dispersion measure, 67.2 +/- 2 pc cmE-3, is consistent with that of the two known pulsars in M15: the 110-ms pulsar 2127+11 reported by Wolszczan et al. (1989, Nature 337, 531), and the 56-ms pulsar recently reported on IAUC 4762. The new pulsar is within 2' of the center of the cluster. In the 1415-MHz Arecibo data taken one year earlier, the pulsar is detected at the 6.5-sigma level with a frequency that is Doppler-shifted relative to the 430-MHz detection by 95 km/s, and a best-fit linear acceleration of 4.9 m/s2. The flux density of PSR 2127+11C is 0.6 +/- 0.2 mJy at 430 MHz."

B.3 Ten-Millisecond Pulsar in M13

(Anderson *et al.* 1989d, IAU Circular #4819)

S. Anderson, S. Kulkarni and T. Prince, California Institute of Technology; and A. Wolszczan, Arecibo Observatory, report: "A 10-ms pulsar has been discovered in the direction of the globular cluster M13 (NGC 6205). The data were obtained from the 300-m Arecibo telescope at a frequency of 430 MHz on 1989 May 20 and analyzed on the Caltech nCUBE/10 supercomputer. The telescope was pointed toward the cluster's optical center (R.A. = 16h39m54s.2, Decl. = +36d33'16", equinox 1950.0); the telescope beamwidth is about 12'. The dispersion measure of the pulsar is 30.5 +/- 1 pc cm-3. The pulse profile consists of a single pulse with a duty cycle of 15 percent."

B.4 Pulsar in Globular Cluster M53

(Anderson *et al.* 1989c, IAU Circular #4853)

S. Anderson, S. Kulkarni, T. Prince, California Institute of Technology; and A. Wolszczan, Arecibo Observatory, write: "We report the discovery of a 33-ms pulsar with a dispersion measure of 24 +/- 1.5 cmE-3 pc towards the globular cluster M53 (NGC 5024). Observations were made with the 305-m Arecibo reflector at a frequency of 430 MHz using the same backend as that used in the discovery of pulsars in the cluster M15 (e.g., IAUC 4772). The analysis was done on the Caltech nCUBE/10 supercomputer. Confirmation observations show that the new pulsar is within the 2' of the optical centroid of M53. The new pulsar is either an isolated pulsar or possibly a member of a very wide binary system."

B.5 PSR 1908+00

(Anderson *et al.* 1990a, IAU Circular #5013)

S. Anderson, S. Kulkarni, and T. Prince, California Institute of Technology; and A. Wolszczan, Arecibo Observatory, write: "We report the discovery of a 3.6-ms binary pulsar at a dispersion measure of 200 +/- 10 pc cmE-3 in the globular cluster NGC 6760. Observations were made with the 305-m Arecibo reflector at 1415 MHz on 1987 Dec. 29. A 2E23 sample time series was formed from a 1.2-hr observation and subject to standard pulsar signal detection analysis. Following a preliminary detection, a search was made over a range of accelerations. The signal peaks at an acceleration of -2.8 m sE-2, indicating that the pulsar is in a binary system. The pulsar has been detected at a consistent dispersion measure in several observations made during 1989 Sept. at Arecibo."

Appendix C

Multiple Observation Sensitivities

In this appendix we calculate the relative sensitivities of coherently and incoherently combining ("stacking") multiple day observations. The probability density functions for normalized power spectrum values and their respective cumulative distribution functions are as follows:

$$\begin{aligned}
\Pr(P_c)\,dp_c &= e^{-p_c}\,dp_c, \\
\Pr(P_i;m)\,dp_i &= \frac{p_i^{m-1}}{(m-1)!}e^{-p_i}\,dp_i, \\
\Pr(P_c > p_c) \equiv 1 - \mathcal{CDF}\,[P_c] &= e^{-p_c}, \\
\Pr(P_i > p_i;m) \equiv 1 - \mathcal{CDF}\,[P_i;m] &= \sum_{i=0}^{m-1}\frac{p_i^m}{m!}e^{-p_i} = Q(2p_i\big|2m) = \int_{2p_i}^{\infty}\frac{p^{m-1}e^{-\frac{1}{2}p}}{2^m\Gamma(m)}\,dp,
\end{aligned}$$

where m is the number of days being combined, $p_{c,i}$ are the normalized powers in the coherent and stack power spectra, with associated random variates $P_{c,i}$ (Middleditch 1975, for example). To calculate flux limits for the two methods it is first necessary to calculate the corresponding power thresholds for detection. Defining a detection as an overall statistical significance of 1:100, the threshold power levels, $\mathbf{p}_{c,i}$ are implicitly defined by,

$$\mathbf{p}_{c,i} = p_{c,i} \quad s.t. \quad \left\{1 - (\mathcal{CDF}\,[P_{c,i}])^{N_{c,i}} = \frac{1}{100} \simeq N_{c,i}\,(1 - \mathcal{CDF}\,[P_{c,i}])\right\};$$
$$N_c = mN_i,\ N_i = \frac{N_{pts}}{2},$$

for m observations of N_{pts} samples each. The $\mathbf{p}_c$ equation is readily inverted to yield, $\mathbf{p}_c = \ln N_c + \ln 100$, however, for $\mathbf{p}_i$ a numerical inversion is required. For comparison, the expected normalized power for a single observation with instantaneous SNR of a/σ is

$$Q \equiv \text{single observation power} = \frac{a^2 N_{pts}}{4\sigma^2} + 1.$$

Relating the threshold powers to equivalent single observation powers yields,

$$\mathbf{p}_c = \frac{a^2 m N_{pts}}{4\sigma^2} + 1 \quad \rightarrow \quad \mathbf{q}_c = \frac{\mathbf{p}_c - 1}{m} + 1$$
$$\mathbf{p}_i = m\left(\frac{a^2 N_{pst}}{4\sigma^2} + 1\right) \quad \rightarrow \quad \mathbf{q}_i = \frac{\mathbf{p}_i}{m}.$$

The two flux limits, $F_{\{c,i\}} \propto \sqrt{Q_{\{c,i\}} - 1}$ are shown in Figure C.1. For example, the flux limit reached by coherently transforming 13 observations is 70% below the single observation limit and 20% lower than the incoherent stack search, requiring a stack of 25 individual observations to reach the same flux limit. These relative flux limits have only a weak dependence on N_{pts}, differing by less than 6% between the $N_{pts} = 2^{22}$ in Figure C.1 and $N_{pts} = 2^{13}$, over the range of m shown.

As a means of searching for binary pulsars or as a result of finite computer memory we show in Figure C.2 the reduction in sensitivity for splitting a single observation into a sequence of shorter segments which are individually transformed and stacked. We also show the number of days that must be stacked to reach the single day single transform flux limit as a function of the number of stack segments per day.

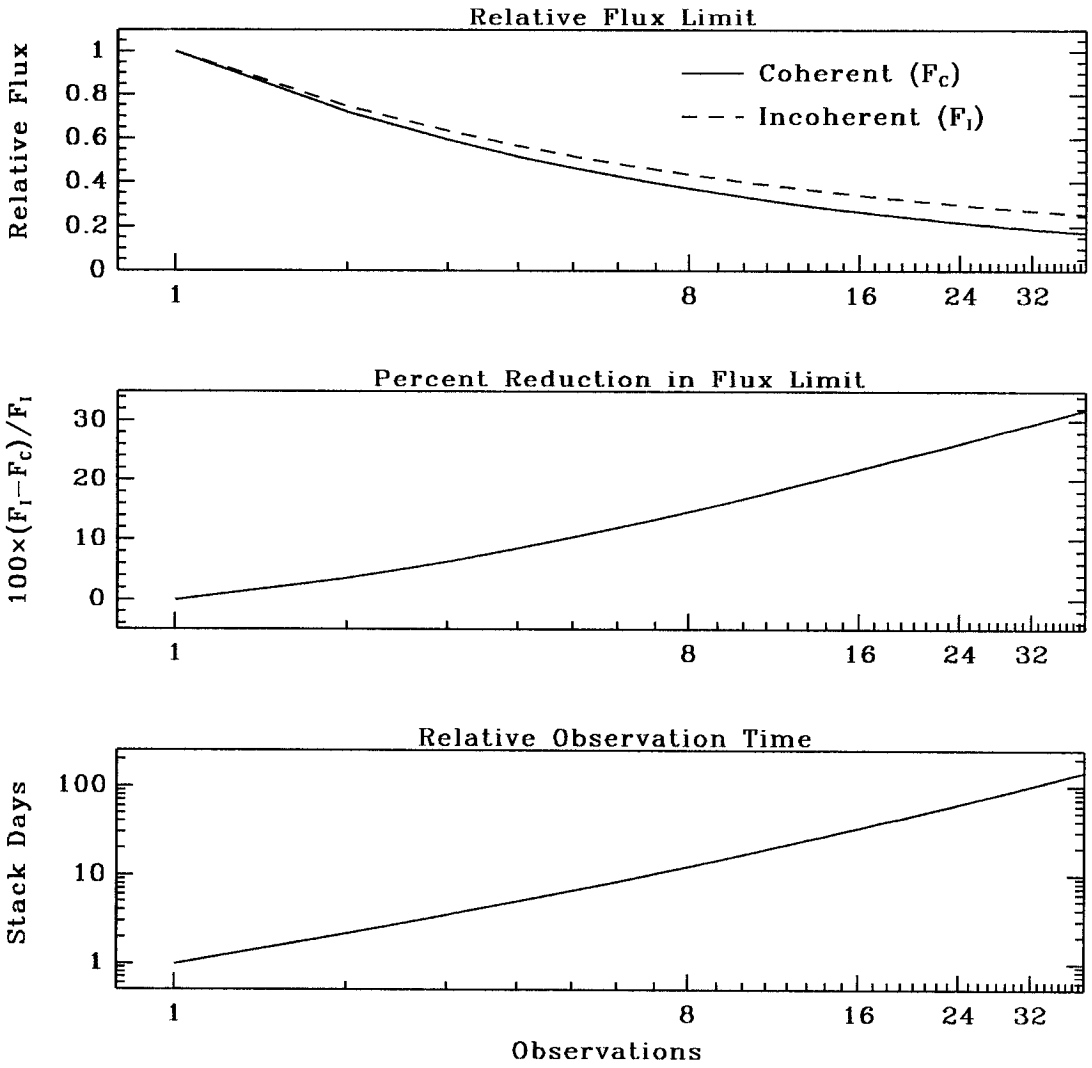

Figure C.1: Relative sensitivity for coherently and incoherently combining multiple day observations.

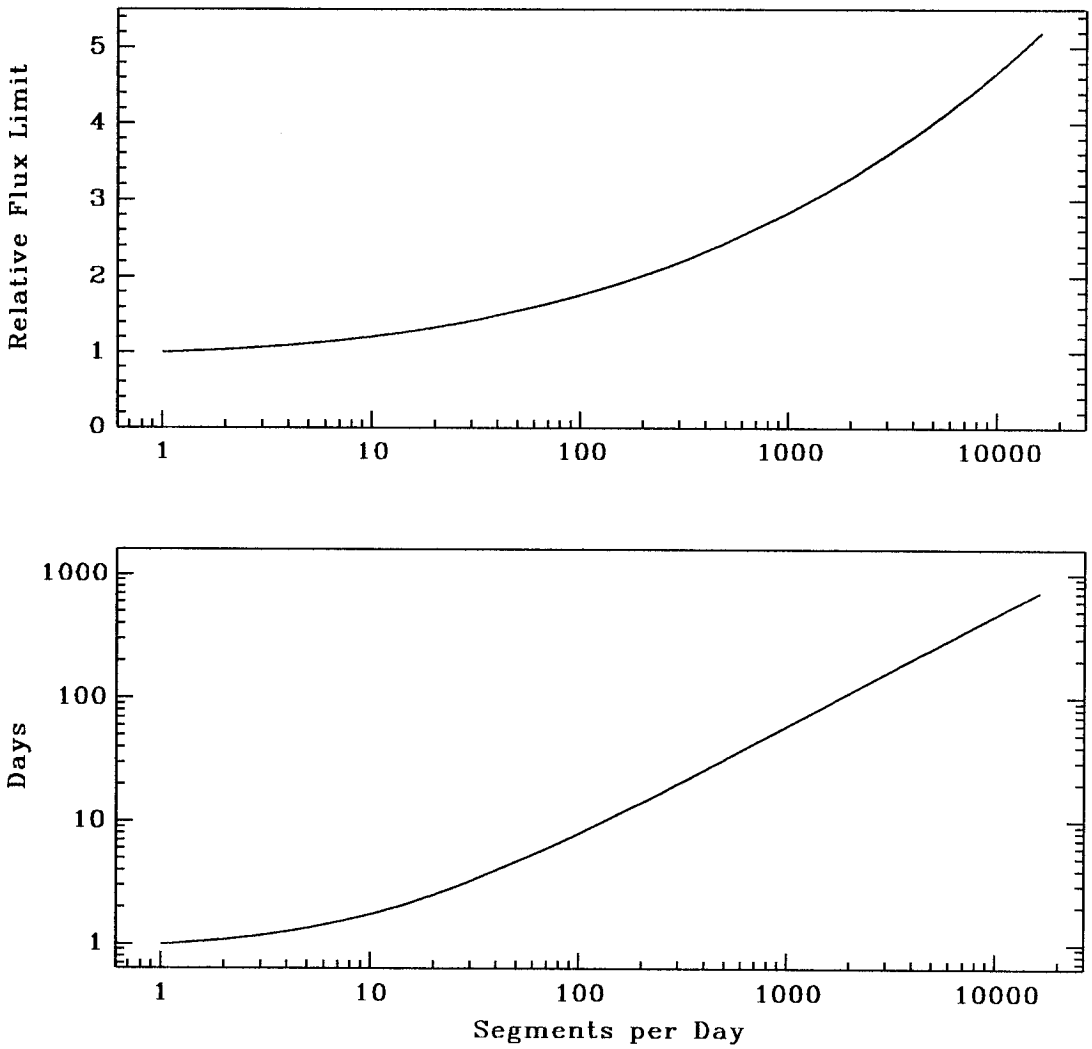

Figure C.2: Relative sensitivity for incoherently stacking short segments of multiple day observations.

Appendix D

Distribution of Cluster Accelerations

In this appendix we calculate the line of sight acceleration distribution for pulsars in the central core region of the globular cluster M15. Following the analysis in Phinney (1992a) we calculate $p(|a_l|\big|R_\perp)$, the probability density of observing a line of sight acceleration of magnitude $|a_l|$ (positive and negative signs being *a priori* equally likely, i.e., no preference for a pulsar to be found in front of rather than behind the cluster center of mass), at an observed projected radius, $R_\perp$. The two quantities necessary to calculate $p(|a_l|\big|R_\perp)$ are the pulsar spatial density distribution, n_p, and and the gravitational mass within a sphere of radius r, $M(<r)$. The pulsar distribution is directly observable, and is found in § 4.6.1 to be $n_p \propto r^{-3}$, i.e., constant population per logarithmic interval of radius. The total mass distribution is currently only partially constrained by the observed negative period derivatives of the two pulsars 2127+11A,D (see § 4.6.2) and must be taken from theoretical studies. Phinney (1992a) argues that even in core collapsed clusters such as M15 where individual mass species have significantly different mass profiles, it remains approximately true that the total cluster mass scales linearly with radius, i.e., an isothermal sphere (cf. Murphy and Cohen (1988), Chernoff and Weinberg (1990), and Murphy, Cohen, and Hut (1990)). Consequently, we assume $M(<r) \propto r$ and use the observed pulsar distribution, $n_p \propto r^{-3}$, in what follows.

The line of sight acceleration in a spherically symmetric cluster is simply the mean field acceleration, $GM(<r)/r^2$ projected by l/r onto the line of sight (see Figure D.2),

$$a_l = -\frac{GM(<r)}{r^3} l.$$

The four extreme values of a_l, assuming an isothermal sphere are,

$$0 = \frac{da_l}{dl} = \frac{d}{dl}\left(\frac{rl}{r^3}\right) = \frac{\partial}{\partial l}\left(\frac{l}{l^2+R_\perp^2}\right) \quad \text{or} \quad l = \pm R_\perp, \pm\infty.$$

Parameterizing a_l by the maximal magnitude acquired at $l = \pm R_\perp$ one finds,

$$a_l = -\left(\frac{2lR_\perp}{R_\perp^2+l^2}\right) a_{max} \qquad \text{and} \qquad a_{max} = \frac{GM(<R_\perp)}{2R_\perp^2}, \tag{D.1}$$

where we again use the isothermal assumption to equate $M(<r)/r$ with $M(<R_\perp)/R_\perp$. Inserting the observed $n_p \propto r^{-3}$ into the *a priori* probability distribution for l yields,

$$p(l\big|R_\perp) = \frac{n_p(r)}{\int_{-\infty}^{\infty} n_p(r)\,dl} \qquad \begin{matrix} n_p \propto r^{-3} \\ \Longrightarrow \end{matrix} \qquad p(|l|\big|R_\perp) = \frac{R_\perp^2}{\left(R_\perp^2+l^2\right)^{3/2}}.$$

Since the inverse function, $l = a_l^{-1}(a)$, is double valued (see Figure D.2) the change of independent variables from $|l|$ to $|a_l|$ is

$$p(|a_l|\big|R_\perp) = \frac{p(|l_1|\big|R_\perp)}{\left|\frac{da_l}{dl}\right|_{|l_1|}} + \frac{p(|l_2|\big|R_\perp)}{\left|\frac{da_l}{dl}\right|_{|l_2|}}, \tag{D.2}$$

where the two roots of the inverse function are found from Equation D.1 to be,

$$l_{1,2} = R_\perp\left(\frac{a_{max}}{a} \begin{matrix} +^{l_2} \\ -_{l_1} \end{matrix} \sqrt{\left(\frac{a_{max}}{a}\right)^2 - 1}\right); \; |l_1| < |l_2|.$$

Calculating the Jacobian for the transformation of Equation D.1 and evaluating Equation D.2 leads to,

$$\begin{aligned}
\left|\frac{da_l}{dl}\right| &= 2a_{max}R_\perp \frac{R_\perp^2 - l^2}{\left(R_\perp^2+l^2\right)^2}, \\
p(|a_l|\big|R_\perp) &= \frac{R_\perp}{2a_{max}}\left(\frac{\sqrt{R_\perp^2+l_1^2}}{R_\perp^2-l_1^2} - \frac{\sqrt{R_\perp^2+l_2^2}}{R_\perp^2-l_2^2}\right), \\
p(|a_l|\big|R_\perp) &= \frac{1}{2a_{max}\sqrt{1-a/a_{max}}}.
\end{aligned}$$

This distribution is quite similar to the "rule of thumb" given in Phinney (1992a) and Phinney (1992b)—with the cumulative distributions differing by at most 11% at a_{max}. In Table D.1 we compare the two probability distributions, their expected values of a_l and cumulative probabilities of $|a_l|$ exceeding a fixed value.

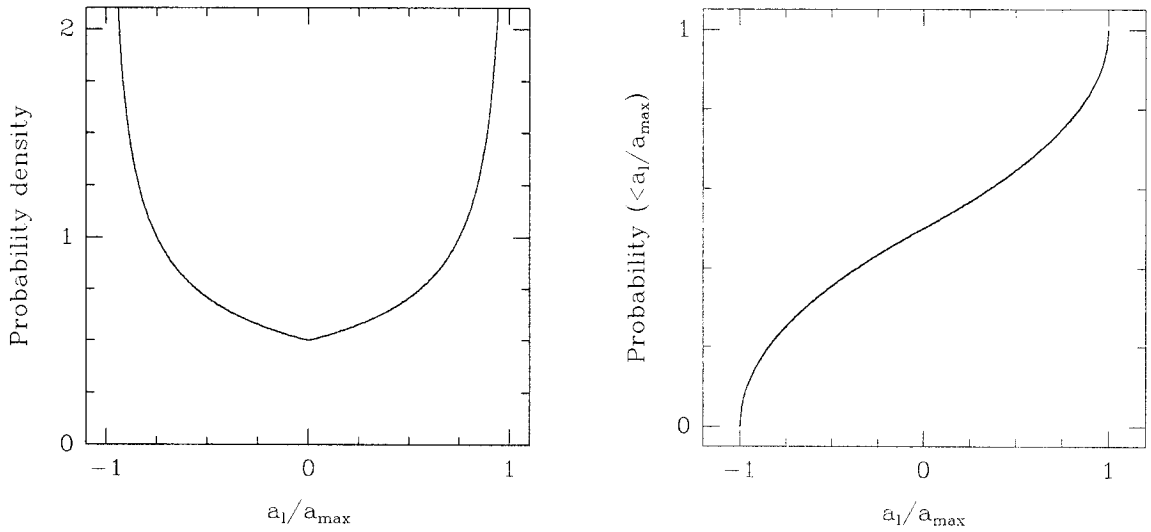

Figure D.1: Cluster acceleration probability distribution ($n_p \propto r^{-3}$).

TABLE D.1

Comparison of Acceleration Probability Distributions

	$n_p \propto r^{-3}$	$n_p \propto r^{-2}$
$p(\lvert a_l \rvert \big\vert R_\perp)$	$\dfrac{1}{2a_{max}\sqrt{1-\lvert a_l \rvert / a_{max}}}$	$\dfrac{2}{\pi a_{max}\sqrt{1-(a_l/a_{max})^2}}$
$\langle \lvert a_l \rvert \rangle$	$\dfrac{2a_{max}}{3} = \dfrac{GM(<R_\perp)}{3R_\perp^2}$	$\dfrac{2a_{max}}{\pi} = \dfrac{GM(<R_\perp)}{\pi R_\perp^2}$
$p(\lvert a_l \rvert > a \big\vert R_\perp)$	$\sqrt{1-a/a_{max}}$	$1-\dfrac{2}{\pi}\sin^{-1}\left(\dfrac{a}{a_{max}}\right)$

The $n_p \propto r^{-3}$ case corresponds to the observed radial distribution of pulsars in M15 (see § 4.6.1). The $n_p \propto r^{-2}$ case is the "rule of thumb" derived in Phinney (1992a). We note that the two cumulative distributions differ by at most 4% near $\langle |a_l| \rangle$.

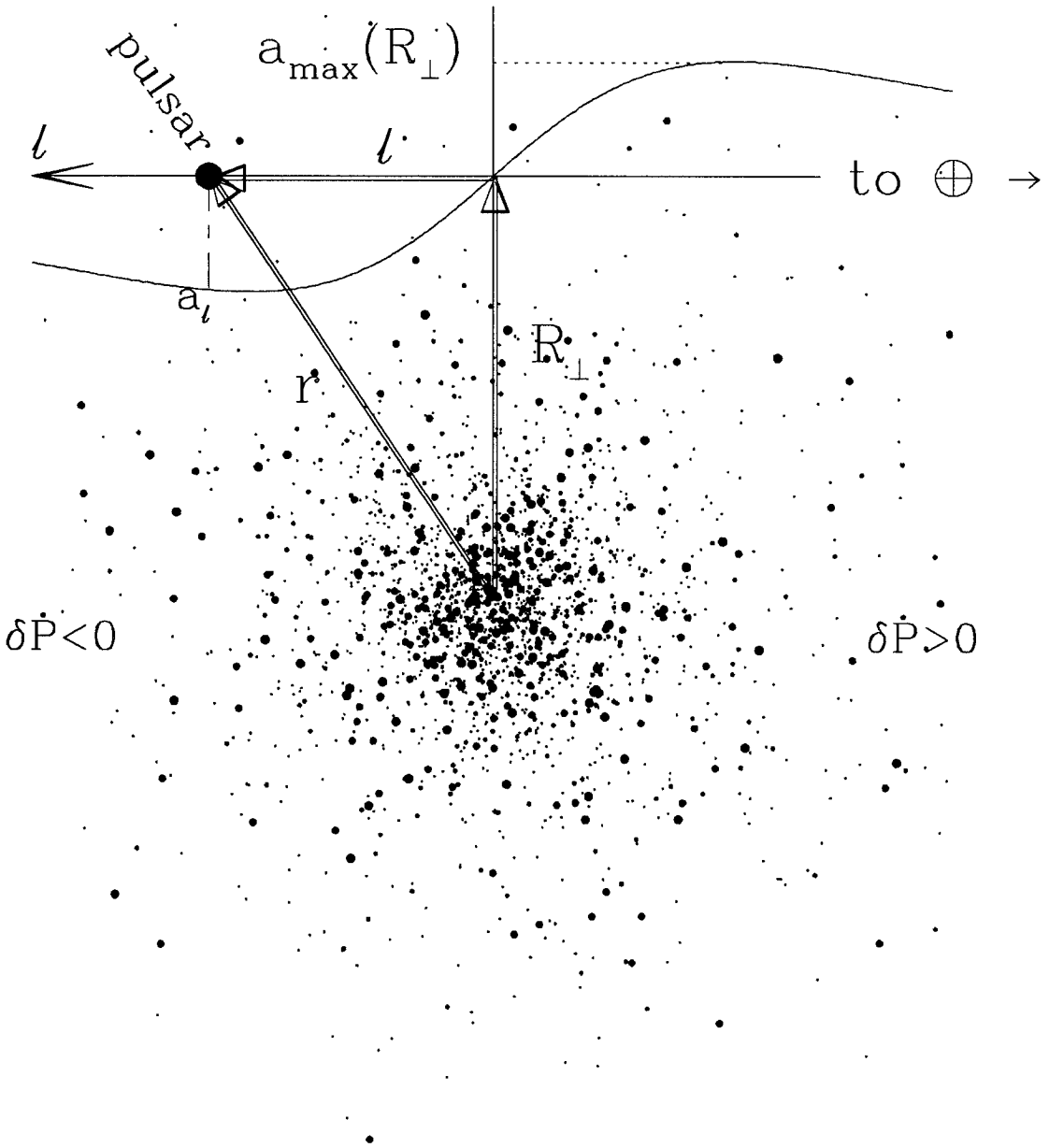

Figure D.2: Schematic drawing of cluster acceleration taken from Phinney (1992b).

Appendix E

Computational Algorithms and Requirements

In this appendix we discuss some of the computational aspects of our pulsar search effort. The following three parallel supercomputers have been used to analyze radio pulsar data: a 576 processor nCUBE/10, a 64 processor iPSC/860, and the 512 processor Intel Touchstone Delta System. The main characteristics of these three computers are listed in Table E.1.

TABLE E.1

Parallel computer specifications

Computer	Processors	Memory (Mbytes)	Speed* (Mflops)	Disk storage (Gbytes)
nCUBE/10	576	256	30	3
iPSC/860	64	1024	250	8
Touchstone Delta	512	8192	2000	95

* The floating point operation rate quoted here is that measured for our search code, the peak performance of these machines is roughly twice this value for the nCUBE/10 and an order of magnitude larger for the iPSC/860 and Delta.

All of the pulsar searches reported in this thesis are based on performing Fourier transforms utilizing the well known FFT algorithm (Bracewell 1986). However, it was initially noted that during the first $\log_2$(number of processors) steps in the standard parallel implementation of the FFT algorithm (Fox *et al.* 1988), that half the floating point numbers are communicated between processors (to avoid redundant floating point arithmetic), operated upon, and communicated back. Consequently, the standard algorithm proceeds as follows: (comm op comm) (comm op comm) ... (comm op comm). We state here without

proof (beyond the estimated Peta floating point operations that have been successfully executed), that a previously unpublished algorithm exists that proceeds as: (comm op) (comm op) ... (comm op comm). This algorithm was motivated by considering the additional degrees of freedom available in a hypercube topology at each stage of the FFT, and may be easily reconstructed by logically relabeling the processors between each inter-processor communication step. This results in the total communication performed dropping quickly to 50% of the standard parallel algorithm as the number of processors exceeds 4, and leads to a reduction in the total FFT time that is typically 25-50%, but depends on the computer architecture, number of data points per processor, and the number of processors.

The only "complication" of this new algorithm is the ordering of the output data. If, as in the pulsar search algorithm, the input data is sorted, then the standard algorithm returns the transform with spectral values in bit-reversed locations, i.e., the frequency value indexed by $(\mathtt{abcdefgh})_2$ (in binary notation) is found at $(\mathtt{hgfedcba})_2$. However in the new algorithm, with the dynamic relabeling of processors, the $\log_2$(number of processors) high order bits of the index are also cyclically permuted, e.g., for an 8 processor machine the value indexed by $(\mathtt{abcdefgh})_2$ is to be found at $(\mathtt{gfhedcba})_2$. We note, however, that since the standard bit-reversed algorithm requires each processor to communicate with every other processor in the final communication step to reorder the frequency spectrum (if necessary, as in pulsar searching, but not so for example in convoluting or correlating two functions) this permutation of processor numbers adds no additional time or complexity to the final reordering.

Bibliography

Adams, S., Seaton, M. J., Howard, I. D., Aurière, M., and Walsh, J. R. 1984, *Mon. Not. R. astr. Soc.*, **207**, 471–489.

Aguilar, L., Hut, P., and Ostriker, J. P. 1988, *Astrophys. J.*, **335**, 720–747.

Anderson, S., Gorham, P., Kulkarni, S., Prince, T., and Wolszczan, A. 1989a. IAU circular 4772.

Anderson, S., Gorham, P., Kulkarni, S., Prince, T., and Wolszczan, A. 1989b. IAU circular 4762.

Anderson, S., Kulkarni, S., Prince, T., and Wolszczan, A. 1989c. IAU circular 4853.

Anderson, S., Kulkarni, S., Prince, T., and Wolszczan, A. 1989d. IAU circular 4819.

Anderson, S., Kulkarni, S., Prince, T., and Wolszczan, A. 1990a. IAU circular 5013.

Anderson, S. B., Gorham, P. W., Kulkarni, S. R., Prince, T. A., and Wolszczan, A. 1990b, *Nature*, **346**, 42–44.

Aoki, S., Sôma, M., Kinoshita, H., and Inoue, K. 1983, *Astr. Astrophys.*, **128**, 263–267.

Aurière, M., Le Fèvre, O., and Terzan, A. 1984, *Astr. Astrophys.*, **138**, 415–420.

Backer, D. C., Fomalont, E. B., Goss, W. M., Taylor, J. H., and Weisberg, J. M. 1985, *Astron. J.*, **90**, 2275–2280.

Backer, D. C. and Hellings, R. W. 1986, *Ann. Rev. Astr. Ap.*, **24**, 537–575.

Bailyn, C. D. 1988, *Nature*, **332**, 330–332.

Bailyn, C. D. and Grindlay, J. E. 1990, *Astrophys. J.*, **353**, 159–167.

Bartel, N., Ratner, M. I., Shapiro, I. I., Cappallo, R. J., Rogers, A. E. E., and Whitney, A. R. 1985, *Astron. J.*, **90**, 318–325.

Bhattacharya, D. and van den Heuvel, E. P. J. 1991, *Phys. Rep.*, **203**, 1–124.

Biggs, J. D., Lyne, A. G., Manchester, R. N., and Ashworth, M. 1990. IAU circular 4988.

Binney, J. and Tremaine, S. 1987, *Galactic Dynamics*, (Princeton: Princeton University Press).

Blandford, R. D., Romani, R. W., and Applegate, J. H. 1987, *Mon. Not. R. astr. Soc.*, **225**, 51P–53P.

Bracewell, R. N. 1986, *The Fourier Transform and its Applications*, (New York: McGraw-Hill), 2^{nd} edition.

Chanmugam, G. and Brecher, K. 1987, *Nature*, **329**, 696–698.

Chernoff, D. and Weinberg, M. 1990, *Astrophys. J.*, **351**, 121–156.

Chernoff, D. F. and Djorgovski, S. D. 1989, *Astrophys. J.*, **339**, 904–918.

Cordes, J. M. and Dewey, R. J. 1988, in *Radio Wave Scattering in the Interstellar Medium, AIP Conference Proceedings No. 174*, ed. J. M. Cordes, B. J. Rickett, and D. C. Backer, (New York: American Institute of Physics).

Cordes, J. M., Weisberg, J. M., and Boriakoff, V. 1985, *Astrophys. J.*, **288**, 221–247.

Cordes, J. M., Weisberg, J. M., Frail, D. A., Spangler, S. R., and M., R. 1992, *Nature*, **354**, 121–124.

D'Amico, N. *et al.* 1990. IAU circular 5013.

Damour, T. and Deruelle, N. 1986, *Ann. Inst. H. Poincaré (Physique Théorique)*, **44**, 263.

Damour, T. and Taylor, J. H. 1991, *Astrophys. J.*, **366**, 501–511.

Damour, T. and Taylor, J. H. 1992, *Phys. Rev. D*, **45**, 1840–1868.

Davis, M. M., Taylor, J. H., Weisberg, J. M., and Backer, D. C. 1985, *Nature*, **315**, 547–550.

Dewey, R. J. and Cordes, J. M. 1987, *Astrophys. J.*, **321**, 780–798.

Dewey, R. J., Stokes, G. H., Segelstein, D. J., Taylor, J. H., and Weisberg, J. M. 1984, in *Millisecond Pulsars*, ed. S. P. Reynolds and D. R. Stinebring, (Green Bank: NRAO), 234–240.

Dewey, R. J., Taylor, J. H., Weisberg, J. M., and Stokes, G. H. 1985, *Astrophys. J.*, **294**, L25.

Elson, R., Hut, P., and Inagaki, S. 1987, *Ann. Rev. Astr. Ap.*, **25**, 565–601.

Fahlman, G. G., Richer, H. B., and VandenBerg, D. A. 1985, *Astrophys. J. Supp. Series*, **58**, 225–254.

Fomalont, E. B., Goss, W. M., Lyne, A. G., Manchester, R. N., and Justtanont, K. 1992, *Mon. Not. R. astr. Soc.* (in press).

Fox, G. C., Johnson, M. A., Lyzenga, G. A., Otto, S. W., Salmon, J. K., and Walker, D. W. 1988, *Solving Problems on Concurrent Processors*, (Englewood Cliffs: Prentice Hall).

Geffert, M., Aurière, M., Ilovaisky, S. A., and A., T. 1989, *Astr. Astrophys.*, **209**, 423–426.

Grindlay, J. E., Hertz, P., Steiner, J. E., Murray, S. S., and Lightman, A. P. 1984, *Astrophys. J.*, **282**, L13–L16.

Groth, E. J. 1975a, *Astrophys. J. Supp. Series*, **29**, 431.

Groth, E. J. 1975b, *Astrophys. J. Supp. Series*, **29**, 443–451.

Groth, E. J. 1975c, *Astrophys. J. Supp. Series*, **29**, 453–465.

Hamilton, T. T., Helfand, D. J., and Becker, R. H. 1985, *Astron. J.*, **90**, 606–608.

Iben, I. and Tutukov, A. V. 1985, *Astrophys. J. Supp. Series*, **58**, 661–710.

Johnston, H. M., Kulkarni, S. R., and Goss, W. M. 1991, *Astrophys. J.*, **382**, L88–L92.

Johnston, H. M., Kulkarni, S. R., and Phinney, E. S. 1991, in *X-ray Binaries and the Formation of Binary and Millisecond Pulsars*, ed. E. P. J. van den Heuvel and S. A. Rappaport, (Dordrecht: Kluwer).

Kaspi, V. M. and Stinebring, D. R. 1992, *Astrophys. J.*, **392**, 530–542.

King, I. R. 1985, in *Dynamics of Star Clusters, IAU Symposium no. 113*, ed. J. Goodman and P. Hut, (Dordrecht: Reidel).

Kulkarni, S. R., M., G. W., Wolszczan, A., and Middleditch, J. 1990, *Astrophys. J.*, **363**, L5–L8.

Kulkarni, S. R., Narayan, R., and Romani, R. 1990, *Astrophys. J.*, **356**, 174–183.

Lauer, T. R. *et al.* 1991, *Astrophys. J.*, **369**, L45–L49.

Lee, H. M. and Ostriker, J. P. 1986, *Astrophys. J.*, **310**, 176–188.

Lestrade, J. F., Bougois, G., Biraud, F., Aubry, D., Drouhin, J. P., and Freon, G. 1990, in *Impact of Pulsar Timing on Relativity and Cosmology*, ed. D. Backer, (Berkeley: Center for Particle Astrophysics), E1–E10.

Lyne, A. G., Biggs, J. D., Brinklow, A., Ashworth, M., and McKenna, J. 1988, *Nature*, **332**, 45–47.

Lyne, A. G., Brinklow, A., Middleditch, J., Kulkarni, S. R., Backer, D. C., and Clifton, T. R. 1987, *Nature*, **328**, 399–401.

Lyne, A. G. *et al.* 1990, *Nature*, **347**, 650–652.

Lyne, A. G., Manchester, R. N., and Taylor, J. H. 1985, *Mon. Not. R. astr. Soc.*, **213**, 613–639.

Manchester, R. N., Lyne, A. G., Johnston, S., D'Amico, N., Lim, J., Kniffen, D. A., Fruchter, A. S., and Goss, W. M. 1989. IAU circular 4905.

Manchester, R. N., Lyne, A. G., Robinson, C., D'Amico, N. D., Bailes, M., and Lim, J. 1991, *Nature*, **352**, 219–221.

Manchester, R. N. and Taylor, J. H. 1977, *Pulsars*, (San Francisco: Freeman).

Masters, A. R. and Roberts, D. H. 1975, *Astrophys. J.*, **195**, L107–L111.

McMillan, S. L. W., McDermott, P. N., and Taam, R. E. 1987, *Astrophys. J.*, **318**, 261–277.

Meylan, G. 1989, *Astr. Astrophys.*, **214**, 106–112.

Michel, F. C. 1987, *Nature*, **329**, 310–312.

Middleditch, J. 1975. Ph.D. thesis, University of California, Berkeley.

Murphy, B. W. and Cohen, H. N. 1988, *Mon. Not. R. astr. Soc.*, **232**, 835–852.

Murphy, B. W., Cohen, H. N., and Hut, P. 1990, *Mon. Not. R. astr. Soc.*, **245**, 335–349.

National Astronomy and Ionosphere Center. *Arecibo Observatory Users's Manual* 1989.

Nice, D. J. 1992. Ph.D. thesis, Princeton University.

Perillat, P. 1989. Timing notes. Technical report, Arecibo.

Phillips, J. A. and Wolszczan, A. 1991, *Astrophys. J.*, **382**, L27–L30.

Phinney, E. S. 1992a, *Mon. Not. R. astr. Soc.* (in press).

Phinney, E. S. 1992b, *Phil. Trans. Roy. Soc. A.* (submitted).

Phinney, E. S. and Kulkarni, S. R. 1991, *Nature.* (in press).

Phinney, E. S. and Sigurdsson, S. 1991, *Nature*, **349**, 220–223.

Prince, T. A., Anderson, S. B., Kulkarni, S. R., and Wolszczan, A. 1991, *Astrophys. J.*, **374**, L41–L44.

Rappaport, S., Putney, A., and Verbunt, F. 1989, *Astrophys. J.*, **345**, 210–221.

Rappaport, S. A. and Joss, P. C. 1983, in *Accretion-Driven Stellar X-Ray Sources*, ed. W. H. G. Lewin and E. P. J. van den Heuvel, (Cambridge: Cambridge University Press).

Ray, A., Kembhavi, A. K., and Anita, H. M. 1987, *Astr. Astrophys.*, **184**, 164–172.

Rickett, B. J. 1990, *Ann. Rev. Astr. Ap.*, **113**, 561–605.

Roberts, D. H., Masters, A. R., and Arnett, W. D. 1976, *Astrophys. J.*, **203**, 196–201.

Romani, R. W., Kulkarni, S. R., and Blandford, R. D. 1987, *Nature*, **329**, 309–310.

Shawl, S. J. and White, R. E. 1986, *Astron. J.*, **91**, 312–316.

Sigurdsson, S. 1992. Ph.D. thesis, California Institute of Technology.

Sigurdsson, S. and Phinney, E. S. 1990, *Bulletin of the A. A. S.*, **22**, 1341.

Smarr, L. L. and Blandford, R. 1976, *Astrophys. J.*, **207**, 574–588.

Spitzer, L. 1987, *Dynamical Evolution of Globular Clusters*, (Princeton: Princeton University Press).

Taylor, J. H. and Weisberg, J. M. 1989, *Astrophys. J.*, **345**, 434–450.

Taylor, J. H., Wolszczan, A., Damour, T., and Weisberg, J. M. 1992, *Nature*, **355**, 132–136.

van den Heuvel, E. P. J., van Paradijs, J. A., and Taam, R. E. 1986, *Nature*, **322**, 153–155.

Verbunt, F. 1988, in *Neutron Stars and Their Birth Events: Proceedings of the NATO Advanced Study Institute on Neutron Stars, Their Birth, Evolution, Radiation, and Winds*, ed. W. Kundt, (Dordrecht: Kluwer), 179–218.

Verbunt, F. and Hut, P. 1987, in *IAU Symp. 125, The Origin and Evolution of Neutron Stars*, ed. D. J. Helfand and J.-H. Huang, (Dordrecht: Reidel), 187–197.

Verbunt, F., Lewin, W. H. G., and van Paradijs, J. 1989, *Mon. Not. R. astr. Soc.*, **241**, 51–57.

Verbunt, F., van den Heuvel, E. P. J., van Paradijs, J., and Rappaport, S. A. 1987, *Nature*, **329**, 312–314.

Webbink, R. F. 1985, in *Dynamics of Star Clusters, IAU Symposium no. 113*, ed. J. Goodman and P. Hut, (Dordrecht: Reidel), 541–577.

Wolszczan, A. 1991, *Nature*, **350**, 688–690.

Wolszczan, A. 1992, *Nature*, **355**, 145–147.

Wolszczan, A., Anderson, S., Kulkarni, S., and Prince, T. 1989a. IAU circular 4880.

Wolszczan, A., Kulkarni, S. R., Middleditch, J., Backer, D. C., Fruchter, A. S., and Dewey, R. J. 1989b, *Nature*, **337**, 531–533.